2013

Producing *In-Situ* Nanoparticles of Griseofulvin using Supercritical Antisolvent Methodology

Pratik Sheth
University of Rhode Island, pratiksheth@hotmail.com

PRODUCING *IN-SITU* NANOPARTICLES OF GRISEOFULVIN USING SUPERCRITICAL ANTISOLVENT METHODOLOGY

BY

PRATIK SHETH

A DISSERTATION SUBMITTED IN PARTIAL FULFILLMENT OF THE REQUIREMENTS FOR THE DEGREE OF

DOCTOR OF PHILOSOPHY

IN

BIOMEDICAL AND PHARMACEUTICAL SCIENCES

UNIVERSITY OF RHODE ISLAND

2013

DOCTOR OF PHILOSOPHY DISSERTATION

OF

PRATIK SHETH

APPROVED:

Dissertation Committee:

Major Professor M. Serpil Kislalioglu Ph.D

David Worthen Ph.D.

Michael L. Greenfield Ph.D

Nasser H. Zawia Ph.D
DEAN OF THE GRADUATE SCHOOL

UNIVERSITY OF RHODE ISLAND
2013

ABSTRACT

Poor aqueous solubility of drug candidates is a major challenge for the pharmaceutical scientists involved in drug development. Particle size reduction to nano scale appears as an effective and versatile option for solubility improvement. Unlike the traditional methods used for the particle size reduction, supercritical fluid (SCF) processing techniques offer advantages ranging from superior particle size control to clean processing. Amongst all of the SCF based techniques, supercritical antisolvent (SAS) processing is of particular interest because most pharmaceuticals, including the model drug for this study-griseofulvin, are insoluble in supercritical carbon dioxide ($scCO_2$), and SAS is one of the technique that can effectively process such compounds. Additionally, SAS is the only technique amongst SCF based technologies that has been successfully applied at an industrial scale.

There are number of factors in effect during SAS processing. These factors can be grouped into two main categories; formulation related, and process related. In order to design a robust SAS process, it is extremely important to understand the impact of all of these variables on the desirable SAS product attributes, such as particle morphology, particle size, particle size distribution, and % yield of the process. Although several researchers have studied these variables, there is widespread disagreement amongst them. Hence, the goal of the studies shown in this dissertation is to address these gaps in the literature by carrying out a screening design of experiment (DOE), where 7 factors were studied, at 2 levels each, for their impact on particle size, particle size distribution, and process yield. A $2^{(7-3)}$ fractional factorial

design of 16 experiments, plus 3 center point runs, for a total of 19 experiments, was performed. The factors that impacted the particle size the most were the nozzle diameter, temperature, and spray rate of liquid, in the order of decreasing importance. In case of particle size distribution, nozzle diameter, spray rate of liquid, drug concentration, pressure, and polymer concentration played significant roles. The yield was affected by polymer concentration, pressure, and the drug concentration. Additionally, we were able to find optimum processing and formulation variables, which would consistently deliver product of high yield (~90%), small particle size (d_{50} of ~ 0.4 μm), and narrow particle size distribution.

Further, we prepared and compared the physical and physicochemical characteristics of griseofulvin-polymer composite particles produced via three different methods: (1) supercritical antisolvent (SAS) process, (2) spray-drying process, and (3) the conventional solvent evaporation process. The polymers used were Kollidon® VA64, HPMCAS-LF, and Eudragit® EPO. Particle properties were analyzed using scanning electron microscopy, powder X-ray powder (PXRD), differential scanning calorimetry (DSC), and Fourier transform infra red (FTIR). Particle size and particle size distribution measurements were made using Malvern laser diffractometer. The dissolution behavior of pure API and solid dispersions were compared. Amorphous solid dispersions of spherical shapes were obtained, independent of the type of polymer used, when spray drying process was used. FTIR spectra indicated the formation of hydrogen bonding between the drug and polymers, during spray drying process. Whereas, the drug remained in its crystalline form when the processing method was SAS or conventional solvent evaporation, and there was no hydrogen

bonding for these formulations. The griseofulvin particles used as unprocessed starting material had a mean diameter of approximately 12 μm with a size distribution range between 5-20 μm. With the spray drying or SAS process, and using any of the three hydrophilic polymers, *in-situ* nanoparticles with the mean particle size of 0.3 to 0.5 μm were obtained. These nanoparticles were associated with improved dissolution performance compared with unprocessed crystalline griseofulvin.

In conclusion the physicochemical properties and dissolution of crystalline griseofulvin could be improved by physical modification such as particle size reduction using SAS process, and generation of amorphous state using spray-drying process.

ACKNOWLEDGMENTS

I would like to express my deepest appreciation to my major professor, Dr. M. S. Kislalioglu, who not only provided me the constant guidance, but she is the most caring, and kind human being, I have ever met in my life. I genuinely appreciate her patience, and ready availability for consultation.

I would also like to thank my mentors at Hoffmann La Roche, Dr. Harpreet Sandhu, Dr. Waseem Malick, and Dr. Navneet Shah. They taught me to think outside the box, and be courageous in research and in life. Without their support, and guidance this dissertation would not have been possible. I would like to thank Hoffmann La Roche company for supporting me by paying the tuition during the course of my PhD studies. It was nothing short of an honor to work with renowned Scientific team of PARD at Roche. I especially would like to thank Mr. Bharat Patel, Mr. Daniel Masaka, and Dr. Petra Inbar for sharing their knowledge and resources with me.

I am sincerely grateful to my dissertation committee member, Dr. David Worthen, whose positive attitude towards life constantly reminded me that there is life at the end of long tunnel of graduate studies!

I am also grateful to my parents Mr. Dinesh Sheth and Mrs. Usha Sheth, for encouraging and supporting me to come to come to USA. I cannot thank enough for the loving support of wife, Nomisha. She always stood by me and carried on a responsibility of a mom and a dad, while I was burning mid night oil. Aarush and Arnav: all the soccer games that I missed in last several years, I will make it up!

PREFACE

This dissertation has been written in the manuscript format. It includes three manuscripts. Manuscript 1 has been published in the journal of *Current Drug Delivery*. Manuscript 2 and 3 are written in the format required by the *Journal of Pharmaceutical Sciences*.

Manuscript 1: Nanoparticles in the pharmaceutical industry and the use of supercritical fluid technologies for nanoparticle production

Manuscript 2: Engineering of nano- and micro-particles of griseofulvin by supercritical antisolvent precipitation (SAS) process

Manuscript 3: Comparing physico-chemical properties of griseofulvin coprecipitates prepared by supercritical antisolvent method, conventional solvent evaporation method, and spray drying method.

TABLE OF CONTENTS

LIST OF TABLES

Manuscript 1

Manuscript 2

Manuscript 3

TABLE **PAGE**

APPENDICES

TABLE **PAGE**

LIST OF FIGURES

Manuscript 1

FIGURE **PAGE**

Manuscript 2

FIGURE **PAGE**

Manuscript 3

APPENDICES

TABLE **PAGE**

MANUSCRIPT 1

Published in Current Drug Delivery, Volume 9, Number 3, May 201 , pp. 269-284

Nanoparticles in the pharmaceutical industry and the use of supercritical fluid technologies for nanoparticle production

Pratik Sheth[a,b], Harpreet Sandhu[a], Dharmendra Singhal[a], Waseem Malick[a], Navnit Shah[a], and M.S. Kislalioglu [b, *]

[a]Hoffman-La Roche, Inc., 340 Kingsland street, Nutley NJ 07110 USA,

[b] Department of Biomedical & Pharmaceutical Sciences, University of Rhode Island, 41 Lower College road, Kingston RI 02881

[*] Corresponding author. Department of Biomedical & Pharmaceutical Sciences, University of Rhode Island, 41 Lower College road, Kingston RI 02881 Tel: (401) 874 5017, email address: Skis@uri.edu

Abstract

Poor aqueous solubility of drug candidates is a major challenge for the pharmaceutical scientists involved in drug development. Particle size reduction appears as an effective and versatile option for solubility improvement. Nanonization is an attractive solution to improve the bioavailability of the poorly soluble drugs, improved therapies, *in vivo* imaging, *in vitro* diagnostics and for the production of biomaterials and active implants.

In drug delivery, application of nanotechnology is commonly referred to as Nano Drug Delivery Systems (NDDS). In this article, commercially available nanosized drugs, their dosage forms and proprietors, as well as the methods used for preparation like milling, high pressure homogenization, vacuum deposition, and high temperature evaporation were listed. Unlike the traditional methods used for the particle size reduction, supercritical fluid-processing techniques offer advantages ranging from superior particle size control to clean processing.

The primary focus of this review article is the use of supercritical CO_2 based technologies for small particle generation. Particles that have the smooth surfaces, small particle size and distribution and free flowing can be obtained more, via few SCF techniques. In almost all techniques, the process variables involved may be of thermodynamic and aerodynamic nature and the result of the design of the particle collection environment.

Rapid Expansion of Supercritical Solutions (RESS), Supercritical Anti Solvent (SAS) and Particles from Gas Saturated Solutions (PGSS) are three groups of processes

which lead to the production of fine and monodisperse powders. Few of them may also control crystal polymorphism. Among the aforementioned processes, RESS involves dissolving a drug in a supercritical fluid (SCF) and passing it through an appropriate nozzle. Rapid depressurization of this solution causes an extremely rapid nucleation of the product. This process has been known for a long time but its application is limited. Carbon dioxide, which is the only supercritical fluid that is preferentially used in pharmaceutical processes, is not a good solvent for many Active Pharmaceutical Ingredients (API). Various researchers have modified the RESS process to overcome its solubilizing limitations, by introducing RESOLV, RESAS, and RESS-SC. Overall, all RESS based processes are difficult to scale up.

The SAS processes are based on decreasing the solvent power of a polar organic solvent in which the substrate (API & polymer of interest) is dissolved, by saturating it with carbon dioxide (CO2) at supercritical conditions. CO2 causes precipitation and recrystalization of the drug. SAS is scalable and can be applied to a wide variety of APIs and polymers. Minor modifications of basic SAS process include GAS, ASES, SAS-DEM and SAS-EM. Processes where SCF is used as an anti solvent and dispersing agent include SEDS, SAA, and A-SAIS. The mechanisms and applications of these processes were briefly discussed. In PGSS, CO2 is dissolved in organic solutions or melted compounds and it is successfully used for manufacturing drug products as well as for drying purposes. The two widely used methods, PGSS-drying and CAN-BD SCF, were also included in discussions.

Among the limitations of the techniques involved, the poor solvent power of CO2, the cost and necessity of voluminous usage of the CO2 can be mentioned. There is still confusion in contribution of each variable on the particle morphology and properties, regardless of the number of mechanistic studies available. The advantages of especially SAS and PGSS based techniques are production of the nano or microsized spherical particles with smooth surfaces and narrow particle size distribution. However, the reasons of why 25 years of active research, and more than 10 years of process development, could not promote the use this technology and produced only few commercial drug products were clarified.

Key Words
Nanoparticles, Supercritical fluid, RESS, SAS, SEDS, PGSS

Abbreviations

BCS: Bio-pharmaceutics Classification System; SCF: Supercritical fluid; scCO2: Supercritical carbon dioxide; SEM: Scanning Electron Microscope; RESS : Rapid Expansion from Supercritical Solvent; RESOLV : Rapid Expansion of a Supercritical Solution into a Liquid Solvent; RESAS: Rapid Expansion from Supercritical to Aqueous Solutions; RESS-SC: Rapid Expansion from Supercritical Solvent ; GAS: Gas Antisolvent Process; SAS: Supercritical Antisolvent Process; ASES: Aerosol Solvent Extraction System; SAS-DEM: Supercritical Antisolvent Drug Excipient Mixing; SAS-EM: Supercritical Antisolvent Enhanced Mass transfer; SAA: Supercritical-Assisted Atomization; A-SAIS: Atomization of Supercritical Antisolvent Induced Suspensions; SEDS : Solution Enhanced Dispersion by

Supercritical fluids; PGSS: Particles from Gas Saturated Solutions; CAN-BD: Carbon dioxide Assisted Nebulization with a Bubble Dryer

1.0 INTRODUCTION

Although there are hundreds, thousands of new drug molecules being discovered and formulated day by day, very few of them reach commercialization. One of the most important reasons for the failure is the poor aqueous solubility of the drug substances. By various estimates up to 40 per cent of new chemical entities (NCEs) discovered by the pharmaceutical industry are poorly soluble or highly lipophilic compounds. Although many drugs do have adequate pharmacodynamic or target activity, due to poor solubility, these drugs are not absorbed by the body causing poor bioavailability. Today, nanonization may help drug substances to be actively targeted to the site of action, or directly taken by the cells and for delivery of the genes. However, their application for solubility enhancement is the most frequently applied reason. Reduction of the particle size of the poorly soluble drugs to nano scale increases their dissolution rate, saturation solubility, and in turn, the oral bioavailability; therefore, nanonization is becoming a very popular process enabling the use of such drugs [1-4].

The effect of nanonization on solubility improvement of a drug substance can be explained by modified Noyes Whitney equation [5] which demonstrates the relationship among the rate of dissolution and solubility as well as the surface area and particle size of a given drug substance. On the other hand, Kelvin equation [6, 7] helps us to understand the physics behind the particle size effect on saturation solubility when the particle size is reduced to nano scale. The Kelvin equation may be written as;

$$\ln \frac{p}{p_0} = \frac{2\gamma V_m}{rRT}$$ Eq. (1)

where p is the actual vapor pressure, p_0 is the saturated vapor pressure, γ is the surface tension, V_m is the molar volume, R is the universal gas constant, r is the radius of the droplet, and T is temperature.

Kelvin equation mathematically describes that, the vapor pressure of lipid droplets in a gas phase (aerosol) increases with an increase in the curvature of the surface of the dispersed phase which is realized by the particle size reduction of such a system. The vapor pressure is equivalent to the dissolution pressure. In the state of saturation solubility, there is equilibrium between the molecules dissolving and molecules recrystallizing. This equilibrium can be shifted when the particle size is reduced, which causes an increase in the dissolution pressure by increasing the saturation solubility.

2.0 USE OF NANOTECHNOLOGY BY THE PHARMACEUTICAL INDUSTRY

Since 1990s, nanotechnology continues to gain popularity not only in the health care industry but in many other industries such as information and communication, energy production, food and agriculture, aerospace, construction etc. The term nanotechnology is used for any system of producing structures or devices in the nanometer range (1 nm=one thousand millionth of a meter, 10^{-9} m). Generally, size range of the nanoparticles fall between 1-100 nanometers. In some drug delivery systems, this range may exceed the nanosizes, while it is still being considered as

nanoparticles. Application of nanotechnology in health care arena is by far the most promising and beneficial for drug delivery, improved therapies, *in vivo* imaging, *in vitro* diagnostics and for production of biomaterials and active implants. In drug delivery application of nanotechnology is commonly referred to as Nano Drug Delivery Systems (NDDS).

Examples of commercially available NDDS are given in Table **1** which includes liposomes, nanosuspensions, nanoemulsions, polymer drug or polymer protein conjugates, dendrimers, fullerenes, carbon nanotubes, and inorganic nanoparticles. Liposomes are spherical lipid bilayers from 50 nm to 1000 nm in diameter that serve as convenient delivery vehicles for biological compounds. Dendrimers are spheroid or globular nanostructures that are precisely engineered to carry molecules encapsulated in their interior void spaces or attached to the surface. Fullerenes is form of carbon nanomaterials that can be functionalized and derivatized with a wide array of molecules that allow them to be used in medical and healthcare applications. The makers and the users of NDDS claim that, nanonization reduces the side effects of the drugs; improve efficacy and therapeutic effectiveness in disease stages that currently cannot be treated with conventional drugs. Interest of the pharmaceutical industry in NDDS is increasing worldwide [8-9]. There are several companies ranging from start up to a large corporations currently working in the field of NDDS, across the world.

Table 1: Commercially available nanotechnology based products.

Product Name	NDDS, Technology, dosage form & Route of administration	Therapeutic effect	Name of company & country
Abelcet	Liposomes for injection	Anti-fungal	Enzon, USA
Ambisome,	Liposomes for injection	Anti-fungal	Gilead/ Astellas, USA
Amphotec	Liposomes for injection	Anti-fungal	Three Rivers Pharmaceuticals, USA
Daunoxome	Liposomes for injection	Anti-cancer (Kaposi's sarcoma)	Gilead, USA
DepoCyt	Liposomes for injection	lymphomatous meningitis	SkyePharma, Enzon UK/USA
Doxil/Caelyx	Liposomes for injection	Anti-cancer (ovarian) (Kaposi's sarcoma,	ALZA, Schering Plough USA
Epaxal	Liposomes for injection	Vaccine against Hepatitis A	Berna Biotech AG Switzerlan
Estrasorb	Liposomes-by topical	To treat symptoms of menopause	Novavax
Inflexal	Liposomes for injection	Vaccine against Influenza	Berna Biotech AG Switzerlan
Myocet	Liposomes for injection	Anti-cancer	Elan, Ireland

		(Breast)	
Visudyne	Liposomes for injection	Wet macular degeneration in conjuction with laser treatment	QLT, Novartis Canada/Switzerland
Triglide	Nanosuspension by IDD solubilisation technology-tablets for oral	Anti/Hypo lipidemic	Skye Pharma/First Horizon Pharma USA
Emend	Nanosuspension by NanoCrystal® technology -Capsules for oral	Anti-emetic (during cancer chemotherapy)	Elan/Merck & Co., Ireland/USA
Megace ES	Nanosuspension by NanoCrystal® technology –Suspension for oral	Anorexia, Cachexia	Elan/Par, USA
Rapamune	Nanosuspension by NanoCrystal® technology –suspension/tablet for oral	Immunosuppressant	Elan/Wyeth Ireland/USA
Tricor	Nanosuspension by NanoCrystal® technology -tablets for oral	Anti/Hypo lipidemic	Elan/Abbott USA
NanoXosan 30	Nanoemulsion –by topical	Dermatological application	Biofrontera, Germany

Renagel	Polymeric Drug Conjugates-for injection	Kidney Failure	Genzyme, USA
Xyotax	Polymer drug conjugates-for injection	Anti-cancer (lung)	Cell Therapeutics, Inc
Adagen	Polymer Protein Conjugates- for injection	Treatment of immunodeficiency diseases	Enzon, USA
Copaxone	Polymer Protein Conjugates- for injection	Treatment of Multiple Sclerosis	TEVA, Israel
Macugen	Polymer Protein Conjugates- for injection	Treatment of Age-related macular degeneration	Eye Tech Pharmaceuticals/Pfizer USA
Neulasta	Polymer Protein Conjugates- for injection	Febrile Neutropenia	Amgen, USA
Oncaspar	Polymer Protein Conjugates- for injection	Treatment of Leukemia	Enzon, Sanofi-Aventis USA/France
PEGASYS	Polymer Protein Conjugates- for injection	Treatment of Hepatitis C	Roche-Nektar Switzerlan/USA
PEGINTRON	Polymer Protein Conjugates- for injection	Treatment of Hepatitis C	Enzon, Schering-Plough USA
Somavert	Polymer Protein Conjugates- for injection	Treatment of Acromegaly	Nektar, Pfizer, USA

Abraxane	Protein (Albumin) bound nanosuspension for injection	Anti-cancer (breast)	Celgene, USA
MagNaGel	Targeted Nanoparticle	Diagnosis & treatment of cancer	Alnis Bioscience, Inc USA

3.0 METHODS USED FOR PARTICLE SIZE REDUCTION TO "NANO" SCALE

A major challenge in reducing the particle size of solids to nano scales is the accurate control of the size and shape, which in turn is directly linked with the nano materials processing method. There are two approaches generally used to reduce particles to nanosizes: bottom-up and top-down methods. In the bottom-up approach a colloidal solution of drug is prepared and the solvent is evaporated obtaining controlled rearrangement of single atoms and molecules into larger nanostructures. Supercritical fluid based technologies utilize this approach. The top-down approach reduces the particle size of drug particles using media milling or high pressure homogenization, or similar alternative methods. Table **2** provides an overview of industry leaders in each of these technologies.

Table 2: Approaches for forming nanoparticle, current industry leaders and their patented technologies**.**

Different approaches for nanoparticle preparation		**Company name (patented technology)**	
TOP DOWN	Media milling [3]	**1.** Elan Drug Technologies (NanoCrystal®)	
	High Pressure Homogenization [2, 10]	**2.** Drug Delivery Services	**3.** Avestin (Emulsiflex®)
		4. Baxter (Nanoedge®)	**5.** Solvay/Abbott
		6. Pharmasol (Nanopure®)	**7.** Soliqs/Abbott (Nanomorph™)
		8. Skye Pharma (IDD™)	**9.** Bend Research, Inc
		10. Novartis (Hydrosol™)	
BOTTOM-UP	Wet Chemical Process (e.g. Supercritical fluid technology)	**11.** Nektar	**12.** PiereFabre (Formuplex®, Formuldisp®, Formulcoat®)
		13. Lavipharm (Infuse-X ™)	**14.** Phasex
		15. Eiffel technologies	**16.** Xspray
		17. RxKinetics	**18.** Alcon
		19. Eurand	**20.** Aphios
		21. Crititech/University of Kansas	**22.** Thar
		23. Crystec	**24.** Activery
		25. Ferro Corp (SFEE)	
	Gas Phase Synthesis (flame pyrolysis, laser ablation, high temperature evaporation) [11 - 13]	**26.** Johnson Matthey Technology Centre, UK	**27.** Particular GmbH
Alternative approaches	Lithography, vacuum deposition, etc [14]	**28.** DENA	**29.** Many academic interests

This article focuses on supercritical fluid use as a method of choice for producing nanoparticles.

4.0 SUPERCRITICAL FLUIDS (SCF)

"Supercritical" is a state of a substance above its critical temperature (TC) and critical pressure (PC). A substance in its supercritical state is defined as Supercritical Fluid (SCF). The critical point represents the highest temperature and pressure at which the substance can exist as a vapor and liquid in equilibrium.

In the supercritical stage, there is no phase boundary between the gas phase and the liquid phase. In short, it can behave as if it is a liquid or a gas, but is actually neither.

The properties of SCF are in between that of gas and liquid. The densities of a substance in its supercritical state are either the same or close to that of same substance in its liquid state. This property allows SCF to enhance solubility of poorly soluble drugs more than the gaseous state could. On the other hand, the diffusivity and viscosity of SCF are close to that of gas; which allow rapid mass transfer or penetration of SCF into materials than that of the liquid states.

SCFs are highly compressible, particularly near the critical point, and their density and thus the solvation power can be carefully controlled by small changes in temperature and/or pressure [15, 16]. Although these unique and complementary physical characteristics allow the development of efficient and versatile processes, the SCFs are not universal "super-solvents". Very few drug substances are soluble in SCFs without the aid of a cosolvent.

Although all gases could reach supercritical state above their critical point, for many, extremely high pressure and temperatures which may not be suitable for pharmaceuticals may be required. The critical P, T values increase with the molecular weight or intermolecular hydrogen bonding and/or polarity. One must also consider the safety and affordability in addition to mild processing conditions, when choosing the SCF. For example, Xenon and Sulfur hexafluoride (when sufficiently purified) have low critical values, but remain too expensive for commercial use. Gases such as Nitrous oxide or ethane have low critical values, but can generate explosive mixtures and are therefore unsafe to handle. Trifluoromethane, which is chemically inert and nonflammable, has low toxicity and a low critical temperature and pressure. Furthermore, trifluoromethane has a strong permanent dipole moment (1.56 D), which helps solubilization of pharmaceutical compounds. However, carbon dioxide is the most preferred SCF for processing of pharmaceuticals including heat sensitive material such as biologicals. It has low critical temperature (31.2 °C) and pressure (73.8 bar or 7.4Mpa) and is nonflammable, nontoxic and environmentally safe.

4.1 Solubility of pharmaceutical compounds in supercritical carbon dioxide

Even though the mechanism of particle formation in different SCF based technologies is different, they all rely on either the solubility or insolubility of the solute (drug &/or polymer) in scCO2. Hence, determining the solubility of a solute of interest in scCO2 is important in choosing the SCF technology. This can be done experimentally or via theoretical estimation. The solubility of a pure solid component

(2) in a supercritical fluid (1) can be expressed as a function of the operating pressure P and temperature T, as described in Equation (2)

$$y_2 = \frac{p_2^{SAT}}{p}\frac{1}{\phi_2^G}\exp\left[\frac{v_2^S(p - p_2^{SAT})}{RT}\right] \qquad \text{Eq. (2)}$$

where y_2 is the equilibrium mole fraction of the solid component (2) in the supercritical fluid phase, P_2^{SAT} is the saturated vapor pressure of the solid component (2) at temperature T, R is the universal gas constant, p is the operating pressure, Φ_2^G is the solute fugacity coefficient in the supercritical fluid phase, and v_2^S is the solute molar volume of the solid component (2). The solute fugacity Φ_2^G is calculated by the equation of state (EOS) with T, P, and the concentration. Several EOSs are available in the literature for calculating the fugacity coefficient of the solid in a supercritical fluid. The Peng–Robinson equation of the state is one of the equations commonly used to evaluate the fugacity coefficient at a high pressure. Physical properties of the solute, such as the critical temperature T_c, critical pressure P_c, and acentric factor ω for high molecular weight compounds can be found in the literature.

By controlling the pressure and the temperature, the density and solvent strength of SCF can be altered to simulate organic solvents ranging from chloroform to methylene chloride to hexane. scCO2 is a relatively non polar solvent, therefore if a compound is soluble in hexane, it should also dissolve in scCO2. It is also possible to modify the solvation power of a particular SCF by incorporating a small amount of volatile cosolvent, like acetone or ethanol.

When scCO2 is used as an anti-solvent, the key to particle production is generally the super saturation of the solution of materials via the counter-diffusion of scCO2 and the solvent. The insolubility of the solute in scCO2 influences the degree of this super saturation.

5.0 APPLICATIONS OF SCF BASED TECHNOLOGIES IN THE PHARMACEUTUCAL INDUSTRY

SCF based technologies are extremely flexible. Some applications are already at industrial capacity, whereas others remain under development. They include particle formation, extraction of trace amounts of organic solvent from the drug substances, impregnation of drug into polymer, coating, and reactive systems such as hydrogenation, biomass gasification, and supercritical water oxidation. Table **3** lists some of the well documented pharmaceutical applications of SCF technologies. However, this review article focuses on its use for nanoparticle production.

Table 3: Pharmaceutical applications using supercritical fluid technologies.

Pharmaceutical & Biomedical Applications	**Reference**
Particle formation/particle size reduction (micron and nano scale)	[17-23]
Residual organic solvent stripping (for drying purposes)	[24-27]
Impregnation of drug into polymer to prepare solid dispersion	[28-30]
Encapsulation, coating	[31-33]
Polymer processing (eg. Extrusion)	[34-42]
Liposome preparation	[43]
Inclusion complexes (eg. Cyclodextrin)	[44]
Product sterilization	[45-47]
Extraction and purification	[48, 49]
Nanostructured materials for biomedical applications and tissue engineering	[50-53]

6.0 SCF TECHNOLOGIES THAT ARE USED FOR PARTICLE PRODUCTION

Conventional techniques for particle size reduction include mechanical processes like crushing, grinding, and milling, recrystallization of the solute particles from their solution by using liquid antisolvents, freeze-drying, and spray-drying. Many of these processes require the use of organic solvents which introduce extra problems like removal of trace amounts of such solvents from the products and their proper disposal for environmental safety. In addition, the high energy and high temperatures involved in these processes may lead to thermal and chemical degradation of some of the drugs and ingredients. Therefore, a method that particulates a drug substance in a cGMP compliant manner, which produces controllable particle properties, and requires minimal downstream processing is definitely the most suitable method for manufacturing a wide range of therapeutic agents [16,38].

Several review articles [23, 38, 39, 54-66] already described supercritical fluid based technologies. Different authors have used different techniques to overcome various challenges faced in controlling the particle size and morphology. A wide variety of organic and inorganic materials have already been successfully processed in the form of nanoparticles employing the supercritical fluids as solvents or as antisolvents. Perrut and Jung [56] and Thakkar et al [66] provided excellent summaries of large variety of pharmaceutical compounds being micronized or nanonized by the use of SCF based technologies. Kiran [39] provided a review of polymer solutions at high pressures with a focus on miscibility, phase separation and morphological modifications in supercritical or compressible dense fluids. The present review is

complementary to such reviews appeared in the literature. It provides a critical version on the current state of nano particle formation and compares their advantages and disadvantages.

Table **4** provides a broad classification of SCF based technologies. The main difference amongst these processes is the role a SCF, whether it acts as a solvent or an anti-solvent or as a solute, in formation of the particles. These technologies are further modified based on the particle growth mechanisms and their collection environment. There are many more modified processes which are not described in this review article as they have not created a wide interest in the production of drugs or drug products.

Table 4: SCF technologies used for particle formation.

Process Acronym	Role of Supercritical fluid	Role of Organic solvent (if used)	Mode of Phase separation
RESS/RESOLV/RESAS/RESS-SC	Solvent	Cosolvent	Pressure/Temperature induced
GAS/SAS/ASES/SAS-DM/SAS-EM	Antisolvent	Solvent	Solvent induced
SEDS/SAA/A-SAIS/CAN-BD	Antisolvent/ dispersing agent	Solvent/non-solvent	Solvent induced
PGSS	Solute		Pressure/temperature/ solvent induced

7.0 INFLUENCE OF OPERATING PARAMETERS

In almost all of the SCF processes ,the morphology (crystalline, amorphous, or both), the particle size, shape and distribution of the resulting product depend on factors like the properties of the material [67, 68], the process variables i.e. the thermodynamic and aerodynamic factors [69-79], and to the design of the particle collection environment [22]. Among the thermodynamic factors temperature, pressure conditions, rate of addition of one component to another and, phase and composition changes during the expansion can be listed. The aerodynamic factors include impact distance of the jet against a surface, nozzle geometry and mechanical shear that a particle undergoes. Table 5 summarizes these functional variables, which affect the properties of the finished product in almost all SCF processes.

Table 5: Material and process variables in SCF based processes that affect formation of particles with desired properties

Material properties	Process variables	Desired outcomes
Properties of Drug Substance: Chemical structure, m.p., Tg, [74]	Thermodynamic properties [71,73]: Temperature [70], Pressure, Phase ratio/composition [67,68], Rate of addition of one component to another	Spherical/fibrous particles Crystalline/amorphous particles Micro/Nano scale particles
Properties of Polymer: Chemical structure, m.p., Tg,	Aerodynamic properties: Nozzle geometry [70], impact distance of jet against a surface, Expansion volume	
Solubility or insolubility in scCO2	Particle collection environment	
Solubility in co-solvent	Reduced agglomeration of particles during expansion	

There are several studies carried out to predict the factors involved in the particle formation, size and properties and to correlate particle morphology with the processing parameters for RESS processes. Kwauk and Debenedetti [70] proposed a mathematical model of aerosol formation. They argued that the particle size was highly responsive to the temperature at which the solute is dissolved in the

supercritical fluid (the extraction temperature), and the temperature to which the saturated mixture is preheated isobarically prior to expansion (the pre-expansion temperature). Reverchon and Pallado [71] proposed a hydrodynamic modeling for the same process. The expansion process was subdivided into three successive steps - at the nozzle inlet, along the nozzle itself, and in the expansion chamber. Three thermodynamic transformations, one for each step of the expansion process, were considered. This also appears to be a successful model since the computed values compared reasonably well with the experimental data.

Hirunsit et al's [72] mathematical model concentrated on the wall friction in the nozzle and heat exchange with the surrounding in the supersonic free jet region. They tested their model experimentally by producing ibuprofen particles using RESS process. Turk [73] demonstrated that the nucleation rate was highly responsive to the solubility of the drug and the unknown surface tension group. He argued that the classical nucleation theory was sufficient to describe the particle formation in RESS experiments. Influence of the thermodynamic behavior and solute properties on the homogeneous nucleation in the supercritical solutions in RESS applications were also theoretically studied [74, 75].

Similar issues were also of interest in SAS applications. Lengsfield et al [76] investigated the atomizing pattern of the jets. Their modeling stressed that the microparticle formation resulted from nucleation and growth of the gas phase within the expanding plume, rather than nucleation within discrete liquid droplets. Werling and Debendetti [77] developed a model to describe the two-way isothermal diffusion between a solvent and a dense gas antisolvent at conditions that are supercritical with

respect to the solvent–antisolvent mixture. The extent of droplet swelling or shrinking as a function of temperature and pressure was correlated to the difference in density and diffusivity between the solvent-rich and antisolvent-rich regions. The difference created in the droplet behavior at subcritical and supercritical conditions and their implications for particle production was also studied by the same researchers [77]. They concluded that supercritical conditions results in faster mass transfer suggesting that in the presence of a solute, in supercritical operations causes a higher degree of droplet super-saturation, resulting in higher nucleation rates and smaller particles.

Reverchon et al. [78], in their highly critical review, summarized the results obtained in a great number of studies. Like Lengsfeld et al., they stressed that the particle formation by supercritical antisolvent precipitation is based on the competition between the jet break up and liquid surface tension vanishing characteristic times. They argued that spherical particles are the result of droplet drying after effective atomization of the liquid solution. At a pressure greater than critical pressure, the particle formation mechanism is in competition with the surface tension vanishing followed by the formation of a gas plume. When the latter mechanism prevails, atomization is not obtained and the nanoparticles are produced by precipitation from the fluid phase. The same group further demonstrated the proposed mechanism via in situ laser scattering techniques. They were able to study the location of first particle precipitation inside the vessel, the partial densities of all species in the system, the super-saturation, and overall mixture composition [79].

Reverchon et al.[78], also tabled a large number of published work and listed drugs that were obtained in micron sizes with SCF, at different processing conditions. They

sought relationships among the solute concentration, the vessel temperature, the pressure inside the vessel, and molar fraction of CO2 (X_{CO2}). Upon studying the data available, they have concluded that the X_{CO2} larger than approximately 0.95 -0.97 is the most useful ratio for small particle production. At this condition, the binary mixture of CO2 and liquid organic solvent achieves the mixture critical point (MCP). The effects of solute concentration, the pressure and the temperature on the particle size and morphology were difficult to generalize, because data available was contradictory.

Although each study has emphasized, the effects of one or two variables that are the most critical in obtaining small particles, due to the complexity of the procedure, there is not a published work which takes into account, expansion in the nozzle and in the jet, along with nucleation, growth, and agglomeration in addition to the factors mentioned above.

8.0 OPERATIONS WHERE SCF ACTS AS SOLVENT

Rapid Expansion from Supercritical Solvent (RESS) [54, 57, 61, 62, 64]: This process is schematically illustrated in Fig. (1) The process is used when the solute (polymer, drug or drug-polymer matrix) freely dissolves in the supercritical fluid. The process involves saturation of the supercritical fluid with drug or drug-polymer matrix, followed by depressurization of the solution by passing through a heated nozzle into a low pressure chamber. The rapid decompression of the supercritical fluid containing the drug drives nucleation and particle formation. While the pressure is relieved, the solution experiences a Joule Thompson cooling due to large volumetric expansion.

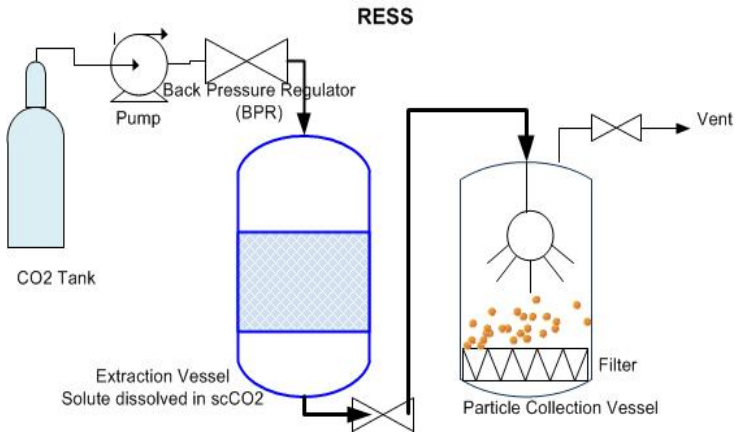

Fig. (1). Simplified schematic representation of **RESS** equipment set up showing different component such as CO2 tank, pump, back pressure regulator, extraction vessel and particle collection vessel.

Mishima and Matsuyama [80] patented a RESS process where an agitator was used in the extraction vessel. They prepared the solution of core and coating material in a supercritical fluid and the solution was expanded rapidly through a nozzle. Thus,

when the solvent power of supercritical fluid was dramatically decreasing, it resulted in the co-precipitation of both substances. However, the process caused heterogeneous dispersion of the drug in the coating material and necessitated the use of a surfactant. In order to avoid the heterogenity problem, the authors proposed the use of a high-pressure apparatus equipped with a column agitator, which can perform high shear mixing of the scCO2, drug particles and the polymer. The column agitator was equipped with holes which facilitated circulation of mixture inside the extraction vessel. The agitating column forced the materials to move towards the inner wall of the vessel, and the shear stress between the column agitator and the inner wall accelerated dispersion of the drug particles in the polymer solution. Fig**. (2)** provides a schematic illustration of the proposed column agitator device.

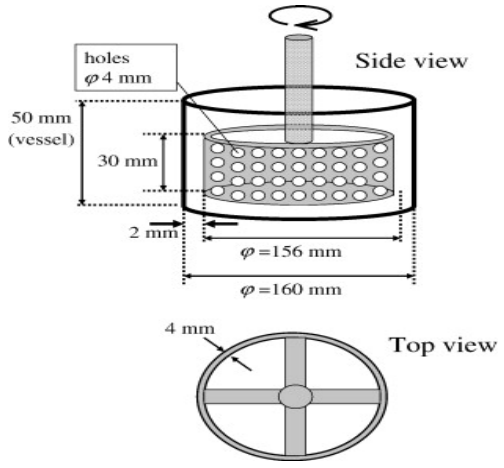

Fig. (2). Schematic diagram of column agitator [80].

In any of the SCF based particle formation techniques, preserving the particle characteristics such as morphology and size is very critical; therefore, the particle collection is an important task. Particle agglomeration is a common problem found during RESS process which is worsened if residual amount of co-solvent remained in

the processed material. Researchers have used different particle collection environments in order to overcome the agglomeration problems which will be presented in the following section of this article.

8.1 Advantages and limitations of RESS

RESS is an attractive method since it is a single step process which requires minimum to no organic solvent, and can be implemented relatively easily at least at a small scale. During the rapid expansion, the solute experiences both the pressure and temperature quenches simultaneously that enhance the precipitation process considerably.

However, RESS process is only applicable to those solutes which exhibit good solubility in scCO2. Majority of the poorly soluble active pharmaceutical ingredients (APIs) have high molecular weights and polar bonds, and are excellent candidates for nanoparticle preparation. Unfortunately, many of them have low to negligible solubility in scCO2 at moderate temperatures (less than 60 °C) and pressures (less than 300 bar). Co-solvents, such as methanol, may be added to carbon dioxide to enhance solubility of the drug. However, such applications will alter environmentally safe nature of the RESS process. The need for removal of residual organic solvents will further increase the cost and complexity of the process.

8.2 Summary of RESS applications for production of spherical nanoparticles

Over the last 2 decades, RESS technology has been successful in the production of nano sized particles of drugs and polymers [38, 56, and 66]. Various modeling studies of RESS were summarized under section 8.0. In this section, few examples from the literature will be provided in order to illustrate the versatility in processing conditions

and show how the researchers have modified the basic RESS process in order to avoid agglomeration problems. It is postulated that due to the fast motion between the solid particles and gas present in the expansion chamber, electrostatic charges that develop on the particle surfaces can be the reason of particle agglomeration which occurs during expansion process. Subsequently, needle like or fibrous particles can form instead of desired spherical particles [63].

Gaddermann et al. [81] produced pure naproxen nanoparticles and coated naproxen with polylactic acid using RESS. The authors demonstrated that the polylactic acid coating, stabilized the naproxen nano particles against agglomeration and coagulation. Using this technique, Varshosaz et al. [82] produced amorphous cefuroxime axetil (CFA) nanoparticles. They studied impact of the of nozzle temperature (changing between 50–70 °C) and the extraction port temperatures (changing between 60–90 °C), on the particle morphology and size. Amorphous particles having an average size of 159 nm were obtained at the nozzle temperature of 60 °C and the extraction temperature at 90 °C. When the temperatures of the nozzle and the extraction column were decreased to 50 °C and 75 °C respectively, the particle size was increased to 465 nm. Reverchon et al. [83] showed the similar effects of both the pre-expansion and the expansion chamber temperature by working with salicylic acid crystals.

There are several variations of the basic RESS process which were designed to minimize the agglomeration problems (Table 5). Amongst these, Rapid Expansion of a Supercritical Solution into a Liquid Solvent (**RESOLV)** [22] and Rapid Expansion from Supercritical to Aqueous Solution (**RESAS)** [84, 85] are the most notable ones.

In RESOLV, the traditional RESS is modified by expanding the supercritical solution into a liquid solvent instead of ambient air. Pathak et al. [22] demonstrated that RESOLV technique can successfully produce individual and spherical particles of naproxen and ibuprofen in nanoscales when they expanded the product into aqueous solution containing PVP as a polymer. Without PVP, the particles obtained were nanosized, but agglomerated and non-spherical. Mechanistically, the liquid at the receiving end of the rapid expansion in RESOLV, suppresses the particle growth in the expansion jet, thus allows nano sized and round particle production.

In RESAS processes, expansion of supercritical solution through an orifice or tapered nozzle into aqueous solution containing a stabilizer(s) is used. This arrangement minimizes the particle agglomeration during the free jet expansion. The stabilizers utilized are mainly surfactants like, polysorbates, poloxamers and lecithins or hydrophilic polymers. Presence of a stabilizer minimizes the particle aggregation by rapidly reducing the surface free energy of the primary particles generated and via steric stabilization [84]. Tozuka et al. [85] successfully used 1% polyvinyl alcohol (PVA) for the same protective effect to produce indomethacin nanocrystals of 300-500 nm, via RESAS process.

In order to overcome the low solubility of polar drugs in the SCF solvent, Thakur and Gupta [86] proposed a modified RESS process that used a solid cosolvent (**RESS-SC**). They tested this process for nanoparticulating phenytoin by the use of menthol, utilized as the solid cosolvent. In the conventional RESS process, each particle is surrounded by the same drug particles in the expansion zone that results in coagulation and formation of larger particles, as illustrated in Fig. **3 (a)**. In the RESS-

SC process, the drug particles were surrounded by particles of solid cosolvent like menthol . Hence, the particle growth could be minimized in the expansion zone resulting in smaller nanoparticles as schematically illustrated in Fig. **3 (b).** Phenytoin particles surrounded by menthol, avoided surface to surface interaction with other phenytoin particles. The cosolvent (menthol) could be easily removed by sublimation using a lyophilizer following the particle recovery from the expansion chamber.

(a)

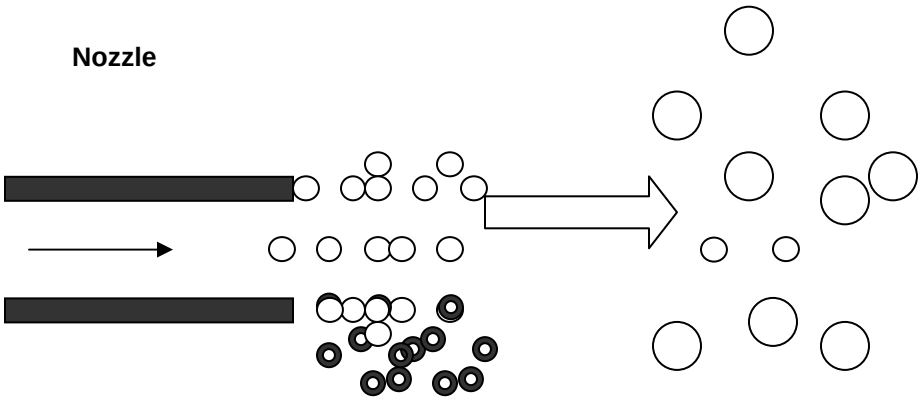

(b)

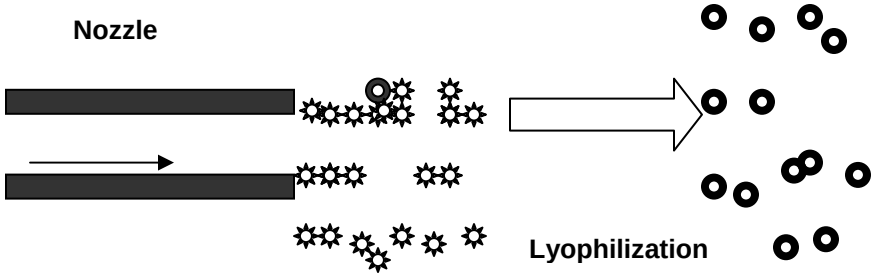

Fig. (3). Schematic representation of particle formation in expansion zone during conventional RESS process (a) with RESS-SC process (b).

9.0 OPERATIONS WHERE SCF ACTS AS AN ANTI SOLVENT

GAS, SAS ASES and SEDS [31, 32]: Gas Antisolvent Process(also known as discontinuous process), (GAS)/ Supercritical Antisolvent Process (SAS) / Aerosol Solvent Extraction System (ASES) / Solution Enhanced Dispersion by Supercritical fluids (SEDS) exploit relatively low solubilities of the pharmaceutical compounds in scCO2. The drug of interest, a polymer (or both) is dissolved in a conventional (organic) solvent to form a solution. Solvents used include, but not limited to,

dimethyl sulfoxide, N-methyl pyrrolidone, methanol, ethanol, acetone, chloroform and isopropanol. In order that the particle precipitation occurs, the solute must be virtually insoluble in carbon dioxide while the organic solvent must be completely miscible with carbon dioxide at the precipitation temperature and pressure.

Collection of the precipitated particles in the antisolvent processes is carried out in the same vessel where solvent extraction takes place. The particles are collected on the filters, located at the bottom of the vessel. Additionally, a drying cycle is performed at the end by passing a generous amount of SCF to remove any un-extracted solvent. Minor modifications of this basic principle are applied in GAS and SAS.

9.1 Mechanism of particle formation in GAS, SAS/ASES

Fig. 4 (a) is the schematic representation of the GAS process. In this process, the solute is first dissolved in a liquid organic solvent or solvent mixture, and a gas is employed to precipitate the solute. The gas used as the antisolvent does not have to be at supercritical condition. It is injected into the solution in a closed chamber, preferably from the bottom, in order to obtain uniform mixing . There is no atomization step. Due to dissolution of the compressed gas in the organic solvent, its solubilizing power on drug molecules lessens and diminishes when it becomes supersaturated with the gas.during which the drug precipitates in the form of the fine particles. The particles produced are washed with additional antisolvent to remove the remainder of the solvent.

GAS processes are batch and semi-continuous operations. They don't work under constant pressure. The pressure varies continuously from 1 bar to the final pressure. GAS is favored by some researchers as it is a slow process and allows the growth of the particles in a controllable manner. However, it has rarely been successfully scaled up to an industrial magnitude.

Fig. **4 (b)** provides the schematic representation of the SAS process. Unlike GAS, this technique utilizes gas in its supercritical stage as an antisolvent for the solute. In addition, the mechanism involved is different than that employed in the GAS process. The solute is first dissolved in a liquid solvent and then this solution is sprayed using a nozzle into a chamber which contains the supercritical fluid (antisolvent). The supercritical fluid dissolves in the liquid solvent droplets followed by a large volumetric expansion by reducing the solvent power of the liquid. As a consequence, the super saturation of the liquid mixture increases causing formation of small and uniform particles. Unlike GAS, this technology has produced favorable results during scale up to industrial capacity [87]. As mentioned before, the **ASES** (aerosol, solvent extraction system) is the same as SAS in principle.

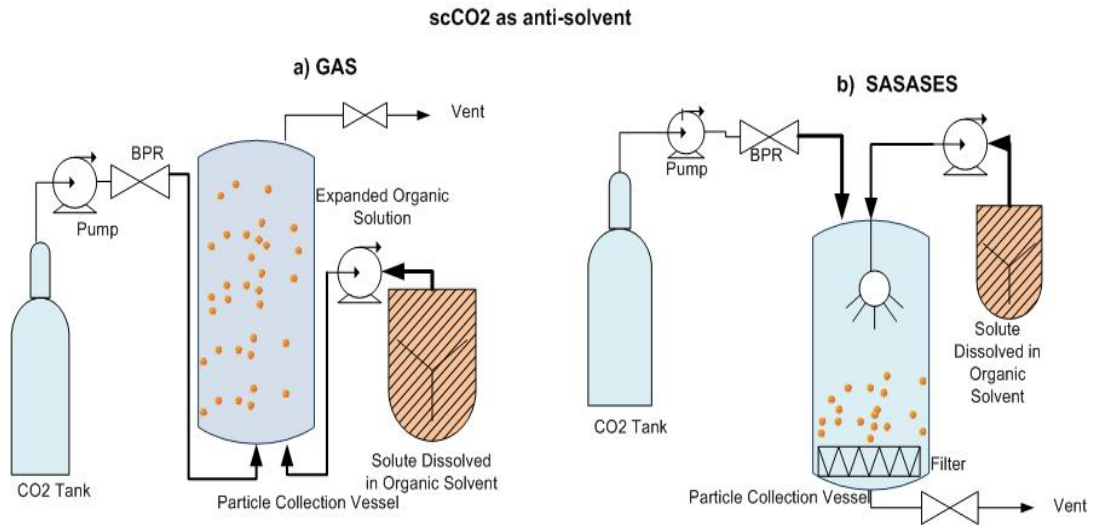

Fig. (4). Simplified schematic representation of GAS **(a)** and SAS/ASES **(b)** equipment set up showing components such as CO2 tank, pump, back pressure regulator, extraction vessel , and solution of API &/or polymer in organic solvent.

9.2 Applications of GAS/SAS/ASES

Kalogiannis et al. [88] used SAS technology to produce amorphous nanoparticles of amoxicillin within the range of 500 nm to 800 nm when they have used DMSO as the organic solvent. When they partially replaced dimethyl sulfoxide (DMSO) with EtOH and MeOH, the particle size was reduced to the range of 350 nm. Reverchon et al. [89] used semi-continuous SAS technique to produce rifampicin micro- and nanoparticles with controlled particle size (PS) and particle size distribution (PSD). SAS experiments were performed using different liquid solvents. When they used DMSO and 40 °C operating temperature, they obtained amorphous nanoparticles with mean diameters ranging from 400 nm to 1000 nm. HPLC analysis showed no degradation during supercritical processing. They also observed that, when the liquid concentration was increased, the mean PS increased and the PSD was widened.

Lee et al. [29] demonstrated that ASES could be a promising technique not only to reduce the particle size, but also to prepare amorphous solid dispersion of itraconazole with a hydrophilic polymer, HPMC 2910. The particle size of solid dispersion prepared, ranged from 100 to 500 nm. Authors verified that itraconazole was molecularly dispersed in HPMC 2910 in an amorphous form.

Production of round nanoparticles with SAS and modified SAS methods is doable. Cefnidir was nanoparticulated to 150 nm size by Park et al. [90] by using methanol as the solvent. They calculated the Intrinsic Dissolution Rate (IDR) of the processed and unprocessed particles and found out that cefidinir nanoparticles prepared with SAS had 9.42-9.94 times more dissolution.

Sanganwar et al [91] and Chattopadhyay and Gupta [92] modified the conventional SAS process in order to minimize the agglomeration of drug particles. Sanganwar et al [91] produced microparticles of a poorly water-soluble nevirapine using SAS method. The drug was simultaneously deposited on the surface of lactose and microcrystalline cellulose respectively in a single step, to reduce drug–drug particle aggregation. Another technique named as "Supercritical Antisolvent-Drug Excipient mixing (**SAS-DEM**)", was used to minimize particle aggregation. In this method, the drug, dissolved in dichloromethane, was precipitated in the scCO2 vessel, which contained suspended excipient particles. The SAS-DEM treatment was effective to minimize particle aggregation but has not interfered with the crystallinity or physicochemical properties of nevirapine. The drug/excipient mixture obtained, had a significantly faster dissolution rate compared to SAS processed drug microparticles

alone or of its physical mixtures prepared with the same excipients. Chattopadhyay and Gupta [92] also modified the conventional SAS technique and included a step where the solution jet was deflected by a surface, vibrating at an ultrasonic frequency, that atomized the jet into small micro droplets. This technique which is called **SAS-EM** (enhanced mass transfer) produced griseofulvin nanoparticles of 130 nm size.

Many more modifications of conventional SAS technique to overcome the challenges faced in SAS were reported. One such modification is called Supercritical-Assisted Atomization (**SAA**). SAA technique that was reported by Reverchon [93] was used to produce micro- and nanoparticles of several pharmaceuticals with controlled size and distribution. In this technique, controlled quantities of scCO2 was mixed with solutions containing a solid solute and the entire ternary solution is subsequently atomized through a nozzle. The technique successfully micronized some superconductor, ceramic, and catalyst precursors as well as several pharmaceutical compounds, such as carbamazepine, ampicillin trihydrate, triclabenzadol, and dexamethasone. Liquid solvents used to form the starting solution were methanol, water and acetone. The author explained the mechanism of the t **SAA** process as, formation of primary small droplets by atomization of the liquid in the thin wall nozzle in Step 1. In Step 2, due to the extremely rapid release of CO2 from inside of the primary droplets, the droplets formed broke up (decompressive atomization), by forming smaller secondary droplets. Creation of primary and secondary droplets eventually resulted in formation of submicron drug particles.

Another modification of SAS was proposed by Rodrigues et al. [94] and is termed **Atomization of Supercritical Antisolvent Induced Suspensions (ASAIS)**.

Mechanistically, ASAIS is similar to SAA where a small volume supercritical antisolvent is dissolved in line, with the liquid solvent before the liquid atomization for the solvent extraction step. Mixing of scCO2 in a small volume immediately before the nozzle orifice, leads formation of conditions such that causes the precipitation of the solute and the suspension formed in this way, is then spray-dried for solvent separation. The process was successfully demonstrated to produce submicron particles of theophylline using tetrahydrofuran as the organic solvent. The authors argued that compared to other similar particle-production techniques, this approach allowed a more efficient control of the antisolvent process and reduced the volume of the high-pressure precipitator by several orders of magnitude.

10.0 SOLUTION ENHANCED DISPERSION BY SUPERCRITICAL FLUIDS (SEDS)

Mechanism of particle formation Fig. (5): This technique is used more frequently in preparation of molecular level drug-polymer combinations and was patented by Hanna and York [95]. It uses SCF as an antisolvent and dispersing agent. The instantaneous contact of the liquid solution containing the drug and the polymer with the SCF, generates a finely dispersed mixture which leads to rapid particle precipitation. This technology is generally used to produce micro-spheres/capsules. The most important feature of the SEDS is the nozzle type. In this process, two types of coaxial nozzles are used; first one is a nozzle with two channels which allows introduction of the supercritical fluid and the drug solution or drug polymer mixture at the same time. The second nozzle used has three channels which allows introduction of three different fluids at once [95], providing more choices in operating

variables. For example, dissolving the drug in an organic solvent and the polymer in an aqueous solution and introducing both solutions and SCF at the same time is possible. Two different SCFs can also be introduced. The experimental arrangement of the SEDS process is shown in Fig. (5). Fig 5(b), shows the schematic representation of the three-channeled coaxial nozzle.

a)

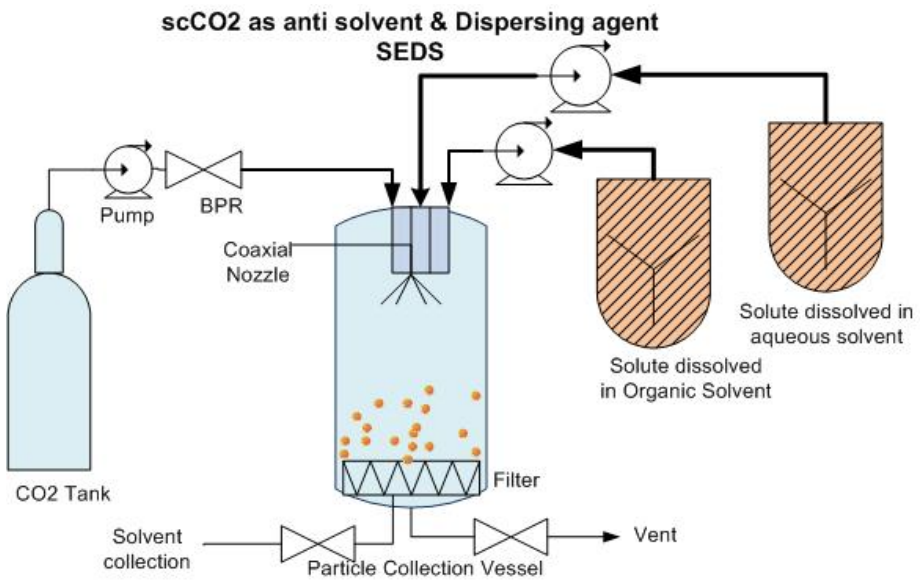

b)

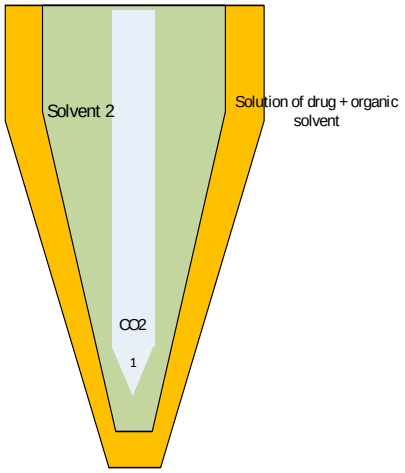

Fig. (5). Schematic drawing of SEDS **(a)** process and a simplified arrangement showing three-channeled coaxial nozzle **(b)** used in SEDS process.

SEDS process produced particles of salmeterol xinafoate with a polymer matrix [95]. Two separate solutions of the active substance and the polymer (hydroxypropylcellulose) which was dissolved in acetone, were prepared, and co-introduced with supercritical CO2 in a precipitator, using a three-passage nozzle. Analysis made, confirmed inclusion of the drug into the polymer matrix. In this manner, Ghaderi et al. [96] produced spherical microparticles of hydrocortisone entrapped within the biodegradable polymer poly($_{D,L}$-lactide-co-glycolide) ($_{DL}$-PLG) by using a combination of supercritical N_2 and CO2, at 130 bar pressure and 38^0C temperature . The use of N_2 simultaneously with CO2 improved the homogeneity of mixing and led to a more efficient integration of the polymer and the drug.

Chen et al. [97] produced nanoparticles of puerarin and microencapsulated them with poly(L-lactide) (PLLA) by using a modified SEDS process. The modification included an "injector" which injected nanoparticles of puerarin inside the polymer solution in dichloromethane . The Puerarin nanoparticles obtained, exhibited good spherical shapes, smooth surfaces and a narrow particle size distribution with a mean particle size of 188 nm. After microencapsulation, the Puerarin–PLLA microparticles had a mean size of 675 nm. A drug load of 23.6% and an encapsulation efficiency of 39.4% was obtained. Data obtained clearly demonstrated that this process is a promising technique to prepare a drug–polymer carrier for a drug delivery system.

11.0 OPERATIONS WHERE SCF ACTS AS SOLUTE

Particles from Gas Saturated Solution (PGSS): Fig. **6** provides schematic illustration of PGSS equipment set up. As discussed earlier, many drug substances are either polar or have high molecular weights. It is difficult to dissolve these compounds in CO2, which is a non polar solvent, even in a supercritical state without the aid of a cosolvent. On the other hand, scCO2 has the ability to diffuse into organic compounds, such as polymers. When scCO2 diffuses into the polymer, it lowers the melting point and decreases its viscosity. These characteristics are made use of in PGSS process.

In the PGSS operations, the physical mixture of the drug and the polymer is first exposed to SCF. In the presence of SCF and elevated pressure conditions, the mixture starts to plasticize and melts. Following melting, further application of the scCO2 dissolves the mixture further and viscosity decreases. This solution is then sprayed via a nozzle and a pressure control valve into a receiver. As the result of rapid depressurization, the dissolved supercritical fluid escapes leading to formation of composite microcapsules. This process is designed for making particles of materials that absorb supercritical fluids at high concentrations like poly(vinylpyrrolidone) (PVP), polyethylene glycol, polyethylene, polyester, $_{D,L}$ –PLA, PLGA.

Sencar-Bozic et al. [98] made composite microparticles of nifedipine and poly ethylene glycol, (PEG 4000), using the PGSS process. They showed that the solid dispersions had increased dissolution rates of Nifedipine. Similar results were

reported for the anti-angina drug felodipine by Kerc et al. [19]. Rodrigues et al. [99] prepared the micro particles of theophylline with hydrogenated palm oil (HPO) by the PGSS process. Particle size obtained was about 3.0 μm in diameter. Spherical morphology with a regular surface was obtained at higher expansion pressures. This technology has successfully enlarged to an industrial scale [100].

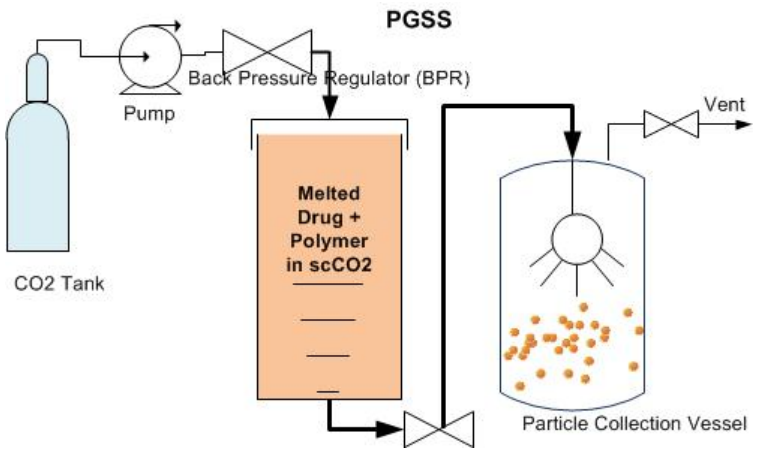

Fig. (6). Schematic representation of equipment set up of PGSS process.

The PGSS process has similar advantages to those of the RESS processes. It can be performed without using an organic solvents. It usually requires lower pressures and gas consumption than the RESS processes . One problem typically associated with the conventional PGSS process is separation of the ingredients as they pass across the pressure drop. This phenomenon can result in segregation of the components. Particles of the drug and the polymer are formed separately, but the polymer microspheres containing the drug could not be obtained

PGSS also has been modified to overcome the agglomeration and non uniform particle size distribution problems.

Skekunov et al. [101] proposed a technique to overcome the segregation problem, by using two separate mixing chambers in the equipment set up. In the first chamber, the drug and the polymer are mixed to homogeneity, allowing them to melt in scCO2. This melt was then passed from first chamber to the second one where it was mixed with more SCF, causing further reduction in the viscosity of the melt. The mixture was finally sprayed and via further expansion occurred, the uniform micro-particles of the polymer-drug mix were obtained.

Another successful modification was proposed by Hu et al. [102] to produce coenzyme Q10 (CoQ10) nanoparticles. First, CoQ10/polyethylene glycol 6000 composite particles were prepared by a PGSS process. Then, CoQ10 nanoparticles were obtained by introducing the composite particles into water. Results showed that CoQ10 slurry product had a median diameter of 190nm, The yield obtained via this method, was 89.8% when an operating pressure of 25 MPa and operating temperature of 80^0C was used.

11.1 PGSS drying

PGSS processes are also used for dependable drying of the drug products, without degrading the drug product or the polymer. This process is termed PGSS-drying , where CO2 is also used as a dispersing agent. Unlike traditional PGSS, PGSS-drying of an aqueous solution of solute (typically a polymer) is as follows: The aqueous solution of a polymer is brought into contact with carbon dioxide in a static mixer that is operating at high pressures (typically 100–150 bar) and relatively high

temperatures (around 100 – 120 ^{0}C). It is then sprayed into a vessel, at ambient pressure and lower temperatures which causes drying as the result of Joule–Thomson effect caused by the expansion.

This is an advantageous technique compared to other drying processes such as spray-drying. It allows drying of the solutions with a reduced thermal degradation or contamination of the solid substance, because the process is carried out in a closed system inertized with CO2. The only instrumental part of the process operating at the high temperature is the static mixer. This process was successfully used by Martin et al [103] to micronize polyethylene glycol from aqueous solutions, by producing spherical PEG particles with average particle sizes of 10 microns and residual water content below 1 %.

11.2 Carbon dioxide assisted nebulization with a Bubble Dryer® (CAN-BD)

This is also an example of a process where CO2 is used for drying purposes. CAN-BD process can dry and micronize pharmaceuticals that are especially used in the pulmonary drug delivery. In this process, the drug is first dissolved in water or an alcohol (or both), and is mixed very well with near-critical or supercritical CO2 by pumping both fluids through a low volume tee to generate microbubbles and microdroplets. These microbubbles are then decompressed into a low temperature drying chamber, where the aerosol plume dries in seconds. Similar to PGSS drying, there is less decomposition of thermally labile drugs. In this method, there is no need for a high pressure vessel and the particles obtained are generally 1-3 microns in size [104].

12.0 CONCLUSION

The SCF literature demonstrates that the complexity of the factors such as fluid dynamics, mass transfer, nucleation kinetics, phase composition, thermodynamics and aerodynamics are the cause of variations in size, surface properties, distribution and amorphous nature of the drug particles obtained. Another problem to overcome, especially for nanosized drugs, is the agglomeration process. The effects of different particle collection environments on the agglomeration should be clarified.

When a drug product is obtained in the presence of one or more polymers, fewer problems are encountered. The challenge is in the preparation of amorphous free flowing nanoparticles of drugs, with round surfaces and narrow particle size distribution, and scaling up related SCF process. Another area which requires further research in order to advance this technology is downstream processing of the drug particles into a suitable dosage form. It would be of no value to generate nanoparticles, if the drug substance cannot be collected as dry, agglomeration free powder or in some cases, in the form of a suspension.

What is the importance of each factor in formation of nanosized particles of an insoluble drug? How do these factors interact during processing? Which of those factors would have stronger influence on the properties of the particles generated? In order to understand their relationship a step further, the morphological changes of particles during the precipitation at the pre entry stage of the orifice versus in the free jet may be examined for a start. The literature does not offer a clear picture of the effects of the solute properties and concentration, the influence of pressure,

temperature, and the nozzle geometry on the particle size, shape, surface properties and distribution. As we continue to improve our fundamental understanding of the SCF chemistry, we can reliably scale up more of the SCF processes to obtain free flowing drug particles of nano sizes.

Throughout the years, various modifications made on the original SCF process, improved the properties of the particles obtained and small spheres with smooth surfaces, and narrow particle size distribution were produced. However, scaling up several of SCF processes is still difficult. It is is disappointing to realize that although the literature has numerous articles that have mechanistically investigated the particle formation process, commercializing this technology for the drug delivery applications has not been very successful.

In spite of the disadvantages mentioned, and the questions remained unanswered to obtain more reliable and repeatable applications, the SCF technology appears to be an exciting tool to process nanoparticulated drugs of the future. It has matured greatly over the last 10 years and has a great potential of becoming a key drug delivery technology in the near future.

REFERENCES

[1] Hecq, J. Preparation and characterization of nanocrystals for solubility and dissolution rate enhancement of nifedipine. *Int. J. Pharm*., **2005**, *299*, 167-177.

[2] Keck, C.M.; Muller, R.H. Drug nanocrystals of poorly soluble drugs produced by high pressure homogenisation. *Eur. J. Pharm. Biopharm*., **2006**, *62*(1), 3-16.

[3] Merisko-Liversidge, E.; Liversidge, G.G.; Cooper, E.R. Nanosizing: a formulation approach for poorly-water-soluble compounds. *Eur. J. Pharm. Sci*., **2003**, *18*(2), 113-120.

[4] Muller, R.H.; Böhm, B.H.L.; Grau, M.J.; Wise, D.L. Nanosuspensions—a formulation approach for poorly soluble and poorly bioavailable drugs. Handbook of Pharmaceutical Controlled Release Marcel Dekker , New York, **2000,** pp. 345-357.

[5] Noyes , A.A.; Whitney ,W. Auflösungsgeschwindigkeit von festen Stoffen in ihren eigenen Lösungen. *Z. Physik. Chemie*., **1897**, *23*, 689 -692.

[6] Junghanns, J.U.; Müller, R.H. Nanocrystal technology, drug delivery and clinical applications. *Int. J. Nanomedicine*, **2008**, *3*(3), 295–310.

[7] Nelson, K.G. The Kelvin equation and solubility of small particles. *J. Pharm. Sci*., **1972**, *61*, 479-480.

[8) Wagner, V.; Dullaart, A.; Bock, A. K.; Zweck, A. The emerging nanomedicine landscape. *Nat. Biotechnol*., **2006**, *24*(10), 1211-1217.

[9] Wagner, V.; Husing, B.; Gaisser, S. Nanomedicine: Drivers for development and possible impacts, European Commission joint research center report. October, **2006**.

[10] Liedtke, S.; Wissing, S.; Müller, R.H.; Mäder, K. Influence of high pressure homogenization equipment on nanodispersions characteristics. *Int. J. Pharm*., **2000**, *196*(2), 183-185.

[11] Cho, J.S.; Ko, Y.N.; Koo, H.Y.; Kang, Y.C. Synthesis of nano-sized biphasic calcium phosphate ceramics with spherical shape by flame spray pyrolysis. *J. Mater. Sci. Mater. Med.,* **2010**, *4*, 1143-1149.

[12] Patey, T.J.; Büchel, R.; Nakayama, M.; Novák, P. Electrochemistry of LiMn2O4 nanoparticles made by flame spray pyrolysis. *Phys. Chem. Chem. Phys,* **2009**, *11*(19), 3756-3761.

[13] Beliatis, M.J.; Martin, N.A.; Leming, E.J.; Silva, S.R.; Henley, S.J. Laser ablation direct writing of metal nanoparticles for hydrogen and humidity sensors. *Langmuir,* **2011**, *27*(3), 1241-1244.

[14] Hulteen, J.C.; Treichel, D.A.; Smith, M.T.; Duval, M.L.; Jensen, T.R.; Van Duyne, R.P. Nanosphere Lithography: Size-Tunable Silver Nanoparticle and Surface Cluster Arrays. *J. Phys. Chem. B,* **1999**, *103*, 3854–3863.

[15] Yasuji, T.; Takeuchi, H.; Kawashima, Y. Particle design of poorly water-soluble drug substances using supercritical fluid technologies. *Adv. Drug Deliv. Rev.,* **2008**, *60*(3), 388-398.

[16] Mishima, K. Biodegradable particle formation for drug and gene delivery using supercritical fluid and dense gas. *Adv. Drug Deliv. Rev.,* **2008**, *60*(3), 411-432.

[17] Youn, Y.S.; Oh, J.H.; Ahn, K.H.; Kim, M.; Kim, J.; Lee, Y.W. Dissolution rate improvement of valsartan by low temperature recrystallization in compressed CO2: Prevention of excessive agglomeration. *J. Supercrit Fluids*, **2011**, *59*, 117-123**.**

[18] Donsi, G.; Reverchon, E. Micronization by means of supercritical fluids: possibility of application to pharmaceutical field. *Pharm. Acta Helv.,* **1991**, *66*(5-6), 170-173.

[19] Kerc, J.; Srcic, S.; Knez, Z.; Sencar-Bozic, P. Micronization of drugs using supercritical carbon dioxide. *Int. J. Pharm.,* **1999,** *182*(1), 33-39.

[20] Snavely,W.K.; Subramaniam, B.; Rajewski, R.A.; Defelippis, M.R. Micronization of insulin from halogenated alcohol solution using supercritical carbon dioxide as an antisolvent. *J. Pharm. Sci.,* **2002**, *91*, 2026-2039.

[21] Mohamed, R.S.; Halverson, D.S.; Debendetti, P.G.; Prud'homme, R.K. Solid formation after the expansion of supercritical mixtures, Supercritical fluid science and technology. In: Johnston K.P., Penninger, JML (eds), ACS Symposium series-406, American Chemical Society, Washington DC, **1989**, 355-378.

[22] Pathak, P.; Meziani, M.J.; Desai, T.; Sun, Y.P. Nanosizing drug particles in supercritical fluid processing. *J. Am. Chem. Soc.,* **2004**, *126*(35), 10842-10843.

[23] Pasquali, I.; Bettini, R.; Giordano, F. Solid-state chemistry and particle engineering with supercritical fluids in pharmaceutics. *Eur. J. Pharm. Sci*., **2006**, *27*(4), 299-310.

[24] Herberger, J.; Murphy, K.; Munyakazi, L.; Cordia, J.; Westhaus, E. Carbon dioxide extraction of residual solvents in poly(lactide-co-glycolide) microparticles. *J. Control. Release,* **2003**, *90*(2), 181-195.

[25] Ruchatz, F.; Kleinebudde, P.; Muller, B.W. Residual solvents in biodegradable microparticles. Influence of process parameters on the residual solvent in

microparticles produced by the aerosol solvent extraction system (ASES) process. *J. Pharm. Sci*., **1997,** *86*, 101-105.

[26] Falk, R.F.; Randolph, T.W. Process variable implications for residual solvent removal and polymer morphology in the formation of gentamycin-loaded poly (L-lactide) microparticles. *Pharm. Res*., **1998**, *15*(8), 1233-1237.

[27] Kamihira, M.; Taniguchi, M.; Kobayashi, T. Removal of organic solvent from antibiotics with supercritical carbon dioxide. *J. Ferment. Technol.,* **1987**, *65*(1), 71-75.

[28] Kazarian, S.G.; Martirosyan, G.G. Spectroscopy of polymer/drug formulations processed with supercritical fluids: in situ ATR-IR and Raman study of impregnation of ibuprofen into PVP. *Int. J. Pharm.,* **2002**, *232*(1-2), 81-90.

[29] Lee, S.; Nam, K.; Kim, M.S.; Jun, S.W.; Park, J.S.; Woo, J.S. Preparation and characterization of solid dispersions of itraconazole by using aerosol solvent extraction system for improvement in drug solubility and bioavailability. *Arch. Pharm. Res*., **2005**, *28*, 866-874.

[30] Berens, A.R.; Huvard, G.S.; Korsmeyer, R.W. Process for incorporating an additive into a polymer and product produced thereby. US Patent 4820752, April 11, **1989**

[31] Wang,Y.; Dave, R.N.; Pfeffer, R. Polymer coating/encapsulation of nanoparticles using a supercritical anti-solvent process. *J. Supercrit. Fluids*., **2004**, *28*, 85-99.

[32] Subramaniam, B.; Saim, S.; Rajewski, R.; Stella, V.J. Methods and Apparatus for Particle Precipitation and Coating Using Near-Critical and Supercritical Antisolvents. US Patent 5,833,891, Nov 10, **1998**

[33] Chattopadhyay, P.; Huff, R.; Shekunov, B.Y. Drug encapsulation using supercritical fluid extraction of emulsions. *J. Pharm. Sci*., **2006**, *95*, 667-679.

[34] Cooper, A.I. Polymer synthesis and processing using supercritical carbon dioxide. *J. Mater. Chem*., **2000**, *10* 207–234.

[35] Kendall, J.L.; Canelas, D.A.; Young, J.L.; DeSimone, J.M. Polymerization in supercritical carbon dioxide. *Chem. Rev*., **1999**, *99*, 543-563.

[36] Tomasko, D.L.; Li, H.; Liu, D.; Han, X.; Wingert, M.J.; Lee, L.J.; Koelling, K.W. A review of CO2 applications in the processing of polymers. *Ind. Eng. Chem. Res,* **2003**, *42*, 6431-6456.

[37] Woods, H.M.; Silva, M.M.C.G.; Nouvel, C.; Shakesheff, K.M.; Howdle, S.M. Materials processing in supercritical carbon dioxide: surfactants, polymers and biomaterials. *J. Mater. Chem*., **2004**, *14*(11), 1663–1678.

[38] Yeo, S.; Kiran, E. Formation of polymer particles with supercritical fluids: A review. *J. Supercrit. Fluids*, **2005**, *34*(3), 287-308.

[39] Kiran, E. Polymer miscibility, phase separation, morphological modifications and polymorphic transformations in dense fluids. *J. Supercrit. Fluids*, **2009**, *47*, 466-483.

[40] Lee, M.; Tzoganakis, C.; Park, C.B. Extrusion of PE/PS blends with supercritical carbon dioxide. *Polym. Eng. Sci.* **1998**, *38*(7), 1112-1120.

[41] Lyons, J.G.; Hallinan, M.; Kennedy, J.E.; Devine, D.M.; Geever, L.M.; Blackie, P. Preparation of monolithic matrices for oral drug delivery using a supercritical fluid assisted hot melt extrusion process. *Int. J. Pharm.,* **2007,** *329*(1-2), 62-71.

[42] Andrews, G.P.; Abu-Diak, O.; Kusmanto, F.; Hornsby, P.; Hui, Z.; Jones, D.S. Physicochemical characterization and drug-release properties of celecoxib hot-melt extruded glass solutions. *J. Pharm. Pharmacol.,* **2010**, *62*(11), 1580-1590.

[43] Frederiksen, L.; Anton, K.; van Hoogevest, P.; Keller, H.R.; Leuenberger, H. Preparation of liposomes encapsulating water-soluble compounds using supercritical carbon dioxide. *J. Pharm. Sci.,* **1997**, *86*(8), 921-928.

[44] Hassan, H.A.; Al-Marzouqi, A.H.; Jobe, B.; Hamza, A.A.; Ramadan, G.A. Enhancement of dissolution amount and in vivo bioavailability of itraconazole by complexation with beta-cyclodextrin using supercritical carbon dioxide. *J. Pharm. Biomed. Anal.,* **2007**, *45*, 243-250.

[45] Kamihira, M.; Taniguchi, M.; Kobayashi, T. Sterilization of microorganisms with supercritical carbon dioxide. *Agric. Biol. Chem.,* **1987**, *51*, 407–412.

[46] Hong, S.; Pyun, Y. Inactivation Kinetics of Lactobacillus plantarum by High Pressure Carbon Dioxide. *J. Food Sci.,* **1999**, *64*(4), 728-733.

[47] Isenschmid, A.; Marison, I.W.; von Stockar, U. The influence of pressure and temperature of compressed CO2 on the survival of yeast cells. *J. Biotechnol.,* **1995**, *39*(3), 229-237.

[48] Andersson, M.B.O.; Demirbüker, M.; Blomberg, L.G. Semi-continuous extraction/purification of lipids by means of supercritical fluids. *J. Chromatogr. A.,* **1997,** *785*(1-2), 337-343.

[49] Kallio, M.H. Supercritical fluid chromatography-gas chromatography of volatiles in cloudberry (Rubus chamaemorus) oil extracted with supercritical carbon dioxide. *J. Chromatogr. A,* **1997**, *787*, 276-282.

[50] Dabbousi, B.O.; Rodriguez-Viejo, J.; Mikulec, F.V.; Heine, J.R.; Mattoussi, H.; Ober, R. (CdSe)ZnS Core−Shell Quantum Dots: Synthesis and Characterization of a Size Series of Highly Luminescent Nanocrystallites. *J. Phys. Chem. B,* **1997**, *101*(46), 9463-9475.

[51] Medintz, I.L.; Uyeda, H.T. Goldman, E.R.; Mattoussi, H. Quantum dot bioconjugates for imaging, labelling and sensing. *Nat. Mater*., **2005**, *4*(6), 435-446.

[52] Reverchon, E.; Cardea, S.; Production of controlled polymeric foams by supercritical CO2. *J. Supercrit. Fluids.* **2007**, *40*, 144-152.

[53] Arora, K.A.; Lesser, A.J.; McCarthy, T.J. Preparation and Characterization of Microcellular Polystyrene Foams Processed in Supercritical Carbon Dioxide. *Macromolecules,* **1998**, *31*(14), 4614-4620.

[54] Marr, R.; Gamse, T.; Use of supercritical fluids for different processes including new developments—a review. *Chem. Eng. Process.,* **2000**, *39*, 19-28.

[55] Pathak, P.; Meziani, M.J.; Sun, Y.P. Supercritical fluid technology for enhanced drug delivery. *Expert Opin. Drug. Deliv*., **2005**, *2*(4) 747-761.

[56] Jung, J.; Perrut, M. Particle design using supercritical fluids: literature and patent survey. *J. Supercrit. Fluids*, **2001**, *20*, 179-219.

[57] Kompella, U.B.; Koushik, K.; Preparation of drug delivery systems using supercritical fluid technology. *Crit. Rev. Ther. Drug Carrier Syst.,* **2001**, *18*(2), 173-199.

[58] Castor, T.P. Phospholipid nanosomes. Curr. Drug. Deliv., **2004**, *2*(4), 329-340.

[59] Tan, H.S.; Borsadia, S.; Particle formation using supercritical fluids: pharmaceutical applications. *Expert Opin. Ther. Pat.,* **2001**, *11*(5), 861-872.

[60] Stanton, L.A.; Dehghani, F.; Foster, N.R. Improving drug delivery using polymers and supercritical fluid technology. *Aust. J. Chem*., **2002**, *55*(6-7), 443-447.

[61] Ye, X.; Wai, C.M.; Making nanomaterials in supercritical fluids: a review. *J. Chem. Educ.,* **2003**, *80*(2), 198-204.

[62] Vemavarapu, C.; Mollan, M.J.; Lodaya, M.; Needham, T.E. Design and process aspects of laboratory scale SCF particle formation systems. *Int. J. Pharm*., **2005**, *292*(1-2), 1-16.

[63] Byrappa, K.; Ohara, S.; Adschiri, T. Nanoparticles synthesis using supercritical fluid technology - towards biomedical applications. *Adv. Drug Deliv. Rev*., **2008**, *60*(3), 299-327.

[64] Pasquali, I.; Bettini, R.; Giordano, F.; Supercritical fluid technologies: an innovative approach for manipulating the solid-state of pharmaceuticals. *Adv. Drug Deliv. Rev*. **2008**, *60*(3), 399-410.

[65] Pasquali, I.; Bettini, R.; Are pharmaceutics really going supercritical?. *Int. J .Pharm.,* **2008**, *364*(2), 176-187.

[66] Maulvi, F.; Thakkar, V.T.; Soni, T.G.; Gohel, M.C.; Gandhi, T.R.; Supercritical fluid technology: A promising approach to enhance the drug solubility. *J. Pharm. Sci. & Res.,* **2009**, *1*, 1-14.

[67] Palakodaty, S.; York, P.; Phase behavioral effects on the particle formation processes using supercritical fluid. *Pharm. Research,* **1999**, *16*, 976 –985.

[68] Reverchon, E.; Caputo, G.; Marco, I.D. Role of Phase Behavior and Atomization in the Supercritical Antisolvent Precipitation. *Ind. Eng. Chem. Res*., **2003**, *42*, 6406-6414.

[69] Perrut, M.; Clavier, J.Y.; Supercritical Fluid Formulation: Process Choice and Scale-up. *Ind. Eng. Chem. Res.* **2003**, *42*(25), 6375- 6383.

[70] Kwauk, X.; Debenedetti, P.G. Mathematical modeling of aerosol formation by rapid expansion of supercritical solutions in a converging nozzle. *J. Aerosol Sci*., **1993**, *24*(4), 445–469.

[71] Reverchon, E.; Pallado, P. Hydrodynamic modeling of the RESS process. *J. Supercrit. Fluids*, **1996**, *9*, 216–221.

[72] Hirunsit, P.; Huang, Z.; Srinophakun, T.; Charoenchaitrakool, M.; Kawi, S. Particle formation of ibuprofen-supercritical CO2 system from rapid expansion of supercritical solutions (RESS): A mathematical model. *Powder Technol.,* **2005**, *154*, 83–94.

[73] Türk, M. Influence of thermodynamic behavior and solute properties on homogeneous nucleation in supercritical solutions. *J. Supercrit. Fluids*., **2000**, *18*, 169–184.

[74] Helfgen, B.; Hils, P.; Holzknecht, Ch.; Türk, M.; Schaber, K. Simulation of particle formation during the rapid expansion of supercritical solutions. *J. Aerosol Sci.,* **2001**, *32*(3), 295–319.

[75] Weber, M.; Russell, L.M.; Debenedetti, P.G. Mathematical modeling of nucleation and growth of particles formed by the rapid expansion of a supercritical solution under subsonic conditions. *J. Supercrit. Fluids,* **2002**, *23*, 65–80.

[76] Lengsfeld, C.S.; Delplanque, J.P.; Barocas, V.H.; Randolph, T.W. Mechanism governing microparticle morphology during precipitation by a compressed antisolvent: Atomization vs nucleation and growth. *J. Phys. Chem. B,* **2000**, *104*(12), 2725-2735.

[77] Werling, J.O.; Debenedetti, P.G. Numerical modeling of mass transfer in the supercritical antisolvent process: miscible conditions. *J. Supercrit. Fluids,* **2000**, *18*, 11–24.

[78] Reverchon, E.; Adami, R.; Caputo, G.; De Marco I. Spherical microparticles production by supercritical antisolvent precipitation: Interpretation of results. *J. Supercrit. Fluids,* **2008**, *47*, 70-84.

[79] Braeuer, A.; Dowy, S.; Torino, E.; Rossmann, M.; Luther, S. K.; Schluecker, E.; Leipertz, A; Reverchon, E. Analysis of the supercritical antisolvent mechanisms governing particles precipitation and morphology by in situ laser scattering techniques. *Chem. Engg. J*., **2011**, *173*, 258-266.

[80] Mishima, K.; Matsuyama, K. Method for preparing composite fine particles, Japan Patent, WO 057374, **2006**

[81] Gadermann, M.; Kular, S.; Al-Marzouqi, A.; Signorell, R. Formation of naproxen/polylactic acid nanoparticles by pulsed rapid expansion of supercritical solutions. *Phys. Chem. Chem. Phys.,* **2009**, *11*, 7861-7868.

[82] Varshosaz, J.; Hassanzadeh, F.; Mahmoudzadeh, M.; Sadeghi, A.; Preparation of cefuroxime axetil nanoparticles by rapid expansion of supercritical fluid technology. *Powder Technol*., **2009**, *189*(1), 97-102.

[83] Reverchon, E.; Donsi,G.; Gorgoglione, D. Salicylic acid solubilization in supercritical CO2 and its micronization by RESS. *J. Supercrit. Fluids,* **1993**, *6*(4), 241–248.

[84] Young, T.; Pace, G.; Johnston, K.P.; Mishra, A. Phospholipid-stabilized nanoparticles of cyclosporine-A by rapid expansion from supercritical to aqueous solution. *AAPS Pharm. Sci. Tech*. **2004**, *5*(1), 70-85.

[85] Tozuka, Y.; Miyazaki, Y.; Takeuchi, H. A combinational supercritical CO2 system for nanoparticle preparation of Indomethacin. *Int. J. Pharm*., **2010**, *386*(1-2), 243-248.

[86] Thakur R., Gupta, R.B. Formation of phenytoin nanoparticles using rapid expansion of supercritical solution with solid cosolvent (RESS-SC) process, *Int. J. Pharm*., **2006**, *308*(1-2), 190-199.

[87] Jung, J.; Clavier, J.Y.; Perrut, M. Gram to kilogram scale up of supercritical anti-solvent process. Proceedings of the 6th International Symposium on Supercritical Fluids. Versailles (France), 1683-1688, **2003**

[88] Kalogiannis, C.G.; Pavlidou, E.; Panayiotou, C.G. Production of Amoxicillin Microparticles by Supercritical Antisolvent Precipitation. *Ind. Eng. Chem. Res*., **2005**, *44*(24), 9339-9346.

[89] Reverchon, E.; De Marco, I.; Della Porta, G. Rifampicin microparticles production by supercritical antisolvent precipitation. *Int. J. Pharm*., **2002**, *243*(1-2), 83-91.

[90] Park, J.; Park, H.J.; Cho,W.; Cha, K.; Kang, Y.; Hwang, S. Preparation and pharmaceutical characterization of amorphous cefdinir using spray-drying and SAS-process. *Int. J. Pharm*., **2010**, *396*(1-2), 239-245.

[91] Sanganwar, G.P.; Sathigari, S.; Babu, R.J.; Gupta, R.B. Simultaneous production and co-mixing of microparticles of nevirapine with excipients by supercritical antisolvent method for dissolution enhancement. *Eur. J. Pharm. Sci*., **2010**, *39*(1-3), 164-174.

[92] Chattopadhyay P., Gupta, R. Production of griseofulvin nanoparticles using supercritical CO2 antisolvent with enhanced mass transfer. *Int. J. Pharm*. **2001**, *228*(1-2), 19–31

[93] Reverchon, E. Supercritical-Assisted Atomization to Produce Micro- and/or Nanoparticles of Controlled Size and Distribution. *Ind. Eng. Chem. Res.*, **2002**, *41* (10), 2405–2411

[94] Rodrigues, M. A.; Padrela, L.; Geraldes, V.; Santos, J.; Matos, H. A.; Azevedo, E. G. Theophylline Polymorphs by Atomization of Supercritical Antisolvent Induced Suspensions. *J. Supercrit Fluids*, **2011**, *58* (2), 303-312

[95] Hanna, M.; York, P. World Patent WO 95/01221, **1994**

[96] Ghaderi, R.; Artursson, P.; Carlfors, J. A new method for preparing biodegradable microparticles and entrapment of hydrocortisone in dl-PLG microparticles using supercritical fluids. *Eur. J. Pharm. Sci.,* **2000**, *10*(1), 1-9.

[97] Chen, A.; Li, Y.; Chau, F.; Lau, T.; Hu, J.; Zhao, Z. Microencapsulation of puerarin nanoparticles by poly(l-lactide) in a supercritical CO2 process, *Acta Biomaterialia,* **2009**, *5*(8), 2913-2919.

[98] Sencar-Bozic, P.; Srcic, S.; Knez, Z.; Kerc, J. Improvement of nifedipine dissolution characteristics using supercritical CO2. *Int. J. Pharm*., **1997**, *148*, 123-130.

[99] Rodrigues, M.; Peiriço, N.; Matos, H.A.; Gomes de Azevedo, E.; Lobato, M.R.; Almeida, A.J. Microcomposites theophylline/hydrogenated palm oil from a PGSS process for controlled drug delivery systems. *J. Supercrit. Fluids*, **2004**, *29*(1-2), 175–184.

[100] Weidner, E. High pressure micronization for food applications. *J. Supercrit. Fluids*, **2009**, *47*(3), 556-565.

[101] Shekunov, B.Y.; Chattopadhyay, P.; Seitzinger, J.S. Method and apparatus for enhanced size reduction of particles using liquefaction of materials, US Patent 6,986,846, January 17, **2006**

[102] Hu, X.; Guo, Y.; Wang, L.; Hua, D.; Hong, Y.; Li, J. Coenzyme Q10 nanoparticles prepared by a supercritical fluid-based method. *J. Supercrit Fluids*, 2011, *57*, 66-72.

[103] Martin, A.; Weidner, E. PGSS-drying, mechanisms and modeling. *J. Supercrit Fluids*, 2010, *55*(1), 271-281.

[104] Sievers, R.E.; Huang, E.T.S.; Villa, J.A.; Engling, G.; Brauer, P.R. Micronization of water-soluble or alcohol-soluble pharmaceuticals and model compounds with a low temperature Bubble Dryer®. *J. Supercrit Fluids*, **2003,** *26*(1)**,** 9-16.

MANUSCRIPT II

Evaluation of factors influencing morphological properties and particle size of Griseofulvin during supercritical antisolvent (SAS) process

Pratik Sheth[a,b], Harpreet Sandhu[a], Waseem Malick[a], Navnit Shah[a], and M.S. Kislalioglu [b, *]

[a]Hoffman-La Roche, Inc., 340 Kingsland street, Nutley NJ 07110 USA,

[b] Department of Biomedical & Pharmaceutical Sciences, University of Rhode Island, 41 Lower College road, Kingston RI 02881

[*] Corresponding author. Department of Biomedical & Pharmaceutical Sciences, University of Rhode Island, 41 Lower College road, Kingston RI 02881 Tel: (401) 874 5017, email address: Skis@uri.edu

ABSTRACT

Particle size reduction to micro and nano scales using supercritical antisolvent (SAS) methodology is an effective and versatile option for solubility and bioavailability improvement of poorly water-soluble drugs. However, there are several factors that influence the particle morphology, particle size, and particle size distribution when SAS methodology is applied to produce nano particles. Hence, a successful application of SAS technology to drug particle production requires a careful evaluation of these factors. A fractional factorial $2^{(7-3)}$ screening design of experiments is applied to supercritical antisolvent precipitation of griseofulvin using carbon dioxide (CO_2) as an anti solvent, and acetone as solvent. The design of experiment (DOE) proposed is useful for identifying the key factors involved in the SAS process in just a few runs at an early stage of experimentation. Seven factors were studied at two levels each. Mean particle size (PS), particle size distribution (PSD), and % yield of the SAS process were chosen as responses to evaluate the process performance.

Statistical analysis of the results from DOE study identified the nozzle diameter and spray rate of organic solvent as two most significant factors affecting PS and PSD. Temperature of the precipitation vessel only impacted the particle size, whereas, the pressure, drug concentration and polymer concentration affected PSD. Lastly, the yield of the SAS process was impacted by drug concentration, polymer concentration, and the pressure condition inside the precipitation vessel. We were able to rank order these factors in terms of their overall impact on all three responses.

Based upon the outcomes of this study, an optimum and robust SAS process was developed. Operating at 45^0C, 80 bar pressure, 20 mg/ml drug concentration, 5 mg/ml polymer concentration, solvent spray rate of 2 ml/min, CO_2 addition rate of 40 g/min, and using nozzle diameter of 150 μm, *in-situ* nanoparticles d_{50} (volume based mean particle size of 50th percentile) of 0.362 μm were produced. Scanning Electron Microscopy revealed that coprecipitates of drug and polymer were fluffy and fibrous in nature. DSC analysis as well as PXRD revealed that the co-precipitates were in crystalline form. FTIR study of the products confirmed that there was no interaction between drug and the polymer. Lastly, formulations obtained with the SAS process had significantly improved rate of dissolution compared to that of the physical mixture of as-is drug and the polymer.

1.0 INTRODUCTION

Technologies that can effectively control particle formation are of utmost importance in the pharmaceutical industry. A reduction in particle size of poorly water soluble drug to the ultra-fine state such as nano scale, increases the surface area, results an increase in the dissolution rate, saturation solubility, and in turn, the bioavailability. Hence, particle size reduction to nano scale for poorly soluble drug has become a very popular process choice, enabling the use of such drugs[1-4].

There are two approaches generally used to reduce particles to the nanosizes: bottom-up and top-down. In the bottom-up approach, a colloidal solution of drug is prepared and the solvent is evaporated obtaining controlled rearrangement of single atoms and molecules into larger nanostructures. Supercritical fluid based technologies utilize this approach. The top-down approach reduces the particle size of the drug particles using media milling or high pressure homogenization. Contrary to the supercritical fluid based technology, in top down methods of particle size reduction, it is difficult to control important characteristics of the final product, such as size, shape, morphology, and surface properties.

"Supercritical" is a state of a substance above its critical temperature (T_C) and critical pressure (P_C). A substance in its supercritical state is defined as a supercritical fluid (SCF). Carbon dioxide is the most preferred SCF for the processing of pharmaceuticals, because it has low critical temperature (31.2°C) and pressure (73.8 bar or 7.4MPa), and is nonflammable, nontoxic and environmentally safe. It is highly

compressible and its density and thus the solvation power can be carefully controlled by small changes in temperature and/or pressure[5, 6]. The solvent strength of supercritical CO_2 can be altered to simulate organic solvents ranging from chloroform to methylene chloride to hexane.

Primarily there are two categories of SCF based particle formation techniques; using SCF as solvent or as an anti-solvent. Example of SCF use as the solvent is Rapid Expansion from Supercritical Solution (RESS) method while the processes that use it as the anti-solvent, include Supercritical Antisolvent Precipitation (SAS), and Solution Enhanced Dispersion by Supercritical fluids (SEDS). There are various other applications to these basic processes and are thoroughly reviewed by Sheth et al.,[7]. In the anti-solvent based process, the solute (drug and polymer) is soluble in the organic solvent, but not soluble in the supercritical CO_2. Therefore, addition of this anti-solvent induces the rapid removal of organic solvent causing the super-saturation and precipitation of the solute. Griseofulvin has negligible solubility in supercritical CO_2, hence SAS technique was chosen for this study.

There are number of factors in effect during SAS processing. These factors can be grouped into two main categories; formulation related, and process related. Physico chemical properties of the drug and the polymer[8] (if used), drug and polymer concentration[8], solubility or insolubility of drug and the polymer in solvent and $scCO_2$[8] are the main formulation variables in effect during SAS processing. Thermodynamic properties[9-10] such as the temperature, pressure, phase composition, rate of addition of one component to another; and aerodynamic properties[11] such as

nozzle geometry and impact distance of jet against a surface are the most important process variables that impact the outcome of SAS precipitation. In order to design a robust SAS process, it is extremely important to understand the impact of all of these variables, on the desirable SAS product attributes, such as particle morphology, particle size, particle size distribution, and % yield of the process.

Although several researchers[12-16] have studied these variables, there is widespread disagreement amongst them. For example, Guha et al., [12] using Cholesterol & Poly (L-lactic acid) in dichloromethane (DCM) found that increase in pressure leads to smaller particle size. Similarly, Reverchon et al.,[13] working with SAS and using griseofulvin, tetracycline, and amoxicillin in dimethylsulfoxide (DMSO), and DCM also concluded that, increase in pressure leads smaller particle size. However, Lee et al.,[14] who carried out SAS precipitation of itraconazole and HPMC2910 in DCM-Ethanol mixture, found that an increase in pressure produced larger particles. Randolph et al.,[15] as well, using SAS, found that an increase in pressure produced larger particles of Poly (L-lactic acid) from methylene chloride. Whereas, when Uzun et al.,[16] carried out SAS processing using methanol on cefuroxime axetil in the presence of PVPK30, concluded that the change in pressure did not affect the particle size significantly.

One of the reason of such wide-spread disagreements amongst the researchers, in defining the variables that impact particle properties during SAS process, is that effective variables in their SAS method were selected without a statistical test, and that optimization studies were conducted only by modifying few selectively chosen

variables. Acceptance of some of the existing factors as insignificant, and not to include them into statistical calculations may mask or influence the degree of importance of the truly effective factors. Another reason of the variability observed in detection of significant variables, could be that the outcome of SAS processing depends on properties of drug and polymer, and their interaction with solvent and anti-solvent.

Griseofulvin is a very difficult drug to transform into a coprecipitate form, and a review of the literature revealed that no author(s) have been successful in producing nanoparticles of GF, when conventional SAS methodology was applied. SAS tests performed using n-methyl pyrollidone (NMP) produced almost complete extraction of this antibiotic[13]; i.e., only traces of GF were found in the precipitation chamber at the end of the experiments. Chen et al.,[17] Reverchon et al., [13, 18] and Foster et al.,[19] using SAS methodology for GF processing, and using organic solvents such as acetone, ethanol, dimethylformamide, and DMSO, obtained needle like particles ranging from 1 μm to several mm.

Chattopadhyay and Gupta [20] modified the conventional SAS technique and included a step where the solution jet was deflected by a surface, vibrating at an ultrasonic frequency, which atomized the jet into small micro droplets. This technique which is called **SAS-EM** (enhanced mass transfer) produced GF nanoparticles of 130 nm, and may be considered as a success. However, there is no evidence that such a process could be scaled up to an industrial scale, whereas today, the conventional SAS process has been scaled up successfully handling 100 kg lots [21.] The failure to produce

nanoparticles of GF using conventional SAS method, suggests that physicochemical property of GF favors precipitation in the form of long crystals.

We have used conventional SAS methodology to reduce the particle size of GF. However, our attempts were unsuccessful to produce nanoparticles of GF, which prompted us to explore a co-precipitation with a polymer. A polymer, which can potentially act as a crystal growth inhibitor would be added to the formulation. Such an approach can be beneficial from two perspectives: firstly, it would prevent the uncontrolled crystal growth, and secondly, the polymer could act as a stabilizer to prevent the aggregation of formed micro particles.

Simonelli et al.,[22] stabilised sulfathiazole by inhibiting its crystal growth with Polyvinylpyrrolidone (PVP). It was found that the concentration and molecular weight of PVP affected the inhibitory function of PVP. These researchers reported that PVP provides a net like coverage, which controls the effective radius of protrusions from the crystal surface. Additionally Jarmer et al.,[23] precipitated GF in the presence of polymer Poly (sebacic anhydride) using a modification of SAS process called PCA (particles from compressed antisolvent). These researchers reported that, the morphology of GF precipitates changed from several hundred micron long acicular structures in the absence of PVP to 1 to 100 μm crystals in the presence of polymer.

Selection of polymer

There are various factors that affect the selection of a polymer in SAS processing, such as: a suitable drug-polymer interaction, solubility of a polymer in water, and in organic solvents, global regulatory acceptance, stabilizing ability of a polymer in an aqueous environment, and ease of processibility. We identified three hydrophilic polymers, having different molecular structure, and ionic properties; namely Kollidon® VA64, HPMCAS, and Eudragit EPO®.

Kollidon® VA64 is manufactured by free radical polymerization of 6 parts of N-vinyl pyrrolidone, and 4 parts of vinyl acetate. It is a non ionic polymer, widely used in the preparation of solid dispersion. It is freely soluble in water, acetone, and DMSO. It does not contain any H^+ donor functional group.

HPMC-AS (hypromellose acetate succinate) is a partially esterified derivative of hypromellose, where succinoyl and acetyl residues are bound to the cellulose backbone. It is practically insoluble in water, and has a pH dependent solubility in a buffered media. It is an anionic polymer, which has both H^+ donor and H^+ acceptor groups.

EUDRAGIT® EPO is a cationic copolymer based on dimethylaminoethyl methacrylate, butyl methacrylate, and methyl methacrylate. It is also practically insoluble in water, and has a pH dependent solubility in buffered media.

We wanted to develop a product that may be relevant clinically, and hence the pharmaceutical polymer selected must be recognized by the United States FDA as

GRAS (generally regarded as safe) and must have prior precedence of being used in an oral dosage form. The polymer should be well tolerated, not known to have any toxicity, and must have been used for decades in the pharmaceutical industry for various applications. Finally, the selected polymer should be freely soluble in the organic solvent chosen for SAS processing, and in water.

Table 1: Properties of pharmaceutical polymers identified for SAS co-precipitation

Property/Polymer	**Kollidon® VA64**	**HPMCAS-LF**	**Eudragit® EPO**
Avg. molecular weight (g/mol)	45,000	18,000	47,000
Functional group	No H^+ donor/acceptor	H^+ donor, and acceptor	H^+ acceptor
Solubility in water	Freely soluble	Practically insoluble	Practically insoluble
Solubility in buffered media	pH independent	pH dependent	pH dependent
Ionic property	Non-ionic	anionic	cationic
Solubility in Acetone	Soluble	Soluble	Soluble
Solubility in DMSO	Soluble	Soluble	Practically insoluble
Insolubility in $scCO_2$	Yes	Yes	Yes
Global regulatory acceptance	GRAS*	GRAS*	GRAS*

* Generally Regarded As Safe by US, Food & Drug Administration
$^+$Soluble in buffered media

Finally, the goal of the studies shown in this dissertation was to address gaps in the literature. First of all, we will carry out a screening design of experiment (DOE), where practically all formulation and processing factors will be included and we believe that such a study will be more reliable in identifying the key variables involved. Secondly, we will follow the changes in the particle size, particle size

distribution, and percent yield of product during the process, as the specific responses for measuring the process performance. Lastly, we will apply the optimum operating variables and produce coprecipitates of GF which, when placed in an aqueous medium would yield *in-situ* micro and nanoparticles of GF having a narrow particle size distribution, while obtaining the highest yield and improved solubility.

2.0 MATERIALS AND METHODS

2.1 Materials

The model drug griseofulvin (GF) was purchased as micronized API (lot # 115H1180) through jet milling process, from Ria International (East Hanover, NJ). dimethyl sulfoxide (DMSO) (purity 99.8%) and acetone (purity 99.5%) were bought from Sigma Aldrich (St Louis, MO). Polystyrene latex microspheres (98 nm, 150 nm, 310 nm, 900 nm, and 2000 nm), for checking the accuracy of Malvern instrument, were purchased from Magsphere, Inc. (Pasadena, CA). Liquid Carbon Dioxide (purity 99.9%, instrument grade 4.0 with siphon tube) was purchased from Airgas USA, LLC (Salem, NH).

Model drug GF (Figure 1), an antifungal drug widely used for the treatment of mycotic diseases of the skin, hair, and nails has very poor aqueous solubility and low bioavailability. In the present study, GF, which has cLogP, measure of intestinal permeability, of 2.88, was selected as a model drug of Biopharmaceutics Classification System (BCS) class II drugs. The Biopharmaceutics Classification System is a guide for predicting the intestinal drug absorption provided by the U.S. Food and Drug Administration. BCS class II drugs have high permeability and low

solubility. The solubility of GF in water is only about 1 µmol/mol at 37 °C[20] and it has dissolution rate limited absorption[24]. Thus, particle size reduction to nanosize is highly desirable. Hence, GF serves as a good model drug for demonstrating the utility of SAS for improving drug solubility and product performance by the formation of nanoparticles.

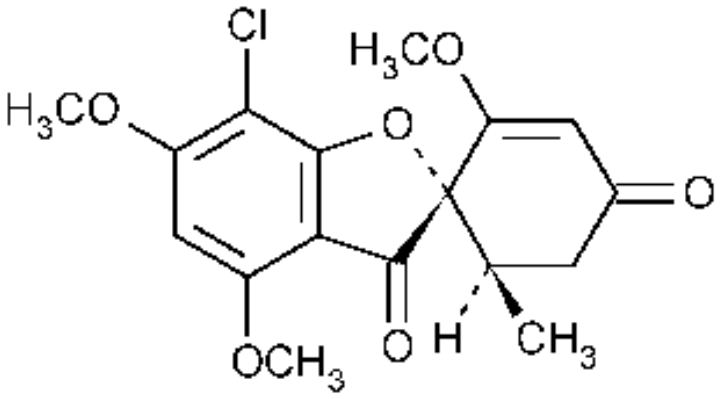

Figure 1: Chemical structure of Griseofulvin

The chemical structure of three hydrophilic polymers (Eudragit EPO®, HPMCAS, and Kollidon® VA-64) is shown in Figure 2. Kollidon® VA64 was obtained from BASF corporation (Florham Park, NJ). The methacrylic polymer, Eudragit EPO® was purchased from Evonik Degussa Corporation (Piscataway, NJ). The cellulosic polymer, HPMCAS-LF, manufactured by Shin-Etsu Co., Ltd. (Niigata, Japan) was donated by Biddle Sawyer Corporation (New York, NY).

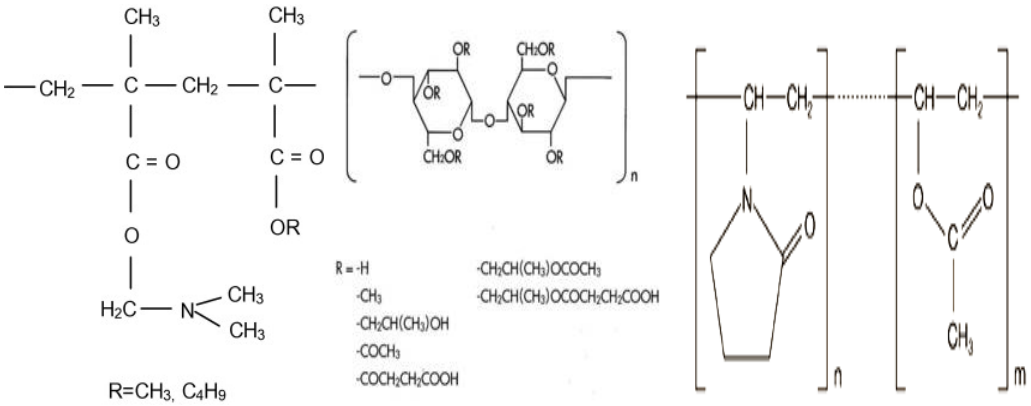

Figure 2: Chemical structure of Eudragit EPO, HPMC-AS, and Kollidon VA64 (from left to right)

2.2 Methods

2.2.1 Description of SAS process

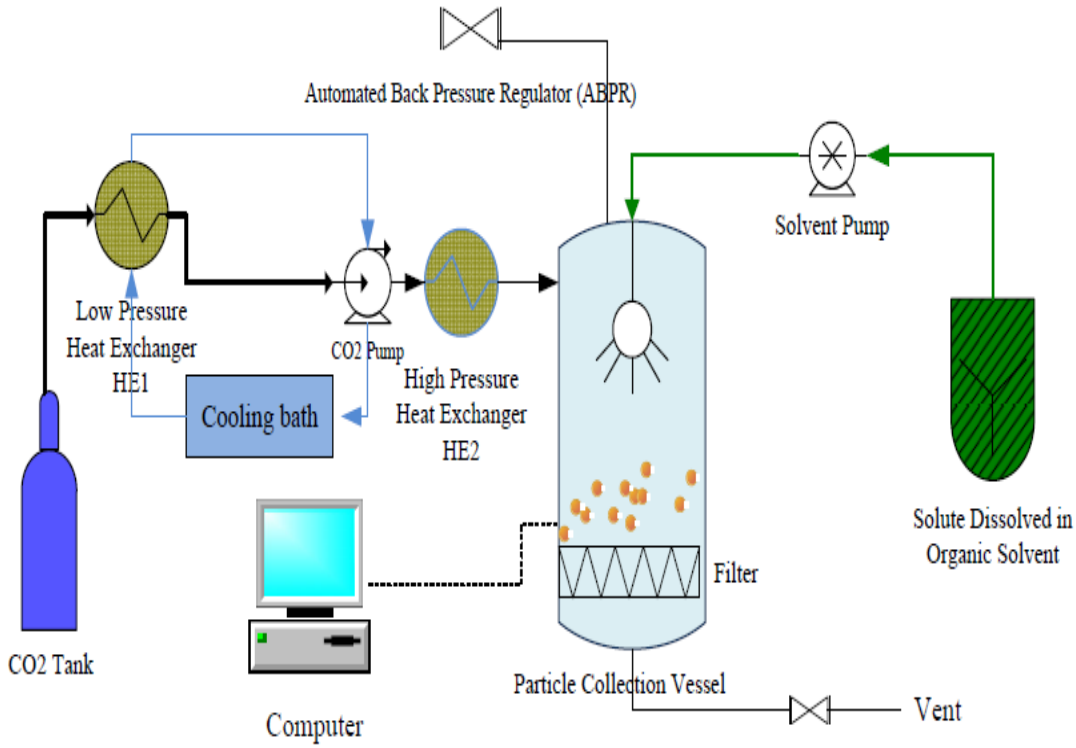

Figure 3: Schematic diagram of Tharr SAS apparatus

An SAS apparatus (model: SAS 50, Thar Technologies Co., USA) was used to generate GF-polymer co-precipitates. Figure 3 shows the schematic diagram of Tharr SAS system using supercritical carbon dioxide ($SCCO_2$) as an anti-solvent. The SAS 50 system is made up of the following components: two high pressure pumps, one for the CO_2 and the other for the organic solvent; a stainless steel particle collection vessel (0.5 L volume, 54 mm internal diameter and 218 mm internal height) consisting of the main body, the frit, and electric heating jacket ; and an automated

back pressure regulator (ABPR) of high precision. Firstly, the CO_2 coming from tank passes through low pressure heat exchanger (HE1) and was cooled down with a cooling bath operating at 4 °C to assure liquid state in the pump. The liquefied CO_2 was then pumped into particle collection vessel using a high-pressure pump through the spray nozzle. CO_2 was heated using another heat exchanger (HE2) before entering the precipitation vessel. Stainless steel orifice nozzles of 100 μ, 150 μ, and 200 μ were used, depending on a particular experiment, as laid out in Table 5. The selection of organic solvent between acetone and DMSO was based on the quality of GF crystals obtained and ease of solvent removal from product. Acetone was preferred as the organic solvent. The flow-rate of CO_2, and acetone were adjusted via using computer software. The pressure in particle collection vessel was controlled using an automatic back-pressure regulator (ABPR), and a temperature controller regulates the amount of heat being applied to the heating jacket.

At the beginning of the experiment, acetone was sprayed for 10 minutes to establish the steady state condition. After that, the solvent pump was used to spray the solution of drug and polymer into the precipitation vessel through the spray nozzle. Approximately 150–200 mL of solution of drug and polymer was sprayed into the precipitation vessel. Rapid mixing between the organic solvent and $SCCO_2$, and the fast diffusion of supercritical CO_2 into the organic solvent produces a supersaturated solution and causes the drug & polymer to precipitate as fine particles, which were collected on a 0.22 μm Nylon filter, placed on top of 5 μ metal frit. Once sufficient powder was collected, the solution pump was switched off while supercritical CO_2 was continuously pumped into the precipitation vessel to wash-up the remaining

solvent residual for duration of approximately 60–80 min. The precipitation vessel was then depressurized gradually to atmospheric pressure using the vent valves. Finally, the powder was collected from the inside of the precipitator for further characterization.

2.2.2 Testing reproducibility of SAS process

In order to find out the variability of the processing method, two sets of experiments were repeated three times each. In these experiments, 150 ml of acetone solution was sprayed in the SAS vessel, and Kollidon VA64 was used as the polymer. All experiments were carried out at 2 ml/min acetone solution spray rate, 20 g/min CO_2 rate, and nozzle diameter was kept at 100 μm. Drug concentration was tested at 15 and 20 mg/mL, polymer concentration at 20% and 70%, temperature at 35 and 45^0C, and pressure at 80 and 85 bar. Particle size and particle size distribution measurements were performed using Malvern light diffraction method, as described in later sections. Table 2 summarizes the results, and shows that the yield of the process was 81 $\pm$ 3.6 % for formulation with 70% polymer, and 88 $\pm$ 3 % for formulation with 20% polymer; whereas d_{50} values were 239 $\pm$ 31 nm, and 370 $\pm$ 3 nm for two different formulations. Lastly, the span values, measure of particle size distribution, were 5.377 $\pm$ 0.47, and 2.534 $\pm$ 0.03. We believe that the higher variability in particle size and particle size distribution for the first set of experiments in Table 2 (experiments 1-3) is due to high polymer content (70%) of those formulations which cause partial precipitation and blockage of nozzle. Considering that these SAS experiments were carried out at a very small scale, overall the results

show that the SAS process is reproducible, while the formulation and processing conditions are varied.

Table 2. Testing reproducibility of SAS process

Exp	Temp	Pressure	Drug Conc.	Poly. conc	Liq. spray rate	CO_2 rate	Noz. dia.	**d_{50}**	**Yield**	**PSD Span**
	^{0}C	Bar	mg/ml	mg/ml(%)	ml/min	g/min	µm	nm	%	
1	35	85	15	35 (70%)	2	20*Liq	100	207	82	5.907
2	35	85	15	35 (70%)	2	20*Liq	100	268	77	5.011
3	35	85	15	35 (70%)	2	20*Liq	100	242	84	5.212
							Average	**239**	**81**	**5.377**
							Std. deviation	**31**	**3.6**	**0.47**
4	45	80	20	5 (20%)	2	20*Liq	100	366	89	2.559
5	45	80	20	5 (20%)	2	20*Liq	100	372	85	2.509
6	45	80	20	5 (20%)	2	20*Liq	100	372	91	2.536
							Average	**370**	**88**	**2.534**
							Std. deviation	**3**	**3**	**0.03**

2.2.3 Evaluation of solubility of drug, and miscibility of organic solvents in $scCO_2$

The RESS 50 (Tharr Technologies Co., USA) system was used for the preliminary solubility and miscibility evaluations. The system, schematically shown in Appendix A, is made up of the following components: a high pressure CO_2 pump; a high pressure agitator; and a stainless steel extraction vessel with a sapphire view cell carved in the middle of vessel. The extraction vessel consists of the main body, an electric heating jacket, and an automated back pressure regulator (ABPR) of high precision.

In this apparatus, firstly, the CO_2 coming from tank passed through low pressure heat exchanger (HE1) and was cooled down with a cooling bath operating at 4 °C to assure liquid state in the pump. The liquefied CO_2 was then pumped into extraction vessel using a high-pressure pump. The CO_2 was heated using another heat exchanger (HE2) before entering the extraction vessel. The pressure in extraction vessel was controlled using an automatic back-pressure regulator, ABPR. A temperature controller provides pre-specified heat to the heating jacket. Agitator mounted on top of the extraction vessel provides mixing to the contents of the vessel.

At the beginning of the experiment, an untreated as-is GF or raw organic solvent (acetone or DMSO) or mixture of GF and organic solvent, was placed in the extraction vessel. Agitator was turned on to gently mix the contents of the vessel. After that, the CO_2 pump was turned on to fill the extraction vessel. Temperature was

gradually raised from 35 to 100^0C, and the pressure gradually raised from 80 to 300 bar. During this time, visual observations were made through the view cell.

2.2.4 Characterization of particles

2.2.4.1 Particle size and particle size distribution

Particle size (PS) and particle size distribution (PSD) were measured using a Mastersizer® 2000 (Malvern Instruments Ltd., Malvern, UK). The Mastersizer® 2000 uses the technique of laser diffraction to measure the size of particles. The technique of laser diffraction is based around the principle that particles passing through a laser beam will scatter light at an angle that is directly related to their size. The instrument can measure particles in the size range of 0.02 to 2000 μm[25].

Particle size distributions are calculated by comparing a sample's scattering pattern by using Mie Theory, which provides a rigorous solution for the calculation of particle size distributions from light scattering data. Mie theory is based on Maxwell's electromagnetic field equations[26]. It predicts scattering intensities for all particles, small or large, transparent or opaque. In order to do particle size measurement by utilizing Mie theory, refractive index of the drug is required, which was measured using Reichert ® AR 200 digital refractometer (Reichert Technologies, Depew NY) and average value of refractive index of 6 replicates was 1.34 ± 0.005.

Approximately 50 mg of SAS samples were added to 10 ml of DI water and sonicated for 1 minute prior to analysis. Each particle size measurement was performed in triplicate, with about 1000 particles being measured at each run.

The results are reported in % volume distribution as it is more pharmaceutically relevant. Appendix B shows a typical report generated for each particle size measurement. We utilised d_{50}, which is the diameter of 50^{th} percentile of distribution, and the span, which is the width of the distribution based on the 10^{th}, 50^{th}, and 90^{th} percentiles, for comparing various SAS samples.

$$\text{Span} = (d_{90} - d_{50})/d_{10} \quad \text{.....} \quad \textbf{Equation 1}$$

Instrument calibration: To verify the accuracy of measurements made by laser light diffraction method, monosized latex standards of 98 nm, 150 nm, 310 nm, 900 nm, and 2000 nm were tested in triplicate, using the method parameters described above. The standards were chosen based on expected particle sizes of SAS samples. d_{50} value obtained after measuring these standards were 86 $\pm$ 0.3 nm, 140 $\pm$ 0.2 nm, 268 $\pm$ 0.5 nm, 803 $\pm$ 0.8 nm, and 2035 $\pm$ 1.1 nm, respectively. The results, shown in Figure 4, provide an assurance that measurements made on SAS formulations will be accurate, within the instrumental limitations.

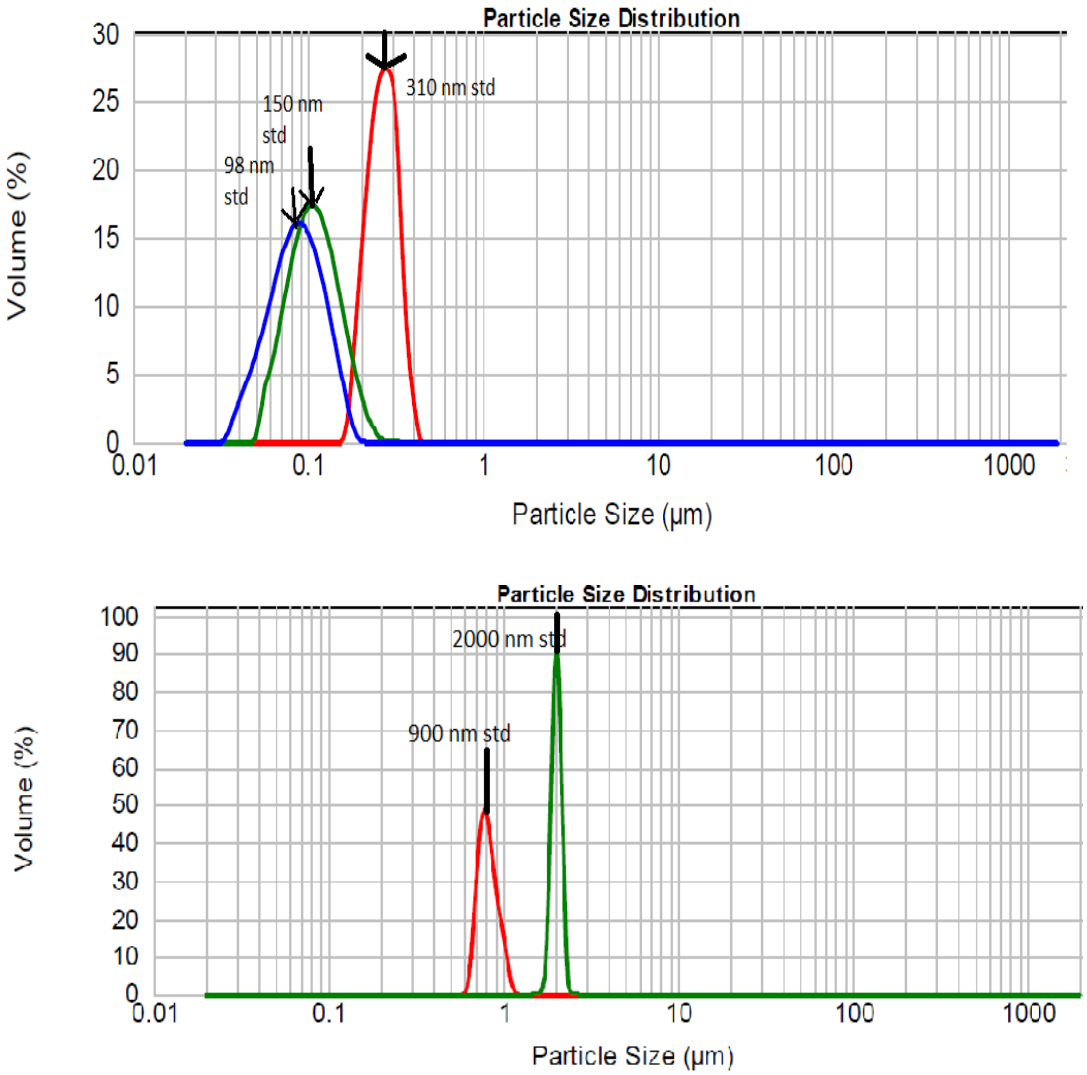

Figure 4. Volume based particle size distribution of polystyrene latex microspheres of various sizes

Since particle size distributions obtained with SAS was bimodal, for testing the accuracy of the instrument in measuring mixture of small and large particles, 150 nm diametered standard was mixed uniformly with 2000 nm diametered standard, in the ratio of 90:10. Results, as shown in Figure 5, showed a bi-modal distribution with d_{50} at 122 nm, and d_{90} at 1807 nm. Similarly, when 310 nm standard was mixed

uniformly with 900 nm standard, in the ratio of 70:30, a bi-modal distribution with d_{50} at 0.314 nm, and d_{90} at 0.937 nm, was obtained.

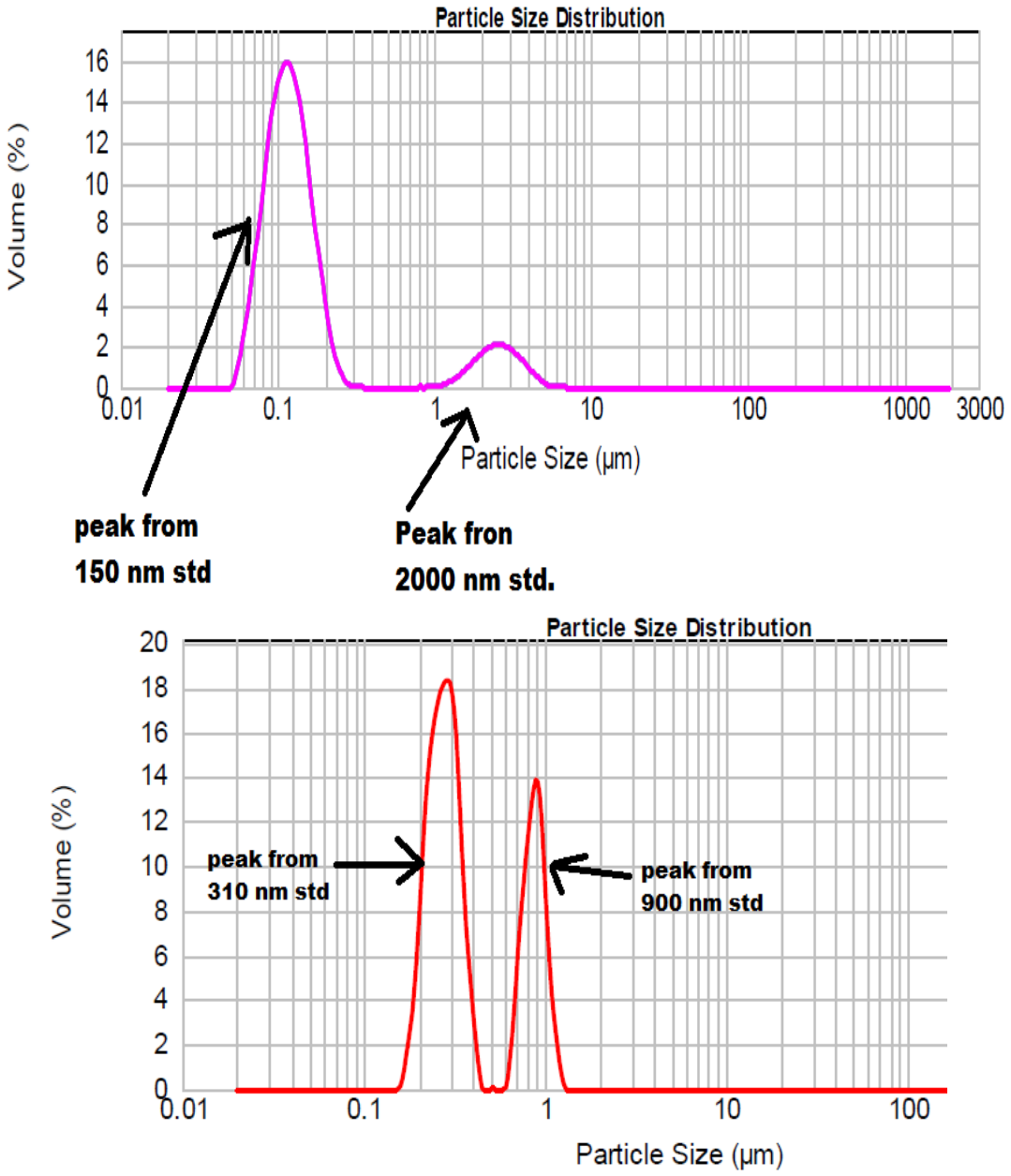

Figure 5. Volume based particle size distribution of 150 nm plus 2000 nm diametered polystyrene latex standards mixed at a ratio of 90:10 (TOP), and 310 nm plus 900 nm standards mixed at a ratio of 70:30 (BOTTOM).

In order to verify the reproducibility of Malvern particle size measurements, one of the SAS formulation sample was run 10 times. The average value for d_{50} was 371.5 $\pm$ 10.7 nm, with a relative standard deviation (RSD), also called coefficient of variation, of 2.88%. The results demonstrate that the reproducibility of measurements is acceptable.

Samples obtained with SAS were sonicated prior to particle size measurement. Samples were exposed for 0, 0.5, 1, 3 and 5 minutes of sonication. Results showed that there was no further reduction in sample particle size after 0.5 minutes sonication. Hence, 1 minute sonication was chosen as the standard sonication, which was sufficient to dissolve the polymer and to obtain sufficient de-agglomeration.

2.2.4.2 Surface appearance

The surface morphological analysis of the sample was performed using an ultra- high resolution digital light microscope , model VHX 600, manufactured by Keyence (KEYENCE America, Elmwood Park, NJ). Scanning Electron Microscopy (SEM) was performed at 15 kV accelerating voltage using model TM-1000 Tabletop Microscope ® manufactured by Hitachi **(**Hitachi High-Technologies Europe GmbH, Germany) . Small amount of SAS formulation sample was applied on mutual conductive adhesive tape on aluminum stubs.

2.2.4.3 Zeta Potential

Surface charge of nanoparticles was determined by zeta potential measurement on a Malvern Zetasizer 2000 HS (Malvern Instrument Ltd., Malvern, UK). The instrument was calibrated routinely with a −50 mV latex standard.

2.2.5 Description of the statistical method

2.2.5.1 Design of Experiment (DOE)

Determination of statistically significant variables of the SAS process was made by the use of DOE approach. Analysis of the data from DOE identifies the statistical importance of different factors on the measured responses, and the methods are described in basic textbooks[27]. We utilized MODDE® software (UMETRICS, version 9.0.0) for designing the fractional factorial study and for performing analysis on the data obtained.

Using a conventional approach, to study *k* different factors, each having only two levels, the minimum number of experimental runs needed is $2 \times 2 \times ... \times 2 = 2^k$. We identified seven factors in our DOE study. The *factorial* design would have required 2^7, i.e., 128, experiments be conducted. To reduce the number of experiments, two level *fractional factorial* design, which is an accepted approach by the United States FDA[28-29] and other researchers[30-32], was selected

In this method, some of the high-order interactions terms are replaced by an additional experimental factor. Although some information can be lost during the testing process, *fractional factorial* designs are very helpful as screening designs, because they allow for the separation of the important effects from the unimportant effects at an early stage of experimentation.[33]

2.2.5.2 Factor and level selection

Seven factors that were identified and used for this screening DOE study were temperature (T) , and pressure (P) of the precipitator; drug concentration (C_d), and polymer concentration (C_p); organic solvent (F_{liq}) and antisolvent (F_{CO2}) flow rates; and nozzle diameter, d_n. The two levels for each of the seven factors selected are shown in Table 3. Values were chosen based on the preliminary experiments conducted with SAS while taking into account limitations of our equipment.

Table 3. Factors and Level selection for DOE

Factor	**Abbr.**	**Levels (Low to High)**
Temperature	T	35 to 55^0C
Pressure	P	80 to 120 bar
Drug Conc.	C_d	10 to 20 mg/mL
Polymer Conc.	C_p	20 to 70 %
solvent spray rate	F_{Liq}	2 to 3 ml/min
CO_2 addition rate	F_{CO2}	10* F_{Liq}, to 20* F_{Liq} g/min
Nozzle diameter	d_n	100 to 200 µm

The lower temperature limit of 35^0C is to ensure that all the experiments were carried out in the supercritical region. The upper temperature limit of 55^0C was established based on experience gained during the preliminary experiments with the process. It is further considered that a range of 20°C is sufficient to estimate the effect of temperature since such an increment leads to a large variation in the binary vapour–liquid equilibrium diagram of the acetone-CO_2 system.

The pressure condition limits of 80 to 120 bar were set to ensure a high solubility of supercritical carbon dioxide in acetone, and with the aim of staying within or near the supercritical region (73 bar). At pressure conditions greater than 150 bar, and in the presence of acetone, the drug was freely soluble in supercritical carbon dioxide and no precipitation was seen inside the vessel.

Drug concentration below 10 mg/mL resulted in no precipitation and hence was chosen as the lower limit. The upper limit of 20 mg/mL was established based on solubility limit of drug in acetone, which is 25 mg/mL. Polymer concentration limit of 20-70% was selected to see the effect of polymer on drug precipitation mechanism over a wide range of polymer concentration.

Flow rate limits for acetone solution and supercritical carbon dioxide were established to obtain both a wide range of acetone mass fraction inside the precipitator vessel and a wide range of CO_2/acetone flow ratio. In all of these experimental conditions, CO_2 mole fraction was always maintained at 0.91 or higher. Maintaining high CO_2 fraction is important to obtain optimum effectiveness of CO_2 as an anti-solvent, as reported by other researchers as well[9].

It was noticed during the preliminary experiments that the low level acetone flow rate of 1 mL/min in combination with 200 μ diametered nozzle did not atomize the solution, and no precipitation could be obtained. As a result, a higher flow rate (2 – 3 ml/min) was selected. We were limited to 100 μm diametered nozzle as the smallest nozzle diameter, because it was the smallest-diametered nozzle available in the market for this instrument. The upper limit of nozzle diameter was setup to 200 μm.

2.2.5.3 Response identification

Three responses which were d_{50} (particle diameter of 50^{th} percentile of distribution), span (the measure of particle size distribution), and % yield, were selected. The yield in percentage is calculated as the ratio of the solute (drug + polymer) processed and the amount collected following SAS processing. Particles are collected on top of 0.22 μm filter paper in the bottom of vessel, as well as scrapped from vessel walls. When a sticky mass is obtained around the nozzle apart from the bulk powder, this portion which was not usable was discarded and not considered in the yield calculation.

2.2.5.4 $2^{(7-3)}$ Fractional factorial design generation & data interpretation

In $2^{(7-3)}$ fractional factorial screening design 16 experiments were required. The design matrix is summarized in Table 4. Designs with factors that are set at two levels implicitly assume that the effect of the factors on the dependent variable of interest is linear. It is however impossible to test whether or not there is a non-linear (e.g., quadratic) component in the relationship between a factor A and a response, if A is only evaluated at two points (.i.e., at the low and high settings). Hence, in order to test that, the relationship between the factors in the design and the response is non-linear,

we included three more runs where all factors are set at their midpoint. Such runs are called **Center-point Runs** (or center points) which provide a measure of process stability and inherent variability and validate the curvature. As a rough guide recommended by National Institute of Standards and Technology (NIST)[34], approximately 3 to 5 center point runs should be added to a fractional factorial design.

The statistical analysis of the data is carried out in three sections. Firstly, fitting of the model accepted to my findings will be evaluated, by performing Analysis of variance (ANOVA). Secondly, the important factors will be ranked, and finally the optimum processing as well as formulation conditions will be identified. The methodology is described in detail in a text book, written by creators of Modde® software[35].

When ANOVA is carried out on the responses obtained from the DOE, four key values are generated for each response: they are R^2, Q^2, Model validity, and Reproducibility. R^2 is the percent of the variation of the response explained by the model. R^2 is a measure of fit, i.e. how well the model fits the data. Q^2 is the percent of the variation of the response predicted by the model according to cross validation. Q^2 provides information, how well the model predicts new data. Model validity is a measure of the validity of the model. When the model validity value is larger than 0.25, there is no Lack of Fit (LOF) of the model. Reproducibility is the variation of the response under the same conditions, compared to the total variation of the response under different conditions.

To interpret the influence of various factors on the measured responses, coefficient plots will be generated. The coefficient plot displays the coefficients, when the selected response is changed from low to high value, with the confidence interval as error bars.

Table 4: A Seven Factor Fractional Factorial (2^{7-3}) Design Matrix for SAS processing.

Exp Name	Run Order	Temp.	Pressure	Drug Conc.	Poly. Conc.	Liq. spray rate	CO_2 rate	Nozzle diameter
		T	**P**	**C_d**	**C_p**	**F_{liq}**	**F_{CO2}**	**d_n**
		^{0}C	Bar	mg/ml	mg/ml(%)	ml/min	g/min	µm
		1	2	3	4	5=123	6=234	7=134
N1	14	35	80	10	2.5 (20%)	2	10*Liq	100
N2	3	55	80	10	2.5 (20%)	3	10*Liq	200
N3	13	35	120	10	2.5 (20%)	3	20*Liq	100
N4	19	55	120	10	2.5 (20%)	2	20*Liq	200
N5	4	35	80	20	5.0 (20%)	3	20*Liq	200
N6	12	55	80	20	5.0 (20%)	2	20*Liq	100
N7	8	35	120	20	5.0 (20%)	2	10*Liq	200
N8	16	55	120	20	5.0 (20%)	3	10*Liq	100
N9	11	35	80	10	23.3 (70%)	2	20*Liq	200
N10	17	55	80	10	23.3 (70%)	3	20*Liq	100
N11	7	35	120	10	23.3 (70%)	3	10*Liq	200
N12	5	55	120	10	23.3 (70%)	2	10*Liq	100
N13	10	35	80	20	46.6 (70%)	3	10*Liq	100
N14	18	55	80	20	46.6 (70%)	2	10*Liq	200
N15	1	35	120	20	46.6 (70%)	2	20*Liq	100
N16	15	55	120	20	46.6 (70%)	3	20*Liq	200
N17	9	45	100	15	12.3 (45%)	2.5	10*Liq	150
N18	6	45	100	15	12.3 (45%)	2.5	10*Liq	150
N19	2	45	100	15	12.3 (45%)	2.5	10*Liq	150

The Table 4 shows that out of 7 variables, three of them were confounded, or aliased. Confounded variables are shown in columns 5-7. We decided to alias spray rate of liquid in column 5, to columns 1-2-3, because the results of preliminary experiments and published literature [30] suggested that the interaction effect of temperature (column 1), pressure (column 2), and drug concentration (column 3) would be negligible compared to main effect of spray rate of the liquid. In a fractional factorial designs, the less probable interactions can be ignored. Therefore, by confounding such less probable three factor interactions of columns 1-2-3 with the spray rate of liquid, we think that the calculated effect of column 5 will mainly be due to spray rate of liquid. Using the similar justification, we confounded interactions between 234 factors with CO_2 flow rate, and interactions between factors 134 with nozzle diameter.

3.0 RESULTS AND DISCUSSION

Prior to initiating SAS experiments of GF and polymer with organic solvent, a series of qualitative experiments were performed, to verify the insolubility of GF in pressurized CO_2, the miscibility of acetone and DMSO in pressurized CO_2, and the insolubility of GF in binary system of organic solvent plus pressurized CO_2. A schematic diagram of the apparatus used for the solubility studies is shown in Appendix A. The results of these experiments, detailed in Appendix C and D, showed that both acetone and DMSO have excellent miscibility with pressurized CO2, and scCO_2 can act as an anti-solvent for GF.

3.1 Production of GF particles with SAS

Before initiating co-precipitation experiments, GF crystals were obtained without any polymer, to observe the changes occurring in the drug morphology and particle size. To define the working domain of SAS process, which was necessary to set up design of experiment; temperature (T) , pressure (P), solution flow rate (F_{liq}), CO_2 flow rate (F_{CO2}), and concentration of GF in solvent(C_d), were tested in the preliminary experiment. Using acetone and DMSO we varied the operating parameters in the range of : T = 45–90°C, P = 80–300 bar, F_{liq} = 1 – 4 ml/min, F_{CO2} =10x to 30x F_{liq} , and C_d = 20% - 80% of saturation solubility in organic solvent. Nozzle diameter (d_n) was kept constant at 100μm.

No precipitation was observed at drug concentration lower than 40% saturation solubility in organic solvent, or pressures greater than 200 bar, due to increasing

solubility of GF in solvent-CO_2 mixtures. In case of acetone, 40% saturation solubility is 10 mg/ml, and in DMSO it is 24 mg/ml. Long fibrous and needle like product was obtained at $C_d \geq 40\%$ of saturation solubility in organic solvent , and $75 \leq P < 200$ bar. Table 5 summarizes the variables tested in preliminary experiments.

Table 5: Preliminary SAS experiments of GF using Acetone and DMSO

Run #	Org. Solvent	Temp. ^0C	Pressure bar	Drug Conc. mg/mL	Spray Rate ml/min	CO_2 flow rate (g/min)	Observation
1	Acetone	45	120	10	4	45	Crystalline long needles/fibers of 500 to 2000 µm
2	Acetone	50	205	10	2	60	no particles
3	Acetone	45	170	10	2	20	Crystalline long needles/fibers of 500 to 2000 microns
4	Acetone	90	90	9	2	20	no particles
5	Acetone	90	150	20	1	20	Crystalline long needles/fibers of 500 to 2000 microns
6	Acetone	75	80	10	2	20	Crystalline long needles/fibers of 500 to 2000 microns
7	DMSO	40	150	20	2	30	no particles
8	DMSO	50	225	23	2	30	no particles
9	DMSO	50	80	25	2	60	Crystalline long needles/fibers several mm long
10	DMSO	50	150	25	2	60	Crystalline long needles/fibers several mm long
11	DMSO	45	200	50	2	30	Crystalline long needles/fibers several mm long
12	DMSO	90	210	50	2	30	no particles

Untreated GF particles (as is GF) comprises of irregular shaped particles (Fig. 6) which have a mean particle size of 14 μ and size distribution of 5–21 μ, as measured by Malvern instrument.

The product obtained by supercritical processing has much larger needle shape, 500 μm to few mm in length (Figure 6). The products obtained with acetone and DMSO were different in size, and uniformity. DMSO produced thicker, longer, non-uniform crystals (Figure 7-a), whereas acetone based GF crystals were thinner, shorter in length, and lot more uniform (Figure 7-b).

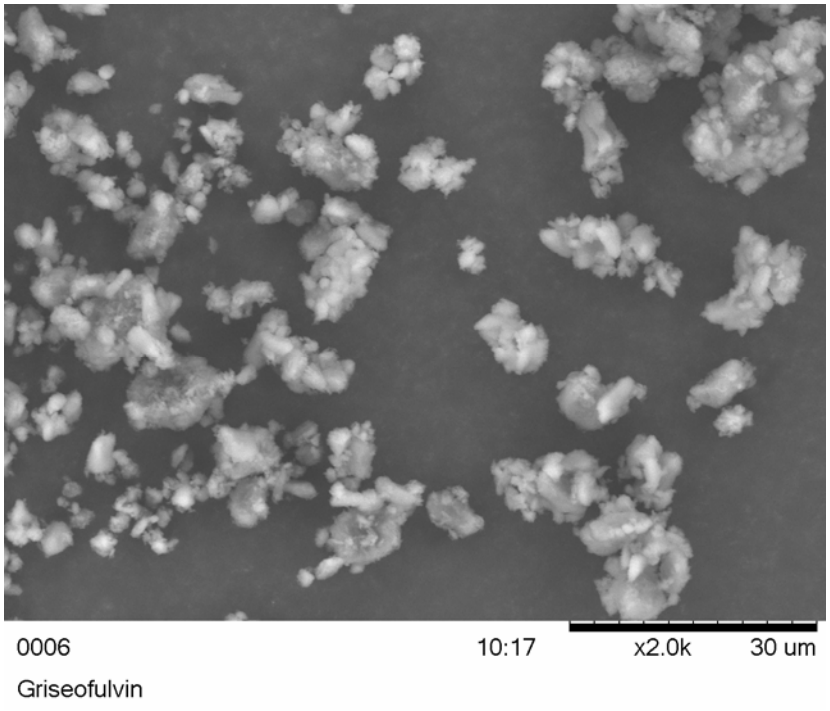

Figure 6: Scanning electron microscopy (SEM) image of untreated as-is GF

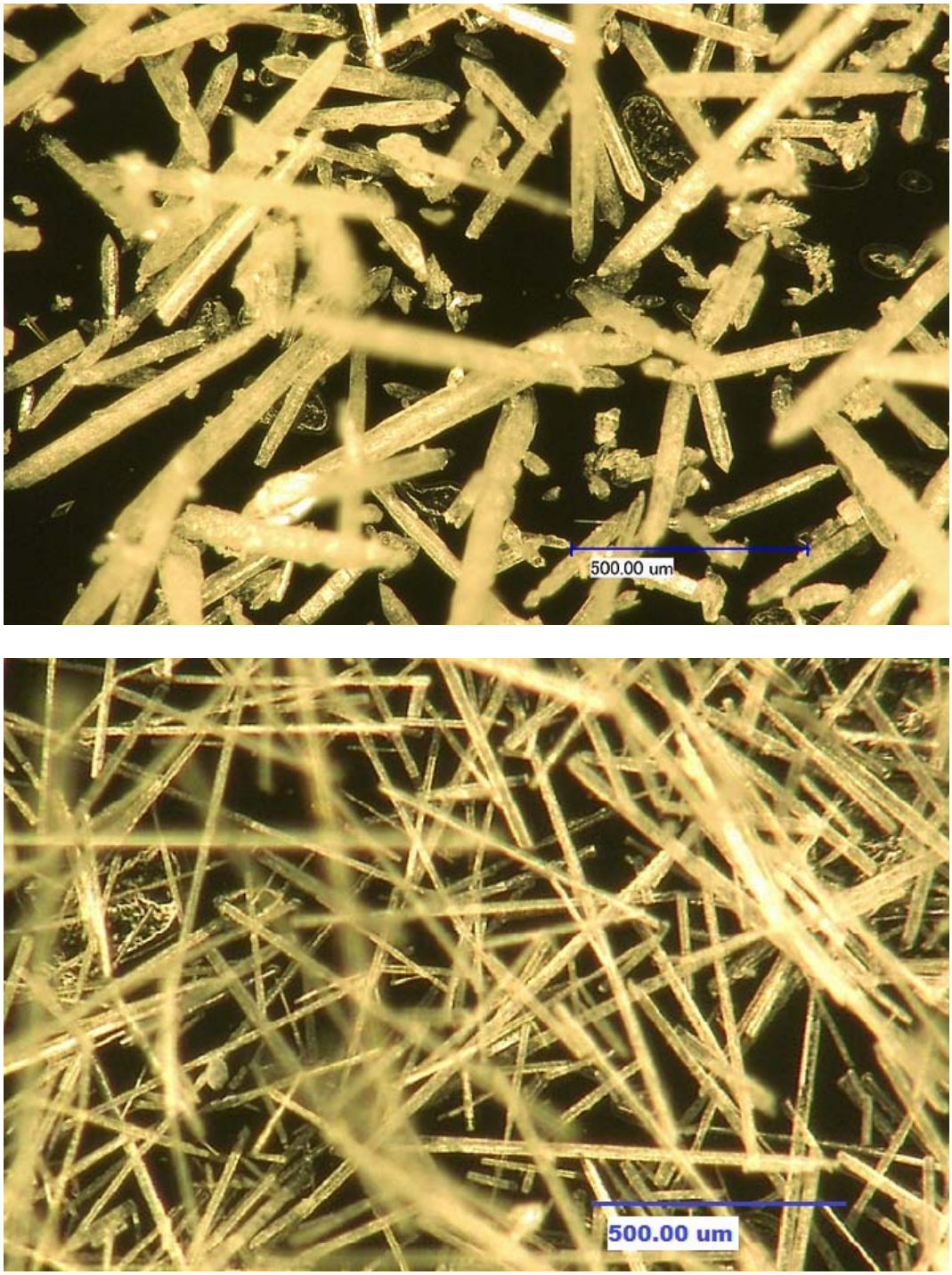

Figure 7: GF precipitated from DMSO (top) and GF precipitated from Acetone (bottom)

3.2 Polymer effect on particle properties of GF

Based on the selection criteria discussed in the introduction section, Kollidon® VA64 (KVa64) was selected as the polymer for coprecipitation. When drug (GF) and polymer (KVa64) were coprecipitated, the size of the crystals changed significantly. Very light, voluminous and fluffy fibrous powders as typical of the $scCO_2$-precipitated samples were obtained in all experiments. Coprecipitated fibers were 1-50 μm in length, as opposed to 500 μm to 2 mm long fibers obtained with GF. This change is likely to be the result of different precipitation mechanisms that the drug undergoes in the presence of polymer. During precipitation of sole GF, a nuclei is formed which can coalesce together to form large stable crystals. The growth of nuclei must be the predominant force causing formation of large and needle-shaped particles.

Some polymers like HPMC[36], polyethylene glycol[36], PVP[22], Poly (sebacic anhydride) [23], are known to inhibit particle growth of the drugs that are treated with, by adsorbing on the surface of drug particles. Surface adsorption of KVa64 on GF drug crystals would have prevented the nuclei coalescence, and hence smaller particles were produced. Additionally, many polymers can act like a stabilizer and minimize the particle agglomeration.

SAS processed material is analyzed for particle size, by dispersing it in an aqueous media. Malvern instrument detected bimodal distributions of particle size through out this study, regardless of the processing conditions. In Figure 8, an example of particle size distribution of the SAS coprecipitates, measured by Malvern instrument is

shown. The appearance of the same material when investigated under SEM, is shown in Figure 9. While performing an SEM analysis, a dry powder obtained from SAS processing is used, and it is difficult to de-agglomerate . The size of intact drug-polymer mixture was approximately 5 to 10 μm.

The size of the products obtained provides some information on the location of the particle precipitation. The bimodal distribution suggest the occurrence of the precipitation at multiple times and locations along the length of the precipitation vessel. The particles that are formed as soon as they come out of the nozzle would be smaller as compared to particles that are formed at the bottom of the vessel. Similar bimodal distribution was reported by Jarmer et al., [23] when they precipitated griseofulvin in the presence of polymer Poly (sebacic anhydride), using a variation of SAS process called PCA (Particles from Compressed Antisolvent). Their particle sizes ranged from 0.5 μm to 100 μm, with one peak observed around 1 μm, and second peak observed around 30 μm. When Varughese et al., [37] precipitated indomethacin from dichloromethane using SAS technology; they also obtained bimodal particle size distribution, ranging from 0.1 μm to 100 μm.

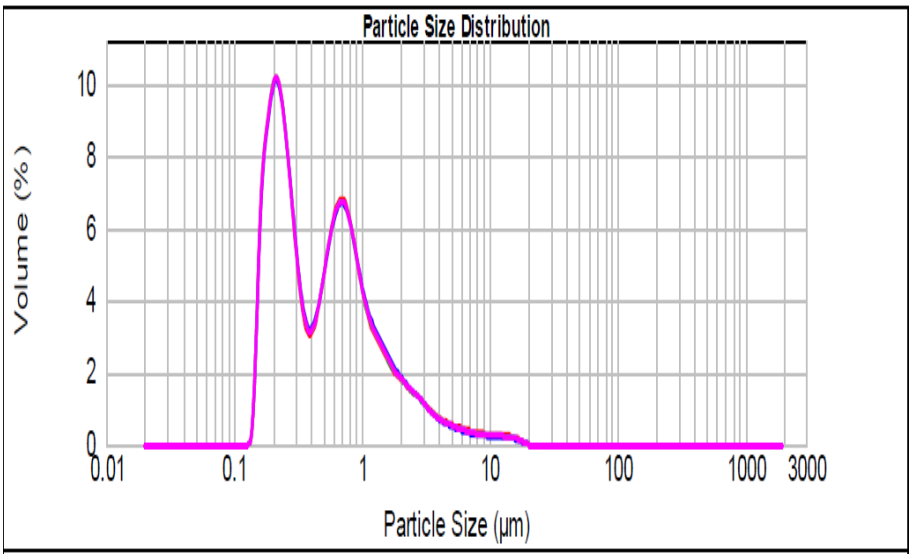

Figure 8: Particle size distribution of SAS formulation containing GF and Kollidon VA64 (processed at 45^0C temperature, 85 bar pressure, 20 mg/ml drug concentration, 5 mg/ml polymer concetration, 2 ml/min liquid spray rate, 40 g/min CO2 addition rate, and 100 µm nozzle diameter), measured by Malvern instrument

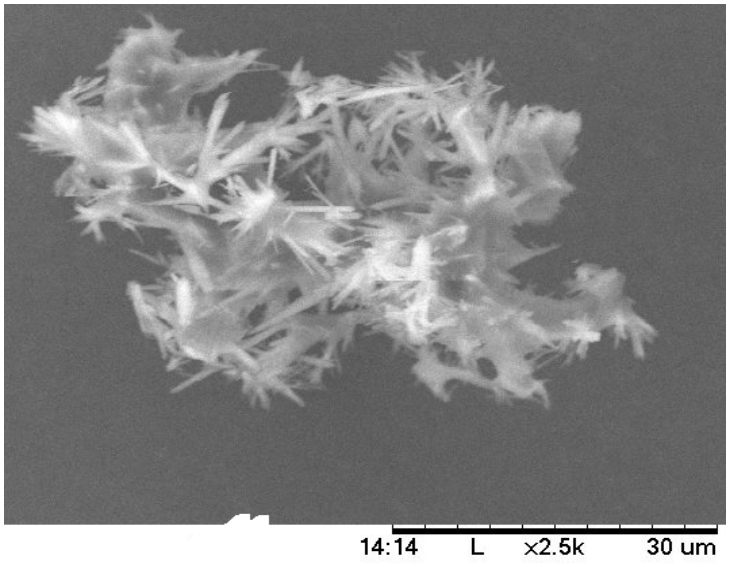

Figure 9: Dry coprecipitates of GF & Kollidon VA64 obtained immediately after SAS processing, observed under SEM

3.3 Statistical analysis of data from DOE

Table 6 summarizes the raw data obtained after executing experiments of Table 4 of each run from DOE. The d_{50} particle size of the products obtained ranged from 140 nm (experiment N8) to 950 nm (experiment N9). The lowest yield was 8%, for experiment N16 and the highest yield was 95%, in experiment N17. The low yields observed in experiments N2, N3, N4, N6, N9-N12, and N15-N16, appear to be the results of low drug concentration, and high pressure. The span value which is the measure of particle size distribution was ranged from 0.494 to 4.962. The smaller the span value, the narrower the distribution.

The zeta potential values obtained ranged from -31.1 mV to -35.5 mV. However the zeta potential values were not used as one of the responses during the statistical analysis.

The raw data was then analyzed using Modde® statistical software. Figures 10 – 13 provide the outcome of analysis in a graphical manner.

Table 6: Results of experiments conducted using DOE

Expt. Name	d_{50} nm	Yield %	PSD Span	Zeta potential (mV)
N1	396	88	4.962	-31.8
N2	281	57	4.665	-32.5
N3	237	17	3.325	-33.0
N4	712	58	0.68	-33.5
N5	711	76	2.599	-32.9
N6	228	58	4.348^{+}	-31.1
N7	900	80	0.5	-31.5
N8	140	87	3.982	-34.0
N9	950	28	0.49	-34.5
N10	175	33	4.469	-35.4
N11	571	40	3.2	-35.5
N12	233	25	3.222	-35.2
N13	322	91	3.97	-33.8
N14	658	75	0.494	-34.9
N15	*	12	*	*
N16	*	8	*	*
N17	596	95	3.201	-34.5
N18	546	85	3.352	-35.2
N19	562	84	3.306	-31.7

* particle size, and zeta potential data could not be obtained since the yield were too low,
+ outlier

3.3.1 Summary of Fit Plot

Summary of fit plot, shown in Figure 10, displays the 4 key values for each response. These values are; R Square (R^2) , Q Square (Q^2) , Model Validity, and Reproducibility.

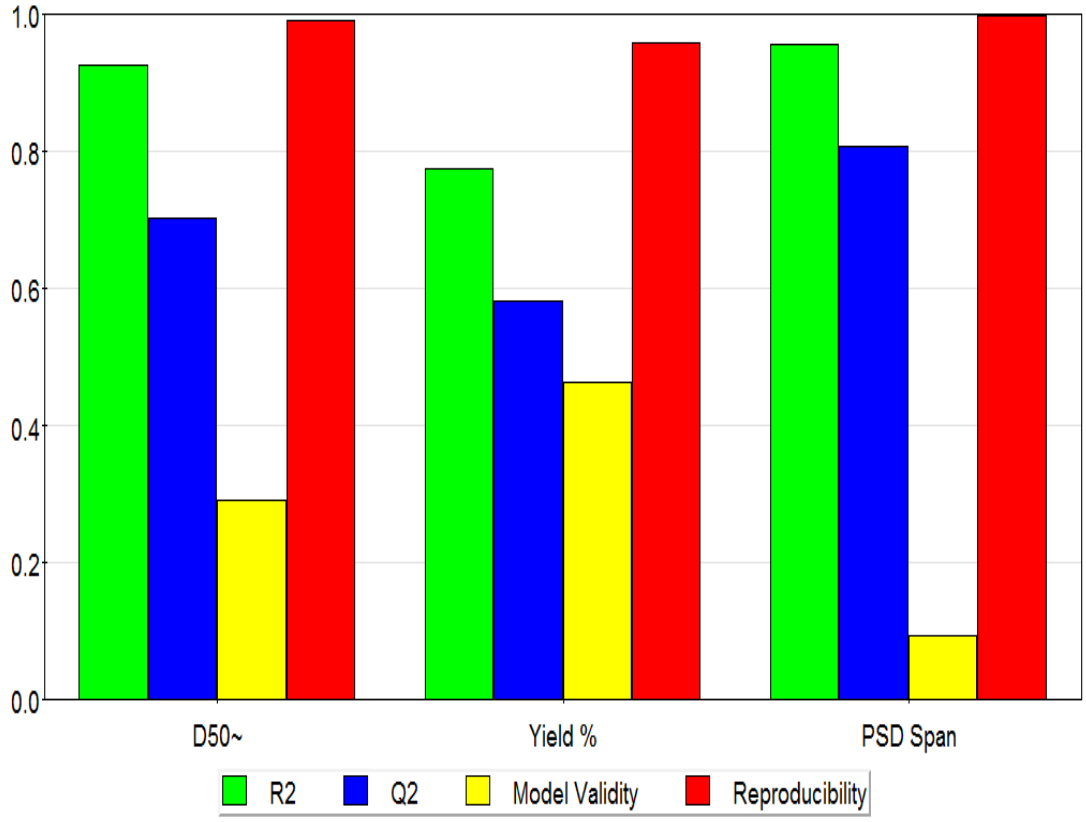

Figure 10: Summary of Fit Plot

Values close to 1 for R^2 indicate very good models with excellent predictive power. R^2 value should be at least 0.5. In our experiments, R^2 values were 0.93 for d_{50}, 0.78 for % yield, and 0.96 for PSD (span).

Q^2 values were 0.70, 0.58, and 0.80 for d_{50}, % yield, and PSD (span) respectively. Q^2 value should be at least 0.1 for a good model, and should be at least 0.5 for a significant difference.

A model validity bar of 1 represents a perfect model. When the model validity is less than 0.25 there is significant Lack of Fit (LOF). Model validity values were 0.29, 0.46, and 0.1 for d_{50}, % yield, and PSD (span) respectively

There are many causes of LOF which result in poor "Model Validity". Statistical outliers as well as non-normally distributed responses can cause LOF. However, when there is true LOF, both R^2 and Q^2 will be small. If there is a good R^2 and Q^2 (> 0.5) and a reproducibility value is close to 1.0, the lack of fit is probably artificial.

We ran a normal probability plot of residuals to find the statistical outliers. The normal probability plot of residuals displays the residuals (standardized or studentized) on a double log scale. This plot helps to detect statistical outliers and assess normality of the residuals. If the residuals are random and normally distributed, the normal probability plot of the residuals has all the points lying on a straight line between -4 and + 4 studentized or standardized standard deviation. When we plotted the normal probability plot of residuals, shown in Figure 11, we found that experiment number 6 was an outlier for particle size distribution. The outlier was not removed from the calculation. Finally, due to the reasons explained here, the low

values for model validity in case of particle size distribution (0.1) , was not cause for concern.

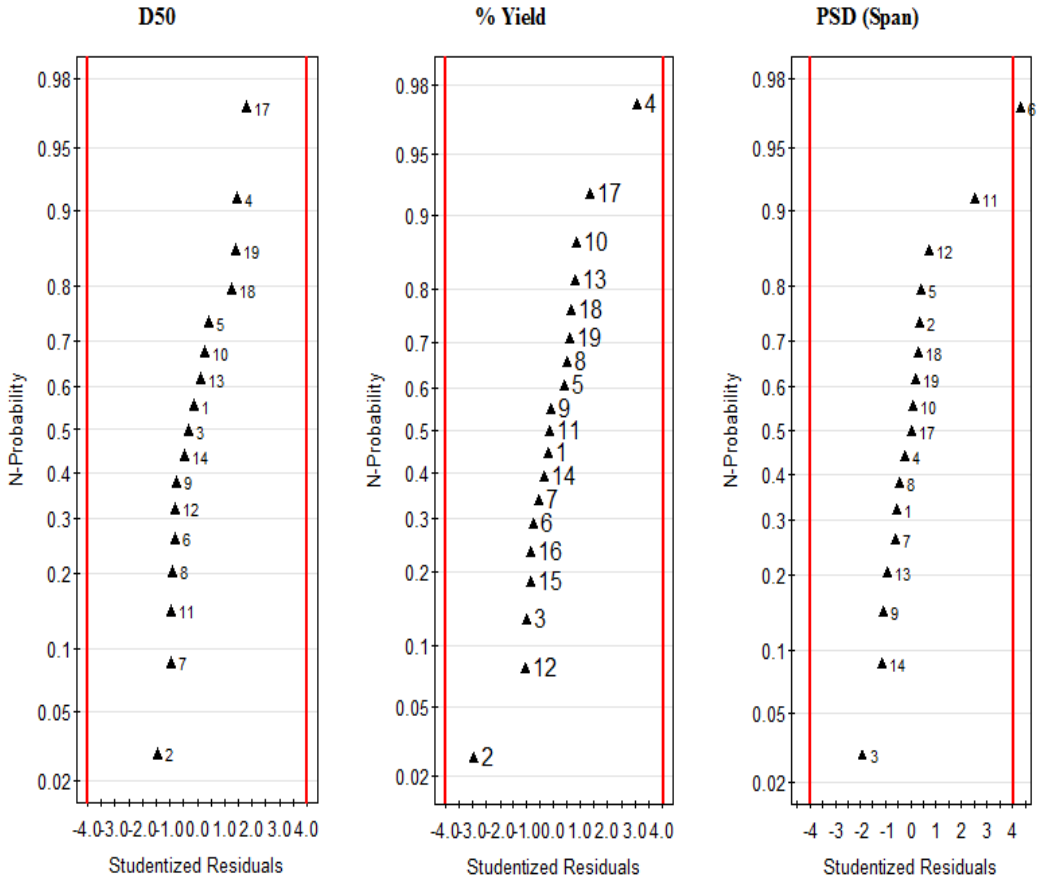

Figure 11: Normal Probability Plot of Residuals

When the reproducibility bar is 1.0, the pure error is 0. This means that under the same conditions the values of the response are identical. If the reproducibility is below 0.5, it implies that there is a large pure error and poor control of the experimental set up (the noise level is high). The validity of such models cannot be assessed. This also results in poor R^2 and $Q^{2.}$. In our experiments, the values for reproducibility were almost 1.0, for d_{50}, % yield, and PSD.

3.3.2 Identification of statistically significant variables of SAS process

The coefficient plot (Figure 12) displays the statistically significant factors that are affecting d_{50} (Figure 12-a), % yield (Figure 12-b), and particle size distribution (Figure 12-c). The data obtained is centered and scaled in this plot. The scaling of the data allows comparable coefficients. The size of the coefficient bar represents the degree of change in a response when a factor varies from low value to high value, while the other factors are kept at their averages. The coefficient is considered significant (different from the noise), when the 95% confidence intervals (shown as bars in Figure 11 a, b, and c) do not cross zero.

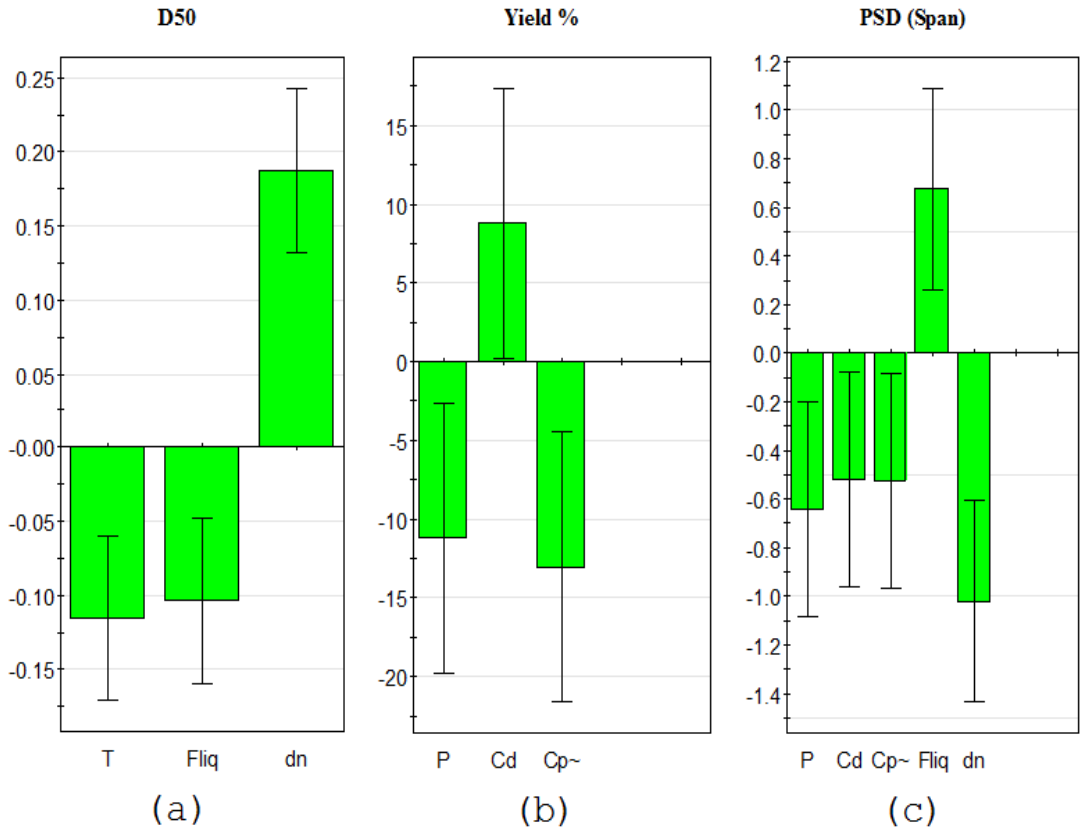

Figure 12: Coefficient Plot

For the particle size (d_{50}) response, three significant factors identified were; temperature, spray rate of liquid, and nozzle diameter. The nozzle diameter was the most important factor impacting the particle size as it is the largest coefficient for d_{50} response. When nozzle diameter increased from 100 to 200 μm, the particle size (d_{50}) was also increased.

Smaller nozzle diameter produced finer droplet and more pronounced atomization of the liquid spray, leading to smaller particles. The spray rate of liquid had an opposite effect on d_{50}, compared to nozzle diameter. Increased spraying rate can produce better atomization of the liquid spray, as more drug is available, super saturation will be reached quicker, leading to smaller particle sizes. Similarly, higher temperature increases the miscibility of acetone with $scCO_2$; at the same time higher temperature of 55^0C may cause evaporation of acetone. Both of these phenomena ultimately result in quicker removal of acetone, and hence smaller particles are produced with increase in temperature. Additionally, higher temperature results in lower viscosity of polymer solution, which enhances mass transfer and more efficient removal of solvent, resulting in quicker precipitation and smaller particle size. The order of importance of the seven factors affecting d_{50} can be summarized as follows;

For d_{50} : d_n (nozzle diameter) > T(Temperature) > F_{liq} (spray rate of liquid) > P(pressure), C_d (drug conc), C_p(pol.conc), F_{CO2}(rate of CO2)

In Figure 12-b, similar analysis is shown for % yield. It can be seen that the polymer concentration has highest influence on % yield. The increase in % of polymer in the formulation causes reduction in the yield. The cause may be the presence of excessive

polymer which leads to precipitation in the nozzle, leading to low yield. Additionally, as stated earlier, higher polymer concentration causes increase in solution viscosity which leads to entanglement of polymer chains and delay in jet break up. This delay in jet break up makes solvent removal and mass transfer difficult, causing drug extraction instead of precipitation, causing low yield. Increase in the pressure also leads to a significant reduction in yield. This is understandable as increased pressure increases the solubility of drug in $scCO_2$, leading to less precipitation of the drug. Drug concentration has an opposite effect on % yield. The yield increases with increasing drug concentration. This is due to availability of more drug in the liquid droplets causing quicker super saturation which prevents extraction of drug from the precipitation vessel.

The order of importance of the factors affecting % Yield can be presented as follows;

For % Yield: C_p(pol.conc) > P(pressure) > C_d (drug conc) > T(Temperature), F_{liq} (spray rate of liquid) , F_{CO2}(rate of CO2), d_n (nozzle diameter)

Finally, a similar analysis conducted for PSD shown in Figure 12-c, revealed that liquid spray rate had the most pronounced influence on PSD. Additionally, there were four more factors that also had significant impact on the particle size. These were pressure, drug concentration, polymer concentration, and the nozzle diameter.

The explanation of this finding is as follows: Consider that there are two opposing effects of increased liquid spray rate: reduction in particle size and increase in particle size distribution. When the flow rate of liquid is increased, the precipitation

vessel contains larger quantity of solute (both drug and polymer). Increased amounts of solute may reduce anti-solvent effect of CO_2, and growth as well as coalescence of nuclei may dominate the process which will cause broader particle size distribution. Within the given operating conditions of our experiments, both of these phenomena are effective at any given time. These competing mechanisms may also explain the bi-modal distribution of the particles.

An increase in pressure, and drug concentration causing smaller PSD is explainable using the same arguments made in previous sections. An increase in polymer concentration provides more availability of polymer for adsorption on drug nuclei, and hence more uniform drug crystals are produced, leading to smaller PSD. An increase in the nozzle diameter creating narrower PSD was unexpected. It could be that increased nozzle diameter, uniformly produced significantly larger particles, and hence the PSD was narrow. The order of importance of the factors for PSD can be summarized as follows;

For PSD: F_{liq} (spray rate of liquid) > d_n (nozzle diameter) > C_d (drug conc) > P(pressure) > C_p(pol.conc) > T(Temperature), F_{CO2}(rate of CO2),

3.3.3 Optimization using Sweet Spot Analysis

Finally, based on the information gathered from the outcomes of statistical analysis, we carried out a Sweet Spot analysis which allowed us to predict the values for formulation and process variables, resulting in responses that we desire. We wanted to produce *in-situ* nano particles, hence we chose d_{50} range of 0 to 900 nm. A desirable yield of 70 to 100% would be efficient for the process. Lastly, a narrow PSD (span value of 0 to 3.0) would allow more predictable dissolution behavior. While performing the sweet spot analysis, drug concentration was kept constant at 20 mg/ml as that was important to obtain high yield. Polymer concentration was fixed at 20%, in order to formulate a product with minimum amount of polymer, and CO_2 addition rate was fixed at 40 g/min which was 20 times the spray rate of liquid.

It can be seen from Sweet Spot analysis shown in Figure 13, that, in order to achieve the responses within the desired range described above, we could choose different set of values for the variables.

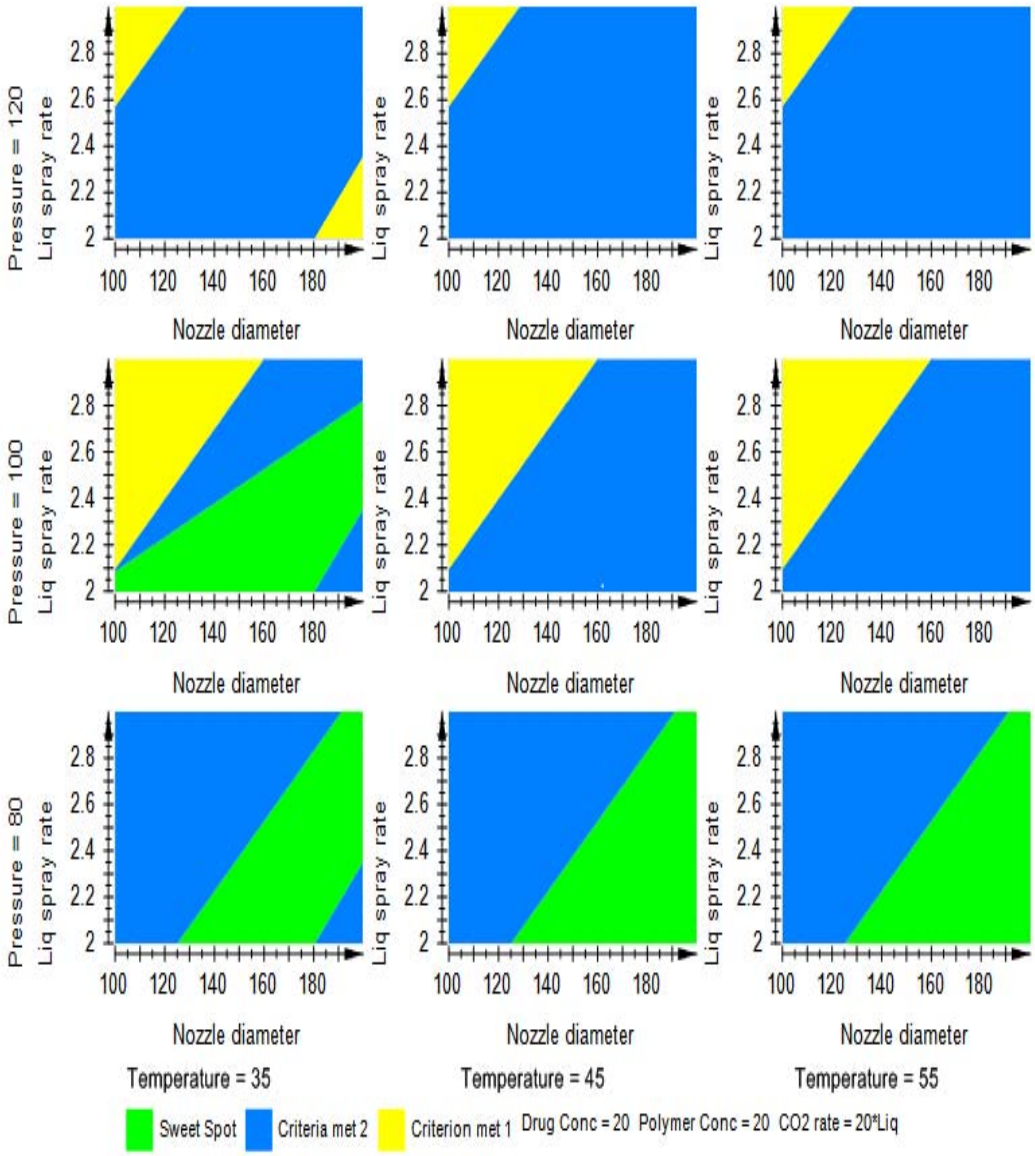

Figure 13: Sweet Spot Analysis

A confirmation run was performed at a temperature of 45^0C, pressure of 80 bar, nozzle diameter of 150 μm, liquid spray rate of 2 ml/min, drug concentration of 20 mg/ml, polymer concentration of 20%, and CO2 addition rate of 40 g/min. Properties of the produced product are summarized in Table 7, and they concur with predictions of sweet spot analysis.

Table 7: Properties of optimized SAS formulation of GF coprecipitated with KVa64

	d_{50}	Yield (%)	PSD (Span)
Optimized Formulation (Lot # OP1)	362 nm	89	2.711

4.0 CONCLUSIONS

A conventional SAS process yields GF crystals which are needle shaped, and several mm long. Using the coprecipitation approach in SAS processing, one can successfully produce *in-situ* nanoparticles of GF having d_{50} value of approximately 0.4 μm. The fractional factorial design $2^{(7-3)}$ was applied for screening of large number of variables, allowing identification of statistically significant factors all within 19 experimental run. The factors that impacted the particle size the most, were the nozzle diameter, temperature, and spray rate of liquid, in the order of decreasing importance. In case of particle size distribution, nozzle diameter, spray rate of liquid, drug concentration, pressure, and polymer concentration played significant roles. Whereas, the yield was affected by polymer concentration, pressure, and the drug concentration. Additionally, we were able to find optimum processing and formulation variables, which would consistently deliver product of high yield, small particle size, and narrow particle size distribution.

Optimized SAS formulation of GF was crystalline in morphology, regardless of changing formulation and processing conditions. There was no evidence of any bonding between the polymer and the drug. BET surface area analysis demonstrated no significant differences in the surface area of optimized SAS formulation (5.2457 m2/g) and the drug itself (5.2095 m2/g). Zeta potential values of the SAS formulations indicated that the coprecipitates when added to an aqueous environment, formed a stable de-agglomerated suspension. The dissolution of the optimized formulation increased from 10% to almost 80% after 100 minutes. Finally, intrinsic

dissolution rate (IDR) of an optimized SAS formulation (0.0065 μg/cm2/min) was 58% better than that of micronized GF (0.0038 μg/cm2/min) in physical mixture**.**

REFERENCES

1. Hecq J, Deleers M, Fanara D, Vranckx H, Amighi K 2005. Preparation and characterization of nanocrystals for solubility and dissolution rate enhancement of nifedipine. Int J Pharm 299:167-177.
2. Keck CM, Muller RH 2006. Drug nanocrystals of poorly soluble drugs produced by high pressure homogenisation. Eur J Pharm Biopharm 62:3-16.
3. Merisko-Liversidge E, Liversidge GG, Cooper ER 2003. Nanosizing: a formulation approach for poorly-water-soluble compounds. Eur J Pharm Sci 18:113-120.
4. Muller RH, Bohm BHL, Grau MJ, Wise DL. 2000. Nanosuspensions-a formulation approach for poorly soluble and poorly bioavailable drugs. In Anonymous Handbook of Pharmaceutical Controlled Release, New York: Marcel Dekker. p 345-357.
5. Yasuji T, Takeuchi H, Kawashima Y 2008. Particle design of poorly water-soluble drug substances using supercritical fluid technologies. Adv Drug Deliv Rev 60:388-398.
6. Mishima K 2008. Biodegradable particle formation for drug and gene delivery using supercritical fluid and dense gas. Adv Drug Deliv Rev 60:411-432.
7. Sheth P, Sandhu H, Singhal D, Malick W, Shah N, Kislalioglu MS 2012. Nanoparticles in the pharmaceutical industry and the use of supercritical fluid technologies for nanoparticle production. Curr Drug Deliv 9:269-284.

8. Palakodaty S, York P 1999. Phase behavioral effects on particle formation processes using supercritical fluids. Pharm Res 16:976-985.
9. Reverchon E, Caputo G, De Marco I 2003. Role of Phase Behavior and Atomization in the Supercritical Antisolvent Precipitation. Ind Eng Chem Res 42:6406-6414.
10. Perrut, M.; Clavier, J.Y.; Supercritical Fluid Formulation: Process Choice and Scale-up. *Ind. Eng. Chem. Res.* **2003**, *42*(25), 6375- 6383.
11. Kwauk, X.; Debenedetti, P.G. Mathematical modeling of aerosol formation by rapid expansion of supercritical solutions in a converging nozzle. *J. Aerosol Sci*., **1993**, *24*(4), 445–469.
12. Guha R, Vinjamur M, Mukhopadhyay M 2011. Demonstration of Mechanisms for Coprecipitation and Encapsulation by Supercritical Antisolvent Process. Ind Eng Chem Res 50:1079-1088.
13. Reverchon E, Della Porta G 1999. Production of antibiotic micro- and nano-particles by supercritical antisolvent precipitation. Powder Technol 106:23-29.
14. Lee S, Nam K, Kim MS, Jun SW, Park JS, Woo JS, Hwang SJ 2005. Preparation and characterization of solid dispersions of itraconazole by using aerosol solvent extraction system for improvement in drug solubility and bioavailability. Arch Pharm Res 28:866-874.
15. Randolph TW, Randolph AD, Mebes M, Yeung S 1993. Sub-micrometer-sized biodegradable particles of poly(L-lactic acid) via the gas antisolvent spray precipitation process. Biotechnol Prog 9:429-435.

16. Uzun Ä, Sipahigil O, DinÃ§er S 2011. Coprecipitation of Cefuroxime Axetilâ€“PVP composite microparticles by batch supercritical antisolvent process. The Journal of Supercritical Fluids 55:1059-1069.
17. Chen H, Lai J, Deng X, Dai G 2001. Fine Griseofulvin particles formation by rapid expansion of supercritical solutions. Huagong Xuebao (Chin Ed) 52:56-60.
18. Reverchon E, Della Porta G, Taddeo R, Pallado P, Stassi A 1995. Solubility and micronization of griseofulvin in supercritical CHF3. Ind Eng Chem Res 34:4087-4091.
19. Foster NR, Meure LA, Barrett AM, Abbasi F, Dehghani F vol. 3, 2003. Micronisation of griseofulvin by the aerosol solvent extraction system. In: Brunner G, Kikic I, Perrut M (eds) Proceedings of the 6th international symposium on supercritical fluids, Versailles, International Society for the Advancement of Supercritical Fluids, Nancy, Franc, 1771 – 1776.
20. Chattopadhyay P, Gupta RB 2001. Production of griseofulvin nanoparticles using supercritical CO(2) antisolvent with enhanced mass transfer. Int J Pharm 228:19-31.
21. Jung J, Clavier JY, Perrut M 2003. Gram to kilogram scale up of supercritical antisolvent process.
22. Simonelli AP, Mehta SC, Higuchi WI 1970. Inhibition of sulfathiazole crystal growth by polyvinylpyrrolidone. J Pharm Sci 59:633-638.

23. Jarmer DJ, Lengsfeld CS, Anseth KS, Randolph TW 2005. Supercritical fluid crystallization of griseofulvin: crystal habit modification with a selective growth inhibitor. J Pharm Sci 94:2688-2702.
24. Griseofulvin, http://www.merckmanuals.com/vet/pharmacology/antifungal_agents/griseofulvin.html, accessed on 02/02/2013.
25. http://www.malvern.com/labeng/products/mastersizer/ms2000/mastersizer2000.htm?specification accessed on 02/02/2013
26. Born M, Wolf E. 1999. Principles of Optics, Electromagnetic theory of propagation, interference and diffraction of light, 7th ed. ed.: Cambridge university press.
27. Anderson MJ, Whitcomb PJ, editors. 2007. DOE Simplified, practical tools for effective experimentation, 2nd ed.: Productivity Press.
28. "US Food and Drug Administration " 2004 Sept. Guidance for industry. Pharmaceutical cGMPs for the 21st century-A risk based approach.
29. International Conference on Harmonization (ICH), Pharmaceutical Development **Q8 (R2)**. 2009. Geneva, Switzerland.
30. Subra P, Jestin P 2000. Screening Design of Experiment (DOE) Applied to Supercritical Antisolvent Process. Ind Eng Chem Res 39:4178-4184.
31. Cotter SC 1979. A screening design for factorial experiments with interactions. Biometrika 66:317-320.
32. Gullberg J, Jonsson P, Nordstrom A, Sjostrom M, Moritz T 2004. Design of experiments: an efficient strategy to identify factors influencing extraction and

derivatization of Arabidopsis thaliana samples in metabolomic studies with gas chromatography/mass spectrometry. Anal Biochem 331:283-295.

33. Devore J, Farnum N. 1999. Applied statistics for engineers and scientists. In Anonymous , Chapter 10 ed., Pacific Grove, CA: Duxbury press.
34. NIST/SEMATECH e-Handbook of Statistical Methods. 2012. http://www.itl.nist.gov/div898/handbook/ accessed on 02/02/2013
35. Eriksson L, Johansson E, Kettaneh-Wold N, Wikstrom C, Wold S 2008. Design of Experiments, Principles and Applications, 3rd ed., Sweden: Umetrics Academy.
36. Raghavan SL, Trividic A, Davis AF, Hadgraft J 2001. Crystallization of hydrocortisone acetate: influence of polymers. Int J Pharm 212:213-221.
37. Varughese P, Li J, Wang W, Winstead D 2010. Supercritical antisolvent processing of Î³-Indomethacin: Effects of solvent, concentration, pressure and temperature on SAS processed Indomethacin. Powder Technol 201:64-69.
38. Wang Y, Pfeffer R, Dave R, Enick R 2005. Polymer encapsulation of fine particles by a supercritical antisolvent process. AIChE J 51:440-455.
39. Kordikowski A, Schenk AP, Van Nielen RM, Peters CJ 1995. Volume expansions and vapor-liquid equilibria of binary mixtures of a variety of polar solvents and certain near-critical solvents. The Journal of Supercritical Fluids 8:205-216.
40. De Gioannis B, Gonzalez AV, Subra P 2004. Anti-solvent and co-solvent effect of CO2 on the solubility of griseofulvin in acetone and ethanol solutions. The Journal of Supercritical Fluids 29:49-57.

41. Feng S, Huang G 2001. Effects of emulsifiers on the controlled release of paclitaxel (Taxol) from nanospheres of biodegradable polymers. J Control Release 71:53-69.

42. Remington JP 2012. 2005. The Science and Practice of Pharmacy, 21st ed.: Lippincott Williams & Wilkins.

MANUSCRIPT III

Comparative physicochemical properties of Griseofulvin coprecipitates prepared by supercritical antisolvent (SAS) process, by spray drying, and by conventional solvent evaporation process

Pratik Sheth[a,b], Harpreet Sandhu[a], Waseem Malick[a], Navnit Shah[a], and M.S. Kislalioglu[b, *]

[a]Hoffman-La Roche, Inc., 340 Kingsland street, Nutley NJ 07110 USA,

[b] Department of Biomedical & Pharmaceutical Sciences, University of Rhode Island, 41 Lower College road, Kingston RI 02881

[*] Corresponding author. Department of Biomedical & Pharmaceutical Sciences, University of Rhode Island, 41 Lower College road, Kingston RI 02881 Tel: (401) 874 5017, email address: Skis@uri.edu

ABSTRACT

The objective of this study was to prepare and compare the physical and physicochemical characteristics of griseofulvin-polymer composite particles prepared using three different methods: (1) supercritical antisolvent (SAS) process, (2) spray-drying process, and (3) the conventional solvent evaporation process. The polymers used were Kollidon® VA64, HPMCAS-LF, and Eudragit® EPO. Particle properties were analyzed using scanning electron microscopy, powder X-ray powder (PXRD), differential scanning calorimetry (DSC), and Fourier transformed infra red (FTIR).

Particle size and particle size distribution measurements were made using Malvern laser diffractometer. The dissolution behavior of pure API and solid dispersions were compared. Amorphous solid dispersions of spherical shapes were obtained, independent of the type of polymer used, when spray drying process was used. FTIR spectra indicated that the drug was hydrogen bonded to the polymers, during spray drying process, whereas, the drug remained in its crystalline form when the processing method was SAS or conventional solvent evaporation. Griseofulvin particles, used as unprocessed starting material, had a mean diameter of approximately 12 μ with a size range range between 5-20 μ. With the spray drying or SAS process, and using any of the three hydrophilic polymers, *in-situ* nanoparticles with the mean particle size of 0.3 to 0.5 μ were obtained. These nanoparticles appeared to be associated with improvement in dissolution performance compared to unprocessed crystalline griseofulvin. It was concluded that physicochemical properties and dissolution of crystalline griseofulvin could be improved by physical modification such as particle

size reduction and generation of amorphous state using spray-drying process. The results also demonstrate that the crystalline nature of griseofulvin particles depends on the method of production.

1.0 INTRODUCTION

The enhancement of solubility and oral bioavailability of poorly water soluble drugs remain as the most challenging aspects of drug development. Amongst several approaches developed to improve the solubility of poorly soluble compounds, preparation of solid dispersion is a formulation strategy that is widely utilized by pharmaceutical scientists [1-2]. Solid dispersions contain one or more active ingredients in an inert carrier or matrix at solid state which can be prepared by melting, solvent or melting solvent method [2]. Many drug products commercially available in the world market[3] contain poorly soluble active pharmaceutical ingredients, and are safe and effective when they are used as solid dispersions for the solubility enhancement. Besides solid dispersions, particle size reduction to micro and nano scale also appears as an effective and versatile option for solubility improvement [4-7]. Other approaches include formation of complexes[8], chemical modification to pro drug or salt formation[9], and lipid based drug delivery systems[10].

Various methods are cited in the literature for preparation of solid dispersion[3]. All of these methods involve mixing of drug with a matrix, preferably at a molecular level. These approaches can be broadly classified into two main categories; 1) Fusion method, 2) Solvent evaporation method. Fusion method, also called melt method,

requires high processing temperature, at which many active pharmaceutical ingredients may undergo degradation. Hot melt extrusion is an example of fusion method. Solvent evaporation method although requires milder processing conditions, has a drawback of utilizing excessive organic solvents and difficulty in removing trace amounts of these toxic solvents left in the processed product. There are three sub-categories of solvent evaporation method: conventional solvent evaporation, supercritical fluid based technologies[11-12], and spray drying[13-14].

Solvent evaporation in its most simple and conventional form is carried out in a rotary evaporator under a reduced pressure and at an elevated temperature. The typical problem encountered in the conventional solvent evaporation process is the removal of the solvent from the mass of solids to an acceptable level quickly during the process. This is because the mass becomes more and more viscous during the "drying", which prevents further evaporation of the residual solvent[15-16].

A modified and an improved version of conventional solvent evaporation technique is spray drying. In its basic form, spray drying is very simple process where droplets/particles are dried while suspended in the drying gas, turning a liquid feed into a small particulated dry powder in a single continuous process step. Spray drying has been a preferred method in the industry for production of spherical, amorphous dispersions. For example, Jung et al.,[17] demonstrated that the morphology of solid dispersions of itraconazole prepared via spray drying method, using methylene chloride and hydrophilic polymers like, Poloxamer® 188, PEG 20,000, PVP, HPMC, AEA® and Eudragit® E 100, were spherical in shape. These researchers performed

the spray drying at: 5 ml/min, pump speed; 800 l/h , air flow rate; 10–15 % aspirator level; 45°C , inlet air temperature; and 38°C, outlet air temperature. During spray drying of tolfenamic acid (dissolved in ethanol), with PVP K30, Thybo et al.,[18] obtained spherical amorphous solid dispersions. The spray drying was carried out in a co-current mode under the following set of conditions: inlet temperature: 115 ± 2°C; process air: 80 ± 2 kg/hr; atomization air flow: 6 kg/hr; and feed rate: 20 ± 2 g/min. These two examples show that irrespective of the processing conditions, the shape of the SD material was spherical.

However, the spray drying process fails to produce high bulk density product. This is not desirable, as it would require further downstream processing for the densification of the material. Additionally, low product recovery and dust collection issues increases the cost of drying, and high initial investment is required compared to other types of dryers. These limitations and a quest to develop a technique that is environmentally cleaner, and preserves the stability of pharmaceuticals, lead us to explore the potential of supercritical fluid (SCF) based technologies for producing ultra fine polymer-drug mixture .

Supercritical fluid (SCF) based technologies particularly gained popularity in the pharmaceutical industry as an alternative to conventional processes for preparation of micro and nano sized solid dispersions, due to several advantages it offers. Carbon dioxide, one of the SCF, has low critical temperature (31.2 °C) and pressure (73.8 bar or 7.4Mpa), is nonflammable, nontoxic and environmentally safe; and hence can be used for processing pharmaceuticals including heat sensitive materials such as

biologicals. There are various categories of SCF based technologies depending on the role of SCF. It may act as a solvent, an anti-solvent, or as a solute, in formation of the particles. These technologies are further modified based on the particle growth mechanisms and their collection environment. Rapid expansion of supercritical solutions (RESS), gas antisolvent precipitation (GAS), supercritical antisolvent precipitation (SAS), precipitation with compressed fluid antisolvent (PCA), solution-enhanced dispersion by supercritical fluids (SEDS), precipitation from gas-saturated solutions (PGSS), are the main variations of SCF based approaches for particle formation[19-22.] These techniques have successfully produced micro and nano particles[23-24] and in some cases amorphous solid dispersions have been successfully prepared[25]. Among all of these SCF based techniques, SAS is of particular interest because most pharmaceuticals are insoluble in supercritical carbon dioxide ($scCO_2$), and SAS is one of the technique that can effectively process such compounds. Additionally, SAS is the only technique amongst SCF based technologies, that has been successfully applied at an industrial scale[26].

Particle precipitation mechanisms are somewhat similar in SAS and in spray-drying. In both methods, a solution is sprayed through a nozzle and is allowed to atomize under elevated temperature in a one-step process. The major difference is that SAS processing is carried out at an elevated pressure conditions, as opposed to an atmospheric condition used in spray drying. In an earlier study, we reported the various processing and formulation factors that affect the reduction of particle size of griseofulvin. The goal of this study is to compare and evaluate the physiochemical and

dissolution properties of the products, produced by three methods mentioned here; SAS, spray drying, and conventional solvent evaporation.

Griseofulvin, an antifungal drug widely used for the treatment of mycotic diseases of the skin, hair, and nails, was chosen as the model drug. The solubility of GF in water is only about 1 μmol/mol at 37 °C[27], it has low permeability (Caco2 cell permeability of -4.44) [28] and it belongs to Biopharmaceutics Classification System (BCS) class II pharmaceuticals. It is a neutral drug, non-ionizable, and has 6 H^+ acceptor functional groups (Figure 1)

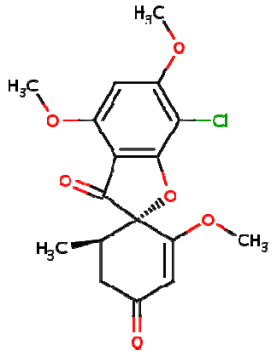

Figure 1: Chemical structure of griseofulvin

There are various factors that affect selection of a polymer in preparing solid dispersions, such as; possibility of drug-polymer interaction, solubility of a polymer in water, and in organic solvents, global regulatory acceptance, stabilizing ability of an ionic polymer in an aqueous environment, and ease of processibility. We identified three hydrophilic polymers, having different molecular structure, and ionic properties; namely Kollidon® VA64, HPMCAS, and Eudragit EPO®, shown in Figure 2. Polymers with different molecular structures, and ionic properties are selected to

understand their interaction mechanisms with griseofulvin in different manufacturing processes.

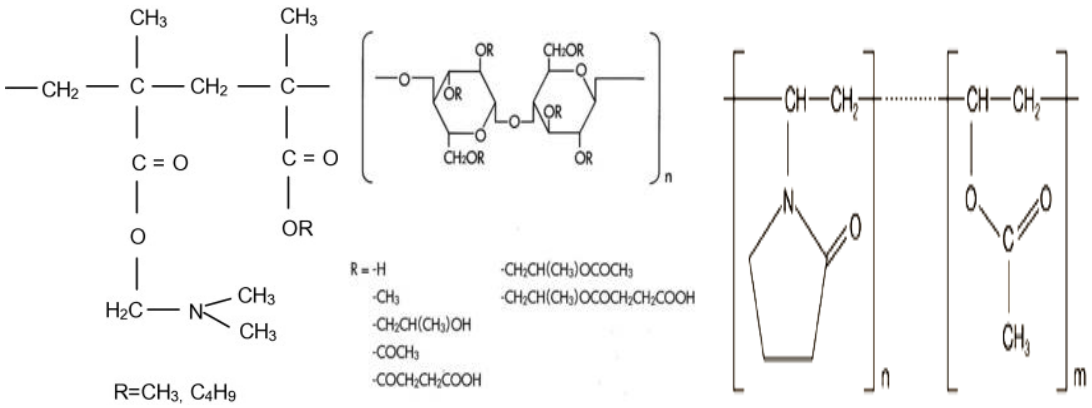

Figure 2: Chemical structure of Eudragit EPO, HPMC-AS, and Kollidon VA64 (from left to right)

Kollidon® VA64 is manufactured by free radical polymerization of 6 parts of N-vinyl pyrrolidone, and 4 parts of vinyl acetate. It is non ionic polymer, widely used in the preparation of solid dispersion. It is freely water soluble and has an excellent solubility in acetone, organic solvent chosen for our process. It does not contain any H+ donor functional group.

HPMC-AS (hypromellose acetate succinate) is a partially esterified derivative of Hypromellose, where succinoyl and acetyl residues are bound to the cellulose backbone. It is practically insoluble in water, and has a pH dependent solubility in a buffered media. It is an anionic polymer, which has both H^+ donor and H^+ acceptor groups. Obaidi et al.,[29] showed that it can form strong hydrogen bonding with griseofulvin, in a spray drying process. Corey, et al.,[30] demonstrated that HPMC AS

can provide a charge when nanoparticles are suspended in an aqueous environment, thus reducing or eliminating agglomeration of nanoparticles.

EUDRAGIT® EPO is a cationic copolymer based on dimethylaminoethyl methacrylate, butyl methacrylate, and methyl methacrylate. It is also practically insoluble in water, and has a pH dependent solubility in a buffered media. Sarode et al.,[31] showed that it can form hydrogen bonding with griseofulvin, in a hot melt extrusion process. Chernysheva et al.,[32] studied the effect of type of hydrophobic polymer on the nanoparticle size obtained through emulsification-solvent evaporation method. They postulated that Eudragit polymers due to their mild surface active properties, and ability to be ionized, provide very low interfacial tension, and produce small droplet upon exiting from the nozzle, and hence produce the smallest particles, compare to poly (D, L, lactide, co-glycolides) polymer which have no ionizable hydrophilic group.

Based on the literature presented here, we propose to compare the production effectiveness of SAS, spray drying, and solvent evaporation methods, using three different polymers (Kollidon® VA64, HPMCAS, Eudragit® EPO) and choose the most practical, and cost effective method that can produce ultra fine particles of griseofulvin, and thus improve its dissolution. Solid dispersions obtained in that manner is further characterized by determining their physicochemical properties via powder X-ray diffraction (PXRD), Fourier transform infrared spectroscopy (FTIR), differential scanning calorimetry (DSC), and microscope . The dissolution behavior of the pure API and in the solid dispersions are also discussed.

2.0 MATERIALS AND METHODS

2.1 Materials

The model drug Griseofulvin (GF) was purchased as micronized API (lot # 115H1180) through jet milling process, from Ria International (East Hanover, NJ). The vinylpyrolidone -vinylacetate copolymer Kollidon® VA-64 was obtained from BASF corporation (Florham Park, NJ). The methacrylic polymer, Eudragit EPO was purchased from Evonik Degussa Corporation (Piscataway, NJ). The cellulosic polymer, HPMCAS-LF, manufactured by Shin-Etsu Co., Ltd. (Niigata, Japan) was donated by Biddle Sawyer Corporation (New York, NY). Acetone (purity 99.5%) was purchased from Sigma Aldrich (St Louis, MO). Polystyrene latex microspheres (98 nm, 150 nm, 310 nm, 900 nm, and 2000 nm), for checking the accuracy of Malvern instrument, were purchased Magsphere, Inc. (Pasadena, CA). Liquid Carbon Dioxide (purity 99.9%, instrument grade 4.0 with siphon tube) was purchased from Airgas USA, LLC (Salem, NH).

2.2 Methods

2.2.1 Supercritical antisolvent (SAS) Process

An SAS apparatus (model: SAS 50, Thar Technologies Co., USA) was used to generate GF-polymer co-precipitates. The schematic diagram of Tharr SAS system using supercritical carbon dioxide ($SCCO_2$) as an anti-solvent is shown in manuscript II. In that previous work, we studied the effect of various formulation and instrumental variables on the effectiveness of SAS process. The optimized processing variables used in this work were: drug/polymer ratio of 80/20 (% w/w), in acetone with total concentration of 2.5 % (w/v); precipitation chamber temperature of 45^0C; pressure of 85 bar; organic solvent addition rate of 2 ml/min ; CO_2 addition rate of 40 g/min; and nozzle diameter of 150 μm. Liquid CO_2 from the tank was pre-heated to 45°C in a heat exchanger and then pumped into the high-pressure precipitation chamber maintained at 45°C. After the system reached 85 bar , pure acetone was pumped for 5 minutes in order to reach equilibrium conditions inside the precipitation vessel. Acetone solution (100 ml) containing drug and polymer was then pumped at 2 ml/min speed into the precipitation chamber through the 100 μm nozzle, and meanwhile steady flow of CO_2 (40 g/min) was maintained. The mixing of the organic solvent with compressed CO_2 resulted in decreased solvation power of the solvent and super saturation developed over a short period of time. Upon completion of spraying of solution, the compressed CO_2 was flushed through the precipitation chamber for another 40–60 min to extract the residual organic solvent from the product. Then the system was slowly depressurized to the atmospheric conditions. Final products were collected from the 0.22 μ Nylon filter element and kept in a desiccator. Formulation

SAS1 contained Kollidon® VA64, SAS2 contained HPMCAS-LF, and SAS3 contained Eudragit® EPO as the polymer matrix.

2.2.2 Spray Drying Process (SD)

SD experiments were performed using a Büchi Mini Spray Dryer B290 (Labortechnik AG, Switzerland) with a co-axial nozzle (1.2 mm diameter) with co-current flow. Approximately 100 ml of solution containing griseofulvin and the selected polymer (weight ratio: 80:20) in acetone were fed to the precipitation chamber of spray dryer. Drug:Polymer ratio of 80:20 was chosen for SD experiments, because this was the ratio used earlier for process optimized with SAS. The total concentration of the solute in solutions was 2.5 w/v %. The inlet temperature at the drying chamber was maintained at $65 \pm 2°C$ and outlet temperature was $30 \pm 2°C$. The aspirator setting was 88% and atomizing air was set at 5.5 cm (750 l/h). The spray feed rate was 6 mL min^{-1}. Formulation SD1 contained Kollidon® VA64, SD2 contained HPMCAS-LF, and SD3 contained Eudragit® EPO as the polymer matrix.

2.2.3 Solvent Evaporation Method (SE)

As conventional for solvent evaporation method, the drug (20 mg/mL) and carrier polymer (5 mg/mL) were dissolved in 100 mL of acetone in a round-bottom flask. The solvent was removed under vacuum in a Buchi RE-111 Rotavapor (Labortechnik AG, Switzerland) at 65°C and 45 rpm over 30-45 minutes. The resultant solid dispersion was scraped out with a spatula. Dispersions were then further dried in a vacuum oven set at 40^0C, for 24 hours. Formulation SE1 contained Kollidon® VA64, SE2 contained HPMCAS-LF, and SE3 contained Eudragit® EPO as the polymer matrix.

2.2.4 Preparation of the physical mixture

The physical mixture of griseofulvin with various polymers were prepared as a control, in 80:20 (drug:polymer) w/w ratio, by simple blending in a vial for 30 minutes.

2.3 Characterization of formulated samples

2.3.1 Microscopy

A scanning electron microscope (SEM), model TM-1000 manufactured by Hitachi **(**Hitachi High-Technologies Europe GmbH, Germany) was used to examine the particle size and morphology. The magnifications were altered in order to get clear images. The samples were fixed by mutual conductive adhesive tape on aluminum stubs. In addition to SEM, an ultra- high resolution digital microscope , model VHX 600, manufactured by Keyence (KEYENCE America, Elmwood Park, NJ) was used to obtain 3-D images.

2.3.2 Laser Diffraction Particle Size Analysis

Particle size (PS) and particle size distribution (PSD) were measured using a Mastersizer® 2000 (Malvern Instruments Ltd., Malvern, UK) . The Mastersizer® 2000 uses the technique of laser diffraction to measure the size of particles.

In our study, the output signal was converted into PSD by using Mie theory. The refractive index of the drug was measured using Reichert ® AR 200 digital refractometer (Reichert Technologies, Depew NY) and average value (n=6) was found to be 1.34. Approximately 50 mg of processed product was added to 10 ml of dispersing media and sonicated for 1 minute prior to analysis. Each particle size measurement was performed in triplicates, with about 1000 particles being measured in each run.

The results are reported in % volume distribution as it is more pharmaceutically relevant. Results are expressed as $D_{(4,3)}$, $d_{50,}$ and span; denoting the volume

weighted mean diameter , diameter of 50th percentile of distribution, and the span is the width of the distribution based on the 10th , 50th, and 90th percentile.

$$\text{Span} = (d_{90} - d_{50})/d_{10} \quad \text{.....} \quad \textbf{Equation 1}$$

Sample measurements were done in two different dispersing media; n-hexane and phosphate buffer (pH 6.8) . Measurements done using n-hexane provides particle size of intact drug-polymer coprecipitates, as neither dissolves in n-hexane. Whereas, all polymers are completely soluble in phosphate buffer (pH 6.8), and hence that dispersing media provides measurement of *in-situ* particles of GF alone.

Prior to performing particle size measurements of processed samples, the accuracy and reproducibility of Malvern laser light diffraction method was challenged using polystyrene latex microspheres of known diameter. The choice of dispersing media did not affect the accuracy, or reproducibility of measurements. The details of these experiments can be found in manuscript II.

2.3.3 Powder X-Ray Diffraction (PXRD)

The morphological characteristics of the substance was determined using Powder X-Ray Diffraction (PXRD). PXRD was performed using Bruker D8 Advance Powder X–Ray Diffractometer (Brukler Corporation, Madison, WI). Samples were analyzed using a Cu (λ=1.54) K α radiation. The X-ray pattern was collected in the 2θ range of 1 to 40^0 in the step scan mode (scan speed 0.27^0/sec and step size 0.0045°). PXRD depicts sharp peaks for crystalline substances and disappearance of these peaks indicates a transformation of a crystalline substance into an amorphous form.

2.3.4 Fourier Transformed Infrared Spectroscopy (FTIR)

FTIR spectra were collected on a Nicolet 6700 from Thermo scientific (Thermo Fisher Scientific Inc., Pittsburgh, PA) . Powders were measured directly using the smart orbit accessory. Spectra were collected from 400 – 4000 cm-1 using 64 scans at a resolution of 4 cm-1. Spectra were analyzed using the Omnic software (v.7.2).

2.3.5 Thermal Analysis

Differential Scanning Calorimetry (DSC) was performed by using a DSC Q 2000 ® differential scanning calorimeter (TA Instruments, New Castle, Delaware). Calibrations were performed prior to analysis using pure samples of indium and zinc. For Melting point (Tm) determination a conventional DSC method was run at 10^0C per minute and samples were scanned from 10^0C to 250 ^{0}C. For glass transition temperature (Tg) determination, a modulated DSC method was run at 3 ^{0}C per minute (modulations were performed at 0.646^0c every 40 seconds) and samples were scanned from 0 to 200^0C . The measurements were carried out in a hermetically sealed aluminum pans under nitrogen atmosphere using approximately 6 - 8 mg of sample. Melting point (T_m) and glass transition temperature (Tg) values were determined by the Pyris software.

2.3.6 Dissolution Rate and Intrinsic Dissolution Rate (IDR)

The dissolution rate and IDR of griseofulvin samples were measured in Distek® Dissolution Apparatus (Distek, North Brunswick, NJ) equipped with UD-lite® fiber optic measurement capability. Solid dispersion samples from SD, SE, and SAS processes were compressed into 100 mg tablets using a flat faced ¼" round tooling,

under carver press. Each tablet contained equivalent of 7 mg of drug, polymer, and lactose was used as filler. The physical mixtures of drug and a polymer were also compressed into tablet having the same ratio of drug to polymer, and the filler. Dissolution media was pH 6.8 phosphate buffer (0.05M) which was considered to be a simulated intestinal fluid (SIF). The dissolution analysis was performed in 500 ml SIF at UV wavelength of 295 nm using USP dissolution apparatus type II, at 37^0C, 50 rpm.

In conventional dissolution studies using tablet or powder, factors such as rate of wetting, effect of particle size and hence specific surface area, disintegration, clumping etc., can affect the rate of dissolution. Whereas, intrinsic dissolution rate (IDR), using Wood's apparatus, provides a constant surface area, and permits a constant hydrodynamic system and in general avoids many of the problems associated with powders or tablet.

For Intrinsic dissolution studies, a Distek stationary disk system was used to prepare the compact pellets and perform the test. Approximately 200 mg of solid dispersion sample from different processing methods, was compressed with the aid of a benchtop Carver press (Carver, Inc., Wabash, IN, USA) at 4000 psi with a dwell time of 10 seconds to form a compact pellet of 0.5 cm^2 exposed surface area. Assemblies, each composed of the pellet, die, gasket, and a polypropylene plastic cap, were immersed with the pellet side up, into the bottom of flat-bottom dissolution vessels containing 500 mL of SIF at 37°C. The USP Apparatus II paddle was positioned 1 inch above the assembly and rotated at 50 rpm.

3.0 RESULTS AND DISCUSSION

3.1 Microscopy

The microscopy pictures showed that the micronized drug purchased had irregularly-shaped, crystalline structures , and were approximately 5 -20 μm in dimensions (Figure 3). The solid dispersion samples obtained by the SAS process, were fibrous, and needle- shaped, independent of the type of polymer used (Figure 4). The length of the intact needles was approximately 1 – 10 μm, and the thickness was less than 1 μm. In contrast, spray-dried micro-particles were spherical (Figure 5) in shape for all three polymers used. Lastly, the morphology of crystalline particles obtained via conventional solvent evaporation process was plate like and irregular shaped (Figure 6).

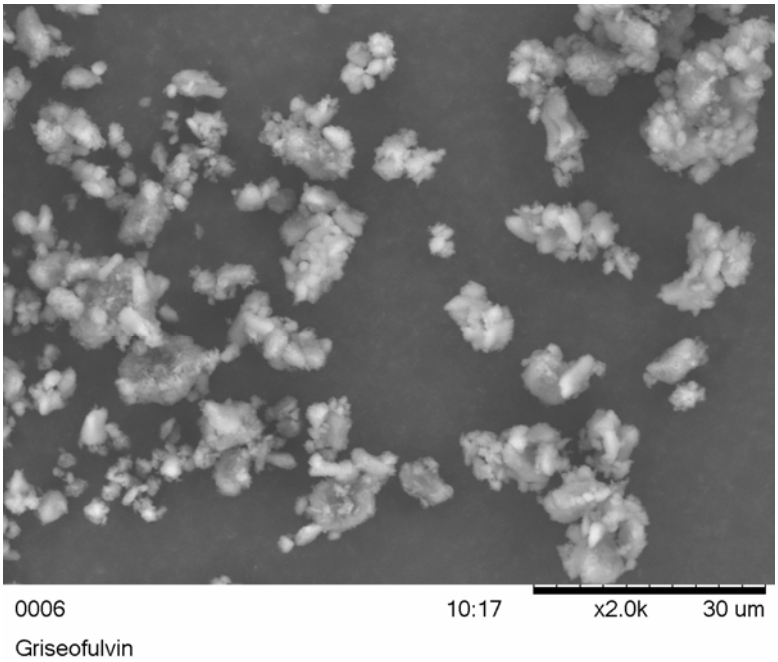

Figure 3. Scanning Electron Microscopy (SEM) image of micronized Griseofulvin API

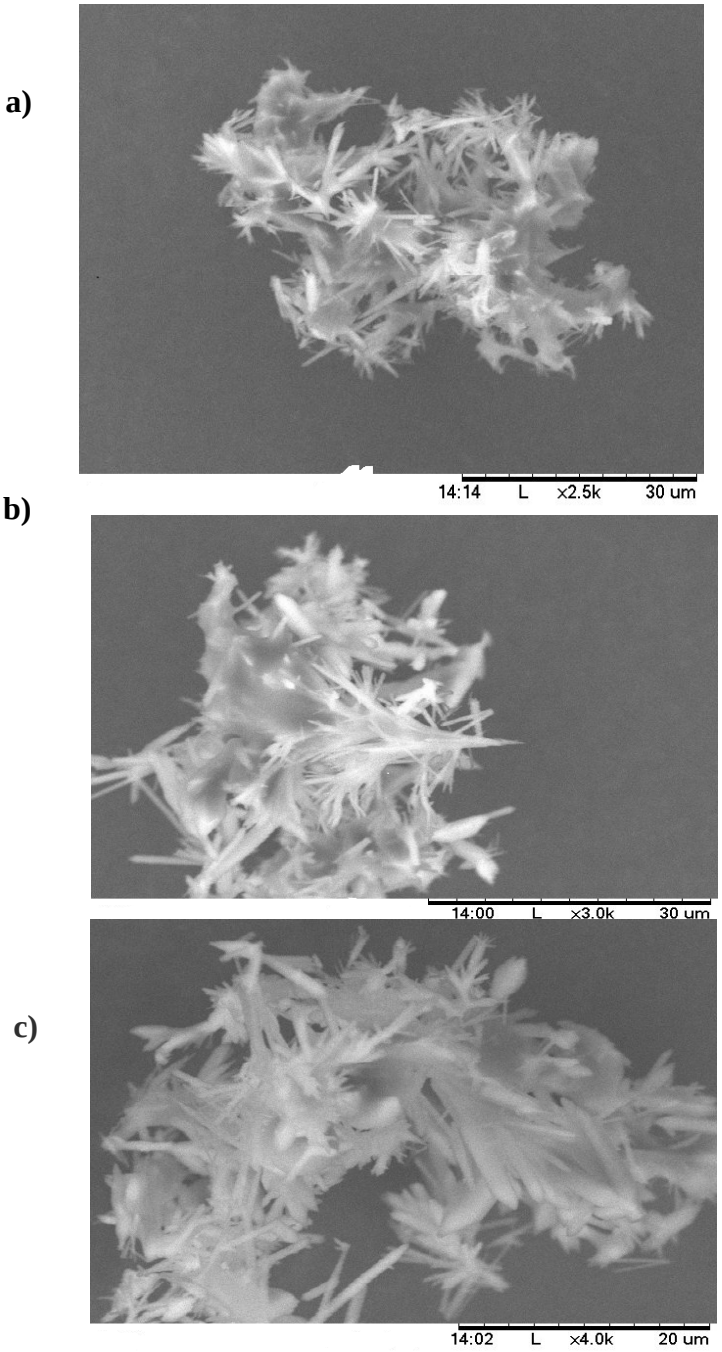

Figure 4. Scanning Electron Microscopy (SEM) images of SAS formulations of GF with Kollidon VA64(a), HPMC-ASLF (b), and Eudragit EPO (c)

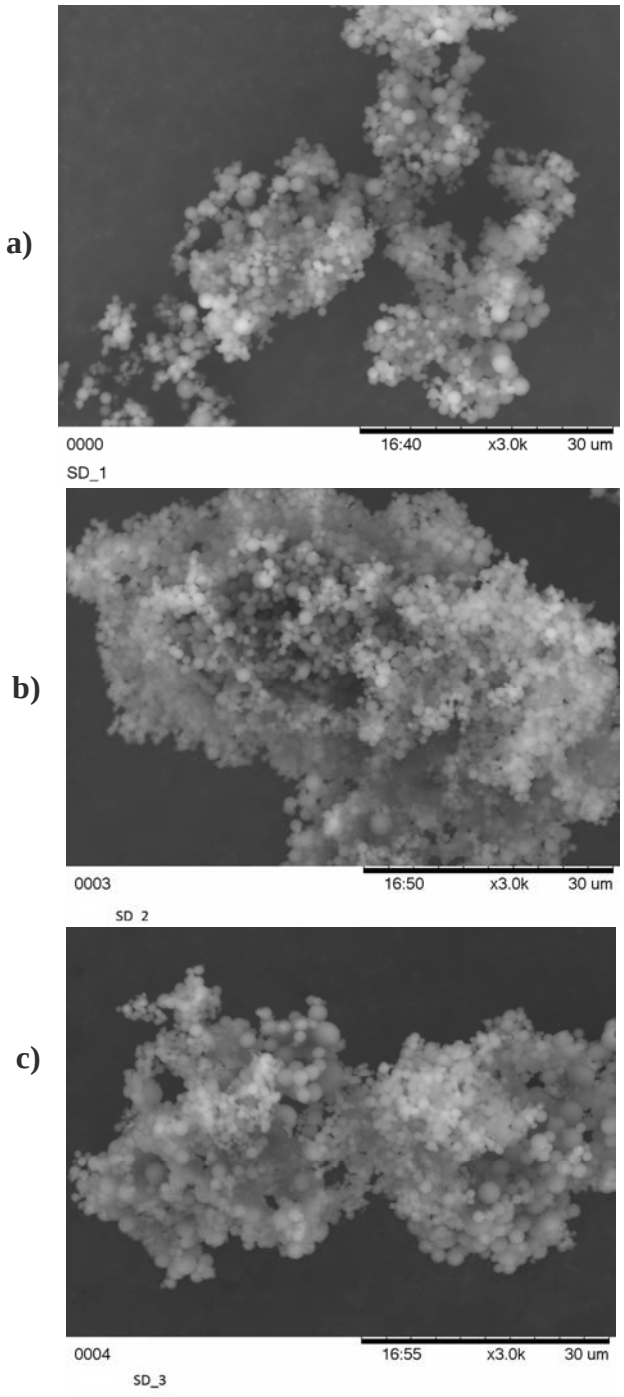

Figure 5. Scanning Electron Microscopy (SEM) images of spray dried formulations of GF with Kollidon VA64(a), HPMC-ASLF (b), and Eudragit EPO (c)

a)

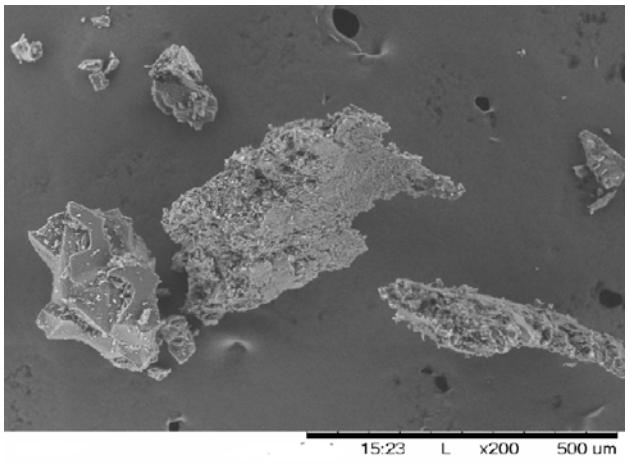

b)

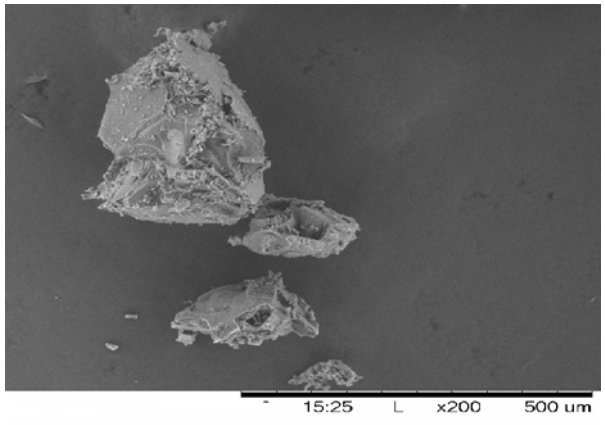

c)

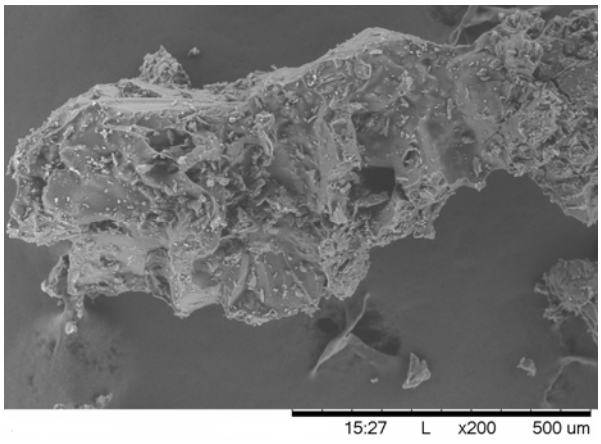

Figure 6. Scanning Electron Microscopy (SEM) images of solvent evaporation method formulations of GF with Kollidon VA64(a), HPMC-ASLF (b), and Eudragit EPO (c)

As it was experienced earlier by many workers[17-18] who studied several drugs of different origin, and very different polymers, our drug, griseofulvin, and selected polymers (Kollidon® VA64, HPMCAS-LF, Eudragit® EPO) also formed spherical amorphous particles, when spray drying process was applied. The mechanism of particle formation during spray drying might explain this roundness and smoothness. At first, there is formation of small or micro sized droplets at the end of nozzle. These droplets meet a stream of hot air and they lose their moisture very rapidly while still suspended in the drying air. The dry powder is then separated from the moist air by centrifugal action in a cyclone separator . This cyclonic movement of particles during the drying process prior to reaching the final collector is most likely giving the particles the spherical shape and smoothness[33-34].

Crystalline, needle shaped morphology of GF particles processed via SAS technique has been observed by other researchers as well. Foster et al.,[35]and Reverchon et al., [36] found that GF by itself (without any polymers) tend to precipitate out as crystalline, long needles of several hundred microns long when SAS process was used. In our study, we applied the coprecipitation approach. Even though the coprecipitates of GF and all three polymers were fibrous and needle shaped, the length of the needle became significantly shorter (d_{50}: 2.3 to 3.7 μm), compared to GF precipitated alone (500 μm to 1mm through SAS process (Figure 7). Obviously, the presence of polymer used is affecting the crystallization of GF resulting in modified morphologies. The reduced size may be the result of adsorption of the polymer onto fast growing drug crystal faces. Researchers like Jarmer et al.,[37] also studied the precipitation of GF

in presence of polymer Poly (sebacic anhydride) using a modified SAS process called PCA (particles from compressed antisolvent). They found that while the particle size of GF, when processed alone was around 500 μm, it reduced to 1-100 μm, when processed with Poly (sebacic anhydride).

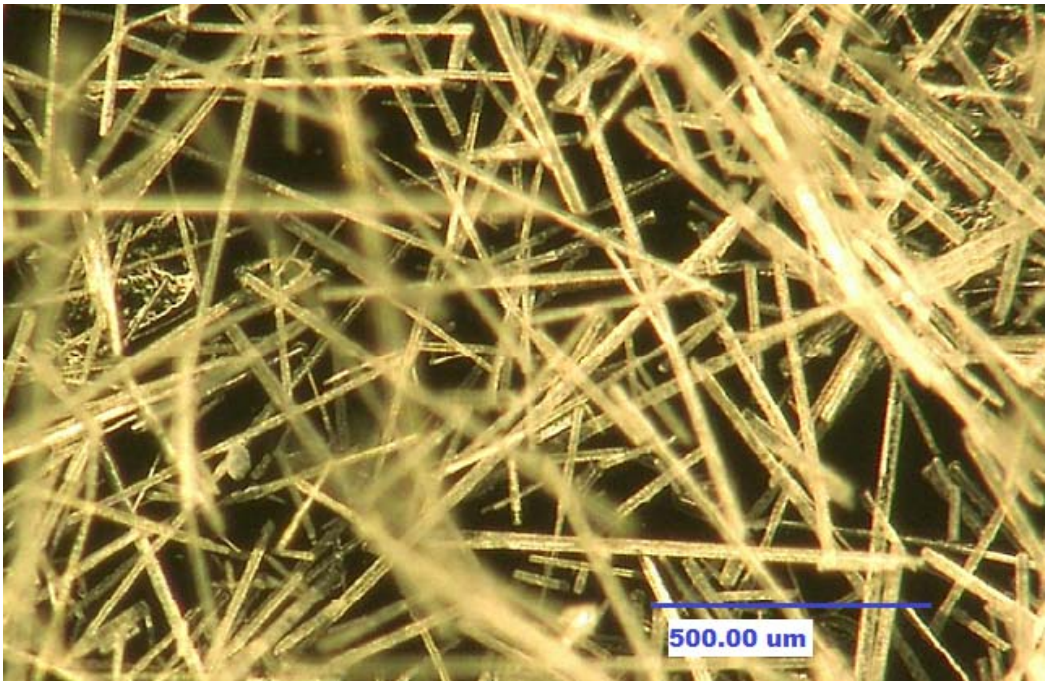

Figure 7: GF precipitated alone from acetone via SAS process

3.2 Particle size (PS) and particle size distribution (PSD) measurement

PS and PSD of SAS, and spray dried formulations were measured by laser diffraction method, as obtained. Samples obtained with solvent evaporation method were collected in the form of films by scraping the walls of glass flask, and hence the samples were crushed using mortar and pestle prior to particle size measurement, in phosphate buffer (pH 6.8) or in n-hexane.

The particle size measurements of the SAS formulations for each polymer, using two different dispersing media, are summarized in Table 1, and Table 2. Using n-hexane as the dispersing media, volume weighted mean diameter ($D_{(4,3)}$) of all intact samples ranged between 2.9 μm to 5.0 μm, whereas d_{50} value ranged between 2.3 μm to 3.7 μm . When the particle size measurement was done using phosphate buffer (pH 6.8) as the dispersion media, an *in-situ* nanoparticles of GF had volume weighted mean diameter ($D_{(4,3)}$) of 0.5 μm, and the d_{50} value was approximately 0.4 μm.

Table 1. Particle size distribution data of SAS, spray dried, and solvent evaporation formulations in n-hexane

		SAS			Spray Drying			Solvent Evaporation		
		$D_{(4,3)}$	d_{50}	Span	$D_{(4,3)}$	d_{50}	Span	$D_{(4,3)}$	d_{50}	Span
Kollidon VA64	Mean (n=3)	5.0	3.7	3.1	15.9	12.9	2.2	332.4	271.2	2.4
	Std. Dev	*0.1*	*0.2*	*0.2*	*0.6*	*0.3*	*0.1*	*10.9*	*9.2*	*0.1*
HPMCAS-LF	Mean (n=3)	4.3	2.8	2.7	2.5	1.9	1.6	377.5	290.7	2.7
	Std. Dev	*0.2*	*0.1*	*0.2*	*0.2*	*0.2*	*0.2*	*22.5*	*27.3*	*0.1*
Eudragit EPO	Mean (n=3)	2.9	2.3	1.9	3.9	2.5	3.0	358.0	287.0	2.5
	Std. Dev	*0.2*	*0.1*	*0.1*	*0.1*	*0.1*	*0.1*	*23.5*	*17.8*	*0.2*

Table 2. Particle size distribution data of SAS, spray dried, and solvent evaporation formulations in phosphate buffer (pH 6.8)

		SAS			Spray Drying			Solvent Evaporation		
		$D_{(4,3)}$	d_{50}	Span	$D_{(4,3)}$	d_{50}	Span	$D_{(4,3)}$	d_{50}	Span
Kollidon VA64	Mean (n=3)	0.50	0.40	2.3	0.91	0.343	4.8	24.70	18.30	3.0
	Std. Dev	0.02	0.02	0.06	0.02	0.01	0.10	1.44	1.66	0.10
HPMCAS-LF	Mean (n=3)	0.55	0.37	2.5	0.76	0.375	3.8	28.30	21.50	2.8
	Std. Dev	*0.04*	*0.01*	*0.1*	*0.05*	*0.022*	*0.1*	*3.15*	*5.35*	*0.1*
Eudragit EPO	Mean (n=3)	0.54	0.37	2.6	0.62	0.340	3.6	82.20	28.10	4.9
	Std. Dev	*0.01*	*0.01*	*0.08*	*0.02*	*0.01*	*0.06*	*4.56*	*5.03*	*0.36*

The particle size measurements of the spray dried formulations for each polymer, was also carried out in the same manner, and results are summarized in Tables 1 and 2. Using n-hexane as the dispersing media, volume weighted mean diameter ($D_{(4,3)}$) of intact SD solid dispersions ranged between 2.5 µm to 15.9 µm, and the d_{50} value for all intact SD formulations ranged from 1.9 µm to 12.9 µm. Once the polymer is dissolved from the spray dried amorphous solid dispersion, the drug crystallizes out in the form of nano particles. We were able to verify the crystalline nature of GF by observing the birefringence under polarized light microscopy (Figure 8). As shown in Table 2, when phosphate buffer (pH 6.8) was used as the dispersion media, the volume weighted mean diameter ($D_{(4,3)}$) of *in situ* nano particles ranged between 0.6 µm to 0.9 µm, whereas the corresponding d_{50} value for all spray dried formulations was approximately 0.3 µm.

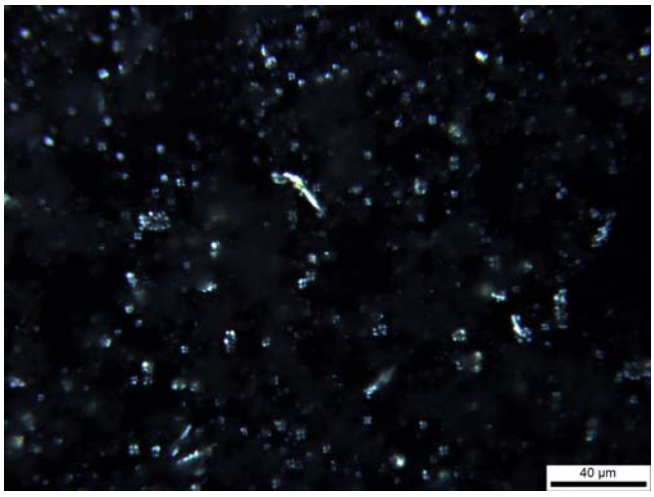

Figure 8. Polarized light microscopy image showing birefringence of spray dried formulation of GF dispersed in phosphate buffer (pH 6.8)

Lastly, the particle size measurements of the solvent evaporation method formulations, carried out in the same manner, are also reported in Table 1 and Table 2. The volume weighted mean diameter ($D_{(4,3)}$) of all intact samples ranged between 332.4 µm to 377.5 µm, whereas d_{50} value ranged between 271.2 µm to 290.7 µm . As mentioned before, solvent evaporation method samples were collected in the form of film, and were gently crushed prior to sample measurement. Hence, these results which are largely different from SAS, and SD process, is explainable. When the particle size measurement was done using phosphate buffer (pH 6.8) as the dispersion media, the *in-situ* particles of GF had volume weighted mean diameter ($D_{(4,3)}$) of 24.7 to 82.2 µm, and the d_{50} value was 18.3 to 28.1 µm. As opposed to SAS and SD process, which produced *in-situ* nanoparticles of GF, solvent evaporation process resulted in extremely large particles of GF *in-situ*.

3.2.1 Analysis of Variance (ANOVA)

ANOVA was performed on d_{50} values to see if the type of polymer used (Kollidon® VA64, HPMCAS-LF, Eudragit® EPO), or the kind of process applied (SAS vs spray drying) had any significant impact on the particle size of intact drug polymer mixture. Results as summarized in Table 3, show that F value of polymers, and that of process (SAS and SD) is larger than their F critical values, hence null hypothesis is rejected, and there is statistically significant difference in particle size amongst three different polymers, and between SD and SAS processes. The d_{50} values from solvent evaporation method formulation were not used for ANOVA test, as it was evident without any doubt that, those particles were significantly larger than the SAS or SD process particles.

It is also evident from the Table 3 that amongst the three polymers tested, ionic polymers (HPMCAS-LF and Eudragit EPO), produced smaller particles in SAS and spray drying process, as compared to non-ionic polymer (Kollidon VA64). Ionic polymers provide low interfacial tension, and tend to produce smaller droplet upon exiting from the nozzle (in both SAS and spray drying process), and hence produced the smallest particles, compare to Kollidon VA64 which have no ionizable hydrophilic group.

Table 3: Statistical comparison of particle size (d_{50})of intact GF coprecipitates produced via SAS vs Spray Drying process, using different polymers, by application of Analysis of Variance (ANOVA)

Summary

Polymer	Process	d_{50}(Mean)	Std.Dev	n
KollidonVA64	SAS	3.7	0.2	3
	Spray Drying	12.9	0.3	3
	Solv.Evap	271.2	9.2	3
HPMCAS-LF	SAS	2.8	0.1	3
	Spray Drying	1.9	0.2	3
	Solv.Evap	290.7	27.3	3
Eudragit EPO	SAS	2.3	0.1	3
	Spray Drying	2.5	0.1	3
	Solv.Evap	287	17.8	3

ANOVA Table

Source of Variation	*SS*	*df*	*MS*	*F*	*P-value*	*F crit*
Polymers	139.3641	2	69.68205	**1790.545**	1.38765E-15	**3.885294**
Process	36.83680556	1	36.83681	**946.556**	8.73047E-13	**4.747225**
Interaction	93.29774444	2	46.64887	1198.686	1.52638E-14	3.885294
Within	0.467	12	0.038917			
Total	269.96565	17				

3.3 PXRD

The micronized GF obtained from supplier, is crystalline with well-defined peaks in PXRD (Figure 9). PXRD of GF solid dispersion samples prepared by the solvent evaporation and SAS methodology show that the material morphology remained crystalline. PXRD patterns of untreated GF matches that of all samples prepared using solvent evaporation and SAS method, independent of type of polymer used. In addition, PXRD patterns of the physical mixtures of GF and polymer samples were similar to that of untreated, GF, indicating the drug remained in crystalline form in the physical mixtures. In contrast, spray drying yielded an amorphous solid dispersion as was evident from the absence of peaks in the powder XRD scans.

The crystal structure is considered to be highly ordered structure, repeating itself in three dimensions. However, in practice, there are always imperfections in the crystal lattice such as point defects (e.g. vacancies, impurity defects etc), line defects (e.g edge dislocation) and plan defects (e.g grain boundaries)[38]. The level of such imperfections are likely to increase many fold during rapid drying process such as spray drying. Hence, spray drying process produced amorphous morphology.

During SAS processing, there was multicomponent system of drug, polymer and solvent. The presence of drug and polymer could have affected the solubility of acetone in $scCO_2$. Reverchon et al.,[36] hypothesized that when there is incomplete miscibility between the organic solvent and the $scCO_2$, the particle formation takes longer duration, and particles are formed at the bottom of the vessel only when the organic phase reaches the super-saturation. This process takes longer duration (as

compared to spray drying) and hence that may have allowed preferred packing of the molecules into its most stable form, the crystalline form. This is why our SAS process yielded crystalline morphology, and spray drying process produced amorphous material.

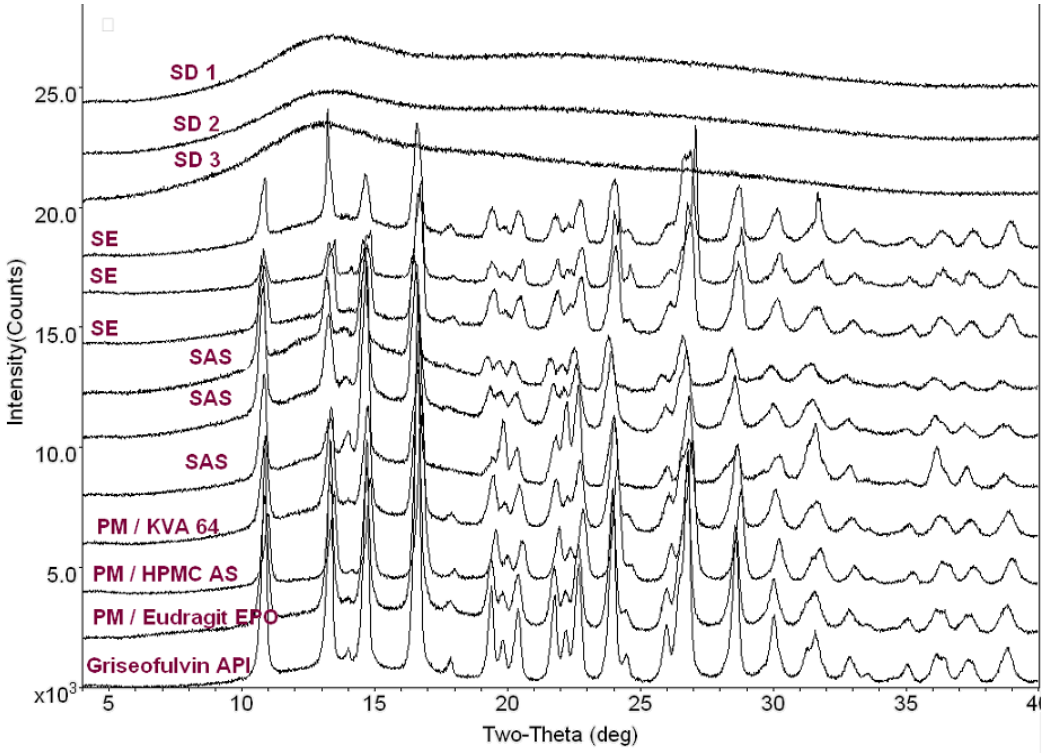

Figure 9. PXRD of untreated as-is GF, SAS formulations, spray dried formulation, and solvent evaporation method formulations.

3.4 Thermal Analysis

DSC curves of micronized GF obtained from supplier, SAS coprecipitate, solvent evaporated solid dispersion, and spray-dried samples to corroborate the amorphicity and/or crystallinity of GF in the solid dispersion, are shown in Figure 10. All samples were dried at 90^0C for 10 minutes to eliminate any plasticizing effect from residual organic solvent. Untreated GF gave a melting endotherm at around 219°C indicating that the drug is in crystalline form. Melting of GF was observed between 215 to 218°C with SAS processed coprecipiates, and the solvent evaporation process samples. DSC analysis is in agreement with PXRD and provided further evidence that the SAS processed material and solvent evaporation process material are crystalline in nature.

There was complete disappearance of drug melting endotherm for spray dried materials. Independent of the type of polymer used, all spray dried formulations of GF were amorphous and their glass transition temperature (Tg) was calculated . Tg of spray dried formulation containing Kollidon VA64, HPMCAS-LF, and Eudragit EPO were 82.7^0C , 93.9^0C and 90.1^0C , respectively. The change in glass transition temperature reflects different noncovalent interaction between the drug, Griseofulvin (Tg 89^0C) and polymers, Kollidon VA64 (Tg 113^0C), HPMCAS-LF (Tg 123^0C), and Eudragit EPO (Tg 55^0C). These findings are also compatible with their PXRD observations. The similarity in DSC curves and PXRD patterns with spray-dried samples indicated that drug was amorphously dispersed in the polymer.

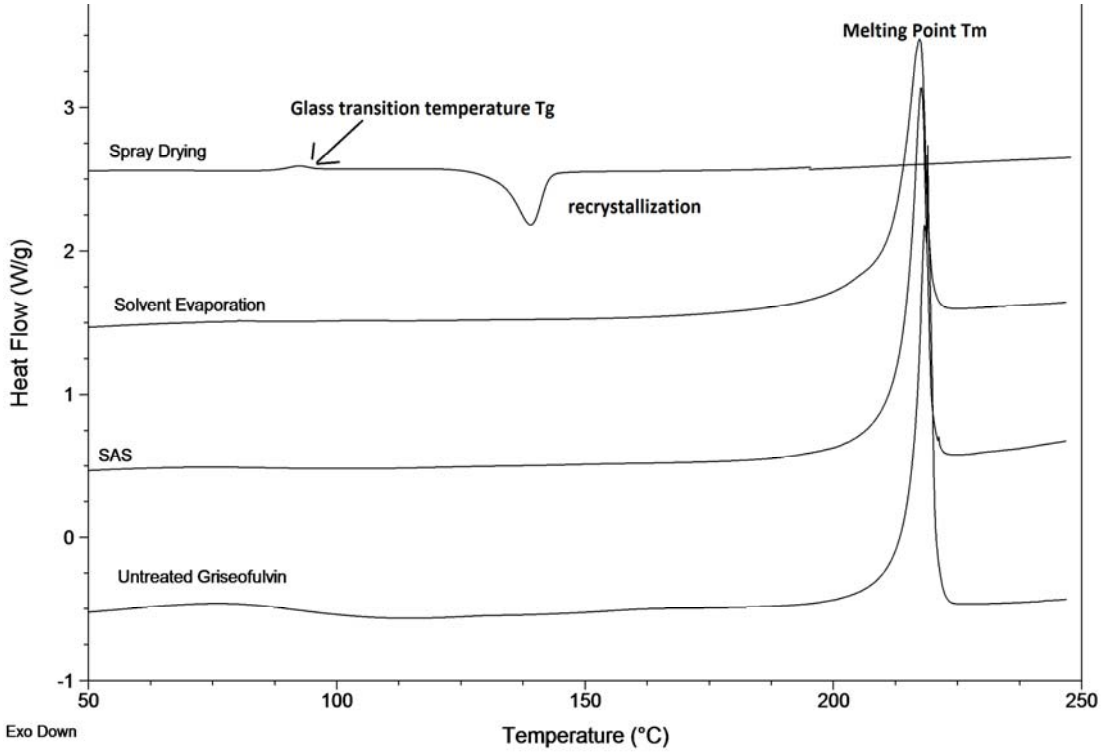

Figure 10. DSC curves of untreated GF, SAS formulation, spray dried formulation, and solvent evaporation method formulation.

3.5 FTIR Analysis

FTIR is an effective technique in detecting presence of interaction in drug-carrier solid dispersions. The appearance or disappearance of peaks and/or the shift of their positions are often an indication of interactions such as hydrogen bonding.[39] To examine the possibility of hydrogen bond formation, an FTIR study was undertaken.

As shown in Figure 11(b), GF has two characteristic peaks; the first peak (1,704 cm^{-1}) corresponds to the stretching of carbonyl group of the benzofuran, and the second peak (1,658 cm^{-1}) corresponds to the stretching of the carbonyl group of cyclohexene. These FTIR spectra of GF were in agreement with published work of Nair et al.,[40].

The FTIR results showed that there is a broadening of the GF carbonyl peak at 1,704 $cm^{-1,}$ and slight shift in 1,658 cm^{-1} peak, in the binary solid dispersion of spray dried formulations with all polymers (Figure 12). The broadened peaks indicated that the drug has formed hydrogen bonds, resulting in the shift of the peak. The broadening also refers to the distribution of free and bound carbonyl groups of GF. FTIR spectrum from SAS and solvent evaporation processes showed no discernible differences.

a)

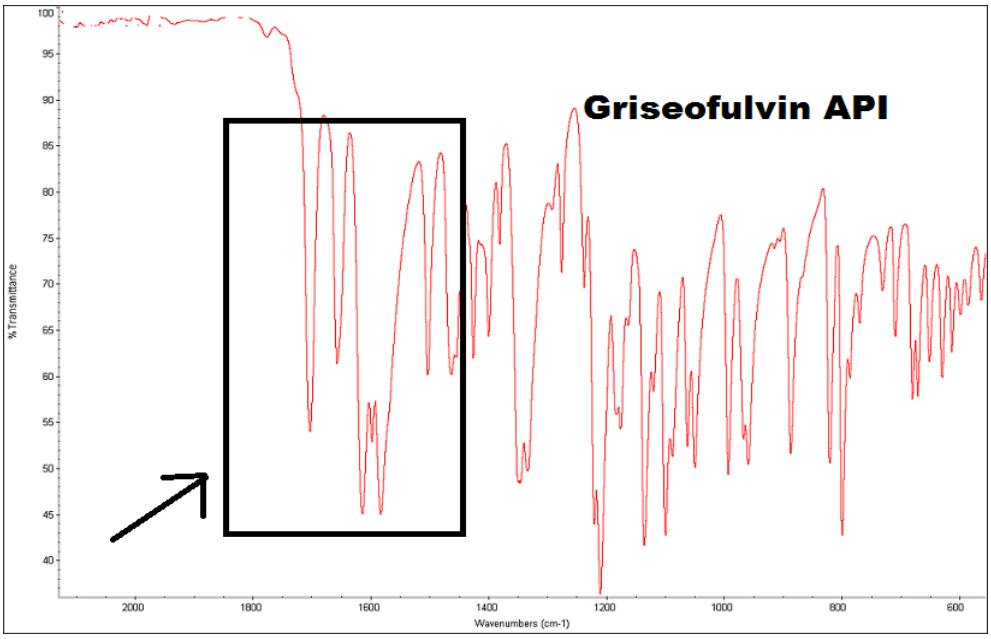

b)

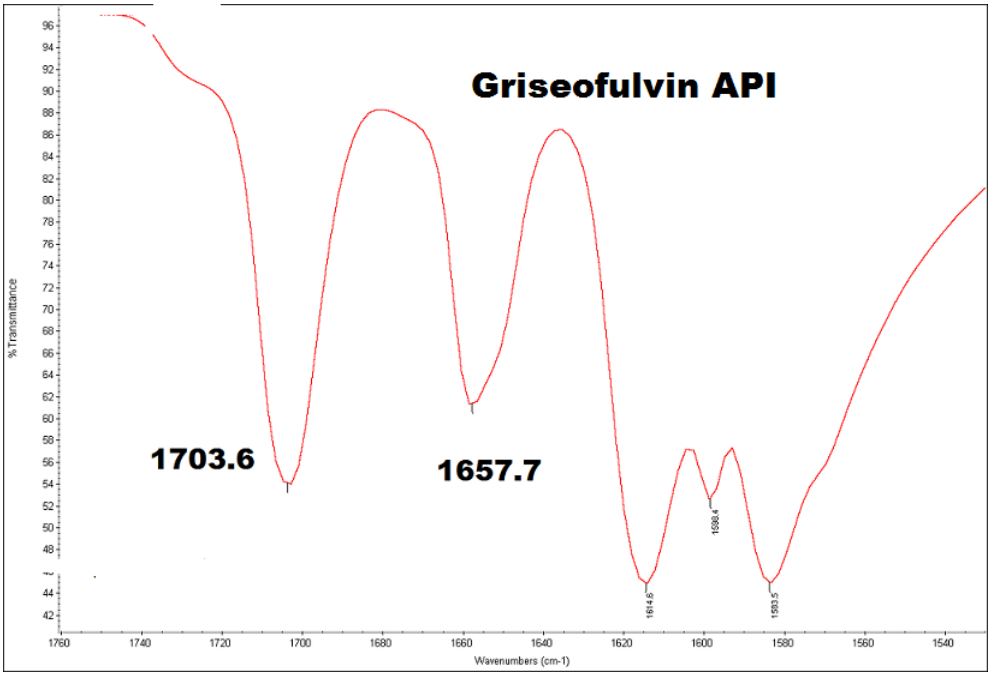

Figure 11: FTIR Spectrum of griseofulvin API (un-processed), showing entire spectrum (a), and the region of interest (b).

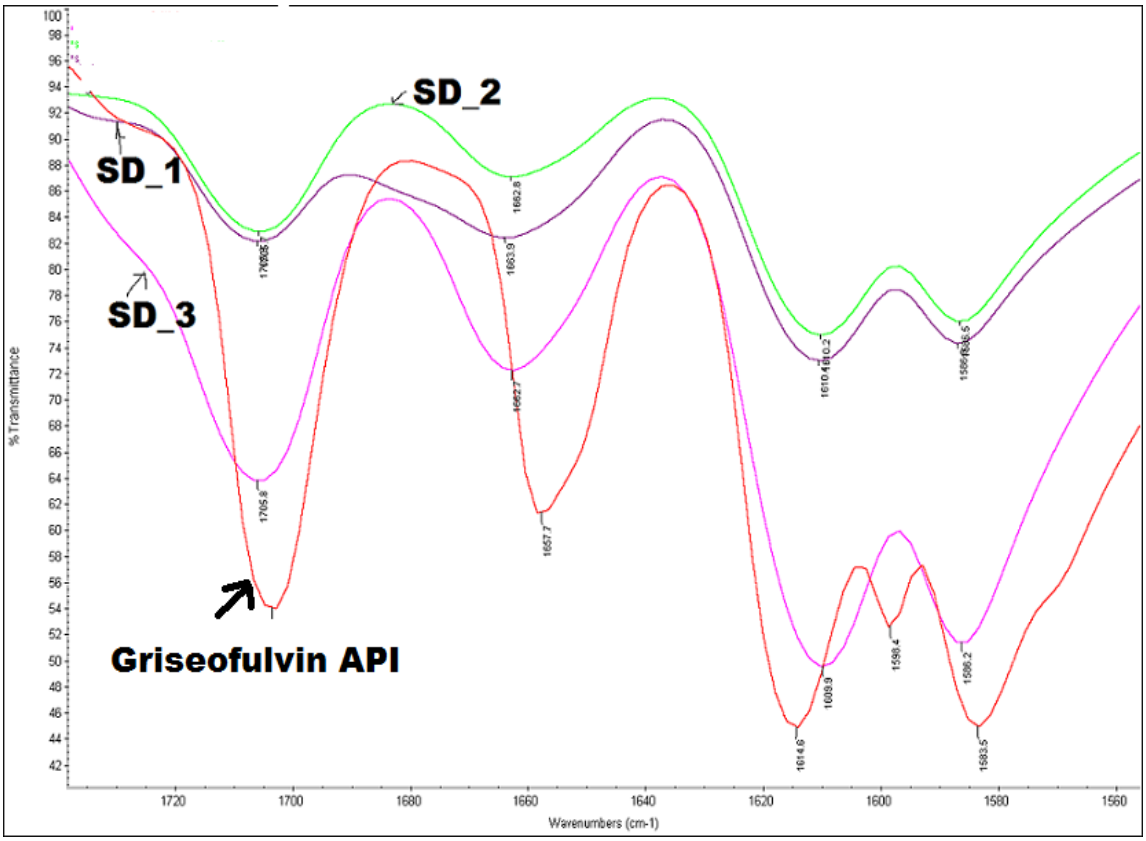

Figure 12. FTIR spectrum of spray dried formulations vs. Griseofulvin API

3.6 Dissolution Study

The drug dissolution behaviors of SAS formulations, spray-dried formulations, and solvent evaporation method formulations, were compared to untreated GF in physical mixture with a water soluble polymer (Kollidon VA64) . It can be seen in the Figures 13 and 14, that enhancement of GF dissolution rate was achieved in SAS and spray dried formulations. Dissolution curves of spray dried and SAS coprecipitates showed the steep initial slope and the dissolution rate was more than 8 times higher than raw drug after 100 minutes of dissolution.

In regards to the physicochemical properties studied in this work, similar mechanisms seemed to govern the dissolution of GF , independent of the type of polymer used in the solid dispersion. The dissolution profiles of products prepared by spray drying, and SAS enhanced the dissolution of GF to all most the same extent; whereas solvent evaporation method formulation did not improve the rate of dissolution of GF.

GF in spray dried solid dispersions was amorphous, however in SAS formulation it was crystalline. Prior to starting the dissolution, our expectation was that spray dried formulation would be better in rate of dissolution compared to SAS formulations. It was surprising to find that there was apparently no difference in rate of dissolution between SAS and spray dried formulations. This is because the improvement in dissolution was due to reduction in particle size. SAS formulation when exposed to phosphate buffer produces nano crystalline GF in situ. Similarly, amorphous GF solid dispersion from spray drying process undergoes fast re-crystallization when exposed to aqueous environment (as confirmed in polarized light microscopy), and leads to

formation of nano crystalline material in situ, identical to SAS formulation. Thus, it is the small particle size (of SAS and spray dried processes) with large surface area, which facilitate the disintegration of the solid dispersions, and provides faster rate of dissolution. It was confirmed by Malvern laser light diffractometer, that particle size of *in situ* GF was identical in SAS and spray drying process.

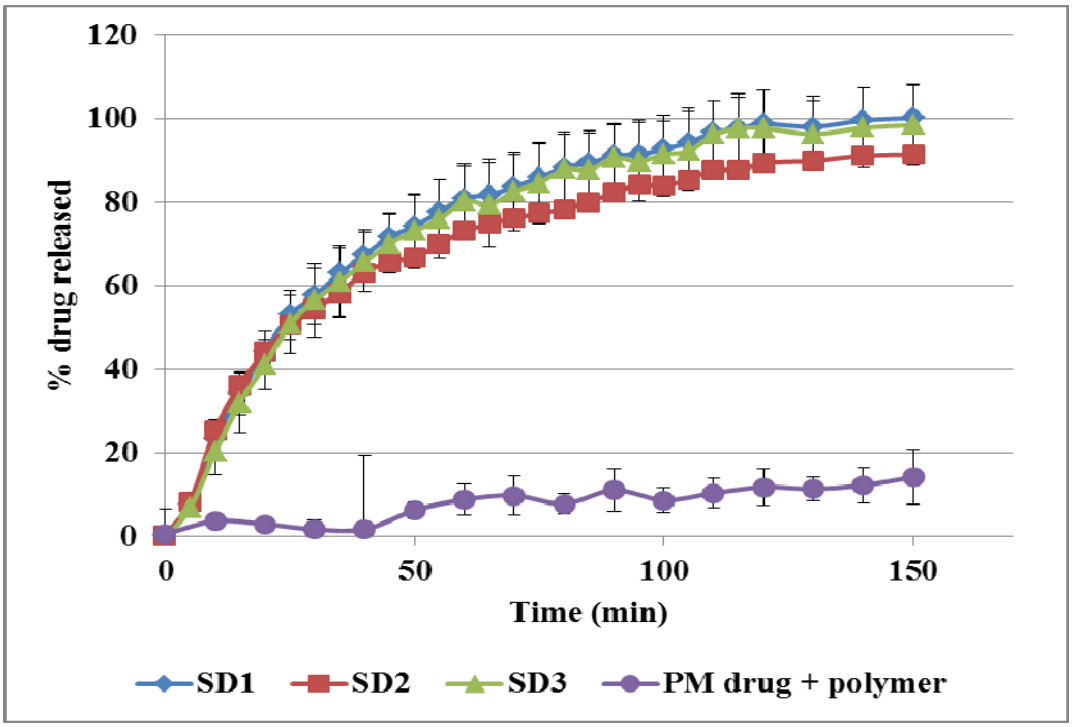

Figure 13. Dissolution of griseofulvin from tablets made with spray dried formulations vs physical mixture of GF with Kollidon VA64

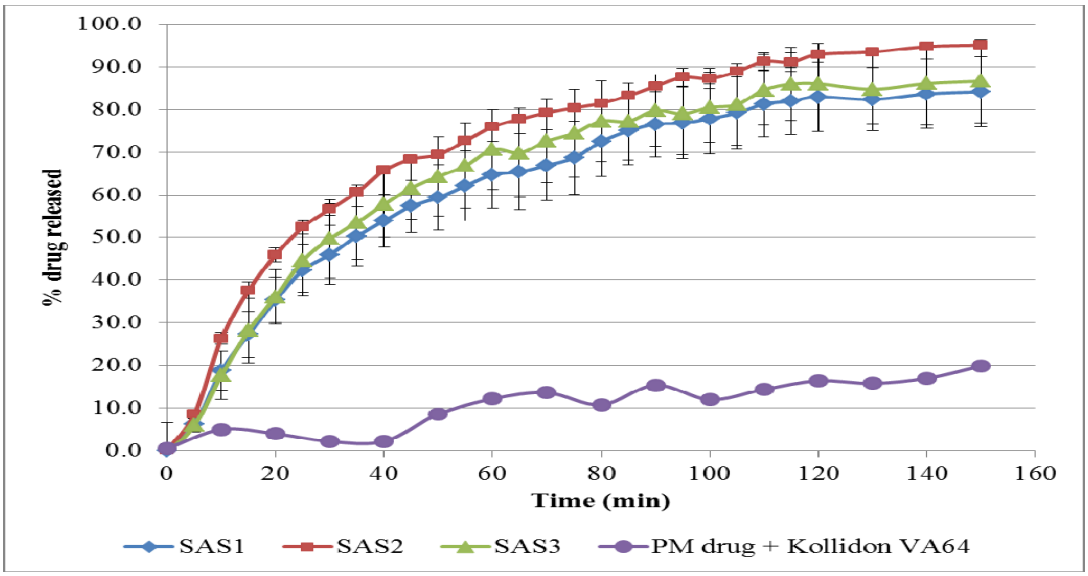

Figure 14. Dissolution of griseofulvin from tablets made with SAS formulations vs physical mixture of GF with Kollidon VA64

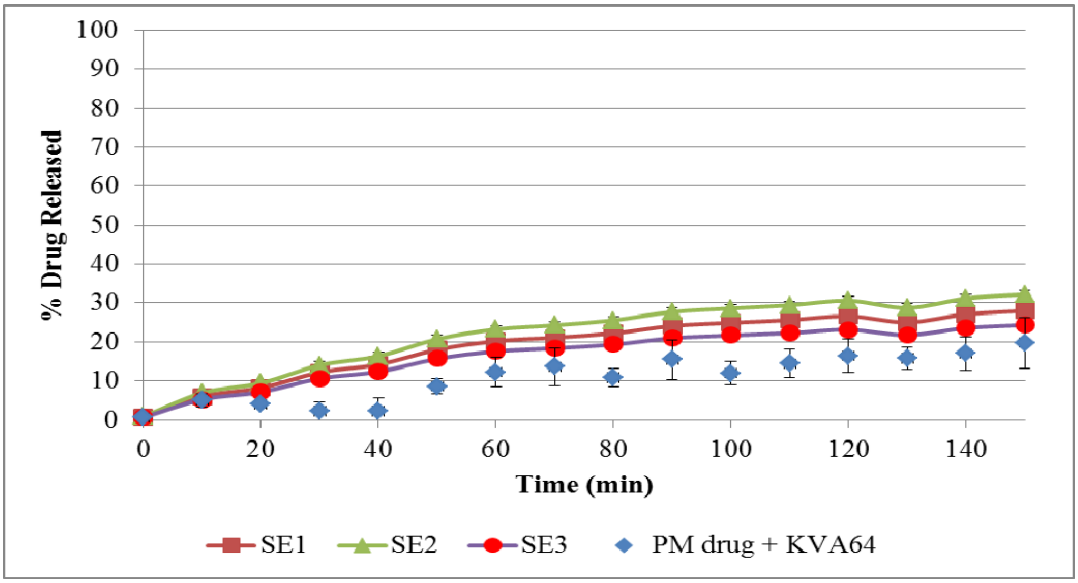

Figure 15. Dissolution of griseofulvin from tablets made with solvent evaporation method formulations vs physical mixture of GF with Kollidon VA64

Intrinsic dissolution rate (IDR)

Apparent IDR of formulations manufactured by three different methods, and three different polymers, were calculated by measuring the slope of concentration (μg/mL) vs time (min) profile; and are compared to that of physical mixture of GF with KollidonVA64. The IDR of pure GF in physical mixture with polymer is 0.0038 $\mu g/cm^2/min$. Table 4 shows the IDR of various formulations prepared by SAS, spray drying, and solvent evaporation processing. The IDR of SAS formulations ranged between 0.0058 $\mu g/cm^2/min$ to 0.0065 $\mu g/cm^2/min$, which was an improvement of 53% to 71%. The IDR of spray dried formulations ranged between 0.0063 $\mu g/cm^2/min$ to 0.0068 $\mu g/cm^2/min$, which was an improvement of 66% to 79%. Whereas, the IDR of solvent evaporation process formulations ranged between 0.0036 $\mu g/cm^2/min$ to 0.0039 $\mu g/cm^2/min$, and showed almost no improvement.

Table 4: Intrinsic Dissolution Rates of various solid dispersions (mean ± SD, n=3)

	Intrinsic Dissolution Rate (μg/cm^2/min)		
	SAS	Spray Drying	Solvent Evaporation
Kollidon® VA64	0.0065 ± 0.0011	0.0063 ± 0.0015	0.0037 ± 0.0008
HPMCAS-LF	0.0058 ± 0.0008	0.0068 ± 0.0007	0.0039 ± 0.0002
Eudragit® EPO	0.0062 ± 0.0014	0.0062 ± 0.001	0.0036 ± 0.0009
Physical Mixture of GF + Kollidon VA64		0.0038 ± 0.0005	

4.0 CONCLUSION

SAS, spray drying, and conventional solvent evaporation techniques were evaluated for their potential to produce rapidly dissolving dosage form of griseofulvin, a BCS class II API, with hydrophilic polymers. The properties of the product, and key processing attributes are summarized in Table 5.

Table 5. Comparison of SAS, spray drying, and solvent evaporation methods, for preparation of GF coprecipitates

		Process Temp. (^{0}C)	Process Yield (%)	d_{50} intact (µm)	d_{50} in-situ (µm)	DSC (T_m /T_g) (^{0}C)	PXRD	FTIR Interaction?	IDR µg/cm^2 /min
SAS	KVA64	45	89	3.7	0.4	T_m 215.0	C	No	0.0065
	HPMC AS-LF	45	91	2.8	0.37	T_m 216.9	C	No	0.0058
	Eudragit EPO	45	60	2.3	0.37	T_m 217.1	C	No	0.0062
SD	KVA64	65	54	12.9	0.343	T_g 82.7	A	Yes	0.0063
	HPMC AS-LF	65	60	1.9	0.375	T_g 93.9	A	Yes	0.0068
	Eudragit EPO	65	63	2.5	0.34	T_g 90.1	A	Yes	0.0062
SE	KVA64	65	95	271.2	18.3	T_m 218.0	C	No	0.0037
	HPMC AS-LF	65	92	290.7	21.5	T_m 216.9	C	No	0.0039
	Eudragit EPO	65	90	287.0	28.1	T_m 217.9	C	No	0.0036

T_m = melting point, T_g = glass transition temperature, C= Crystalline, A= Amorphous,

It was shown that the properties of GF-polymer coprecipitates are influenced by the processing methods. Overall, SAS is the most desirable process, as it had reasonably high product yield. The product obtained was crystalline, and was subjected to the lowest temperature during processing. Due to crystalline morphology and exposure to milder processing conditions, it is expected to have the least stability complications. On the whole, it is a promising approach to produce crystalline solid dispersions in a few processing steps. However, the complexity of the process must be weighed against its benefits.

From downstream dosage form processing perspective, spray dried products being spherical in shape, would be desirable compounds as they would have good powder flow characteristics. The amorphous GF was molecularly dispersed in the spray dried solid dispersions of each polymer through hydrogen bonding. However, due to low polymer content (20%), the drug re-crystallizes rapidly in an aqueous environment. Therefore, it is assumed that the drug would undergo rapid recrystallization during storage. In spite of several prediction methods available to measure reversion to crystallinity, it is still a difficult task to determine accurately and to control. Hence, we conclude that the spray drying process is not desirable for this formulation.

We expect almost the same cost of operation for SAS and SD processes. Conventional solvent evaporation process was the least desirable one even though it was the least expensive, as it did not improve the rate of dissolution of GF.

REFERENCES

1. Stegemann S, Leveiller F, Franchi D, de Jong H, Linden H 2007. When poor solubility becomes an issue: from early stage to proof of concept. Eur J Pharm Sci 31:249-261.

2. Chiou WL, Riegelman S 1971. Pharmaceutical applications of solid dispersion systems. J Pharm Sci 60:1281-1302.

3. Bikiaris DN 2011. Solid dispersions, part I: recent evolutions and future opportunities in manufacturing methods for dissolution rate enhancement of poorly water-soluble drugs. Expert Opin Drug Deliv 8:1501-1519.

4. Hecq J, Deleers M, Fanara D, Vranckx H, Amighi K 2005. Preparation and characterization of nanocrystals for solubility and dissolution rate enhancement of nifedipine. Int J Pharm 299:167-177.

5. Keck CM, Muller RH 2006. Drug nanocrystals of poorly soluble drugs produced by high pressure homogenisation. Eur J Pharm Biopharm 62:3-16.

6. Merisko-Liversidge E, Liversidge GG, Cooper ER 2003. Nanosizing: a formulation approach for poorly-water-soluble compounds. Eur J Pharm Sci 18:113-120.

7. Muller RH, Bohm BHL, Grau MJ, Wise DL. 2000. Nanosuspensions-a formulation approach for poorly soluble and poorly bioavailable drugs. In Anonymous Handbook of Pharmaceutical Controlled Release, New York: Marcel Dekker. p 345-357.

8. Ruan LP, Yu BY, Fu GM, Zhu DN 2005. Improving the solubility of ampelopsin by solid dispersions and inclusion complexes. J Pharm Biomed Anal 38:457-464.

9. Cheong HA, Choi HK 2002. Enhanced percutaneous absoption of piroxicam via salt formation with ethanolamines. Pharm Res 19:1375-1380.

10. Odeberg JM, Kaufmann P, Kroon KG, Hoglund P 2003. Lipid drug delivery and rational formulation design for lipophilic drugs with low oral bioavailability, applied to cyclosporine. Eur J Pharm Sci 20:375-382.

11. Lee S, Nam K, Kim MS, Jun SW, Park JS, Woo JS, Hwang SJ 2005. Preparation and characterization of solid dispersions of itraconazole by using aerosol solvent extraction system for improvement in drug solubility and bioavailability. Arch Pharm Res 28:866-874.

12. Moneghini M, Kikic I, Voinovich D, Perissutti B, Filipovic-Grcic J 2001. Processing of carbamazepine-PEG 4000 solid dispersions with supercritical carbon dioxide: preparation, characterisation, and in vitro dissolution. Int J Pharm 222:129-138.

13. Paradkar A, Ambike AA, Jadhav BK, Mahadik KR 2004. Characterization of curcumin-PVP solid dispersion obtained by spray drying. Int J Pharm 271:281-286.

14. Takeuchi H, Nagira S, Yamamoto H, Kawashima Y 2005. Solid dispersion particles of amorphous indomethacin with fine porous silica particles by using spray-drying method. Int J Pharm 293:155-164.

15. Thakkar AL, Hirsch CA, Page JG 1977. Solid dispersion approach for overcoming bioavailability problems due to polymorphism of nabilone, a cannabinoid derivative. J Pharm Pharmacol 29:783-784.

16. FernÃ¡ndez M, Carmen RodrÃguez I, Margarit MV, Cerezo A 1992. Characterization of solid dispersions of piroxicam/polyethylene glycol 4000. Int J Pharm 84:197-202.

17. Jung J, Yoo SD, Lee S, Kim K, Yoon D, Lee K 1999. Enhanced solubility and dissolution rate of itraconazole by a solid dispersion technique. Int J Pharm 187:209-218.

18. Thybo P, Kristensen J, Hovgaard L 2007. Characterization and Physical Stability of Tolfenamic Acid-PVP K30 Solid Dispersions. Pharm Dev Technol 12:43-53.

19. Del Valle EMM, Galan MA 2005. Supercritical Fluid Technique for Particle Engineering: Drug Delivery Applications. Rev Chem Eng 21:33-69.

20. Foster N, Mammucari R, Dehghani F, Barrett A, Bezanehtak K, Coen E, Combes G, Meure L, Ng A, Regtop HL, Tandya A 2003. Processing Pharmaceutical Compounds Using Dense Gas Technology. Ind Eng Chem Res 42:6476-6493.

21. Knez Z, Weidner E 2003. Particles formation and particle design using supercritical fluids. Current Opinion in Solid State and Materials Science 7:353-361.

22. Kompella UB, Koushik K 2001. Preparation of drug delivery systems using supercritical fluid technology. Crit Rev Ther Drug Carrier Syst 18:173-199.

23. Kerc J, Srcic S, Knez Z, Sencar-Bozic P 1999. Micronization of drugs using supercritical carbon dioxide. Int J Pharm 182:33-39.

24. Snavely WK, Subramaniam B, Rajewski RA, Defelippis MR 2002. Micronization of insulin from halogenated alcohol solution using supercritical carbon dioxide as an antisolvent. J Pharm Sci 91:2026-2039.

25. Won D, Kim M, Lee S, Park J, Hwang S 2005. Improved physicochemical characteristics of felodipine solid dispersion particles by supercritical anti-solvent precipitation process. Int J Pharm 301:199-208.

26. Jung J, Clavier JY, Perrut M 2003. Gram to kilogram scale up of supercritical antisolvent process.

27. Chattopadhyay P, Gupta RB 2001. Production of griseofulvin nanoparticles using supercritical CO(2) antisolvent with enhanced mass transfer. Int J Pharm 228:19-31.

28 http://www.drugbank.ca/drugs/DB00400 , accessed on 02/25/2013

29. Al-Obaidi H, Buckton G 2009. Evaluation of griseofulvin binary and ternary solid dispersions with HPMCAS. AAPS PharmSciTech 10:1172-1177.

30. Corey JB, Marshall DC, Dwayne TF, Warren KM, Michael MM, Daniel TS. 2008. Patent. US 2010/0215747 A1

31. Sarode AL, Sandhu H, Shah N, Malick W, Zia H 2013. Hot melt extrusion (HME) for amorphous solid dispersions: Predictive tools for processing and impact of

drugâ€“polymer interactions on supersaturation. European Journal of Pharmaceutical Sciences 48:371-384.

32. Chernysheva YV, Babak VG, Kildeeva NR, Boury F, Benoit JP, Ubrich N, Maincent P 2003. Effect of the type of hydrophobic polymers on the size of nanoparticles obtained by emulsificationâ€“solvent evaporation. Mendeleev Communications 13:65-67.

33. Masters K. 1991. Spray drying handbook, 5th ed., New York: John Wiley and Sons.

34. Lacasse FX, Hildgen P, McMullen JN 1998. Surface and morphology of spray-dried pegylated PLA microspheres. Int J Pharm 174:101-109.

35. Foster NR, Meure LA, Barrett AM, Abbasi F, Dehghani F vol. 3, 2003. Micronisation of griseofulvin by the aerosol solvent extraction system. Proceedings of the 6th International Symposium on Supercritical Fluids, Versailles. International Society for the Advancement of Supercritical Fluids, Nancy, France, pp 1771–1776.

36. Reverchon E, Della Porta G 1999. Production of antibiotic micro- and nano-particles by supercritical antisolvent precipitation. Powder Technol 106:23-29.

37. Jarmer DJ, Lengsfeld CS, Anseth KS, Randolph TW 2005. Supercritical fluid crystallization of griseofulvin: crystal habit modification with a selective growth inhibitor. J Pharm Sci 94:2688-2702.

38. Brittain HG, Fiese EF. 1999. Effects of pharmaceutical processing on drug polymorphs and solvates. In Brittain HG, editor. Polymorphism in pharmaceutical solids, New York: Marcel Dekker.

39. Van dM, Augustijns P, Blaton N, Kinget R 1998. Physico-chemical characterization of solid dispersions of temazepam with polyethylene glycol 6000 and PVP K30. Int J Pharm 164:67-80.

40. Nair R, Nyamweya N, GÃ¶nen S, MartÄ±Ì nez-Miranda LJ, Hoag SW 2001. Influence of various drugs on the glass transition temperature of poly(vinylpyrrolidone): a thermodynamic and spectroscopic investigation. Int J Pharm 225:83-96.

APPENDICES

Appendix A

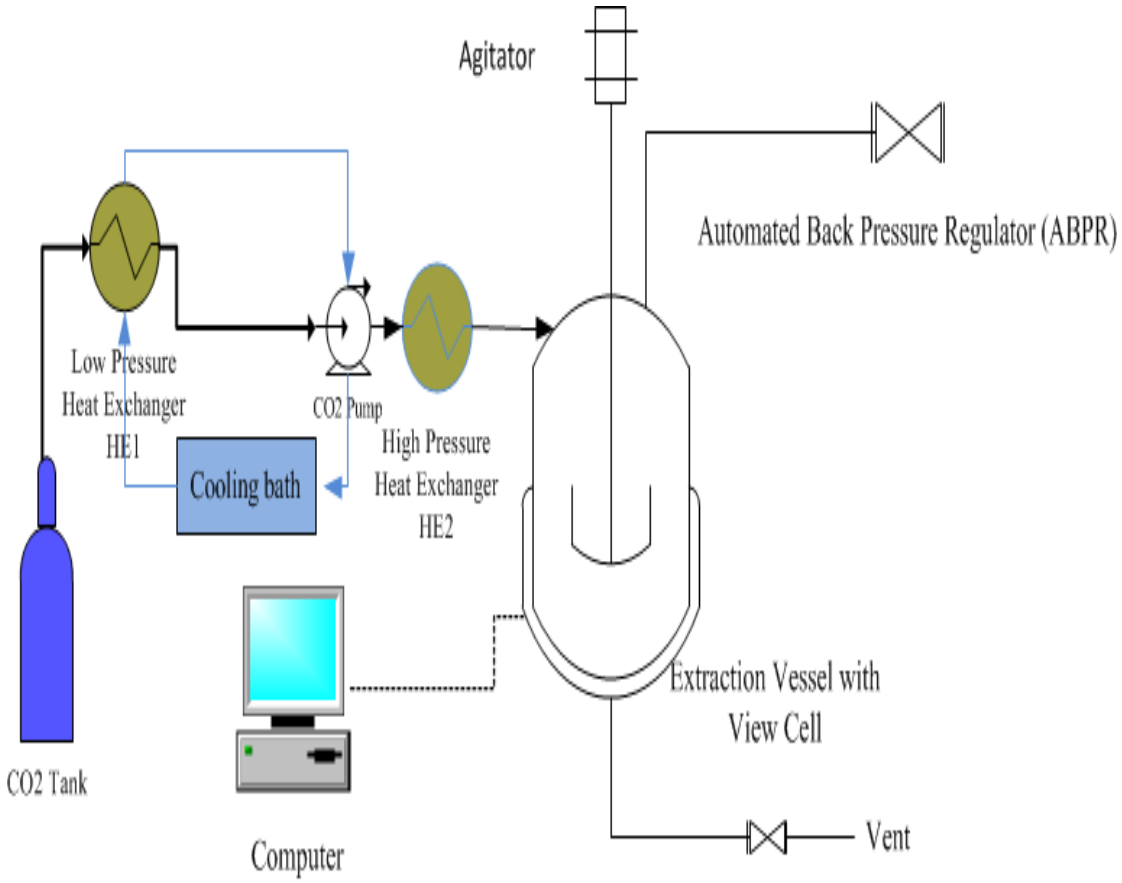

Figure A.1: Schematic representation of RESS apparatus for solubility and miscibility evaluations

Appendix B

MASTERSIZER 2000

Result Analysis Report

Sample Name: SAS Expts (Gris + KVa64) OP1 - Average
SOP Name:
Measured: Thursday, December 20, 2012 12:13:55 PM

Sample Source & type: KT = Griseo + KVa64
Measured by: masakad
Analysed: Thursday, December 20, 2012 12:13:57 PM

Sample bulk lot ref: OP1-Repeat 2
Result Source: Averaged

Particle Name: Griseofulvin
Accessory Name: Hydro 2000S (A)
Analysis model: General purpose
Sensitivity: Normal

Particle RI: 1.340
Absorption: 0.01
Size range: 0.020 to 2000.000 um
Obscuration: 9.00 %

Dispersant Name: Water
Dispersant RI: 1.330
Weighted Residual: 20.235 %
Result Emulation: Off

Concentration: 0.0201 %Vol
Span : 2.536
Uniformity: 0.82
Result units: Volume

Specific Surface Area: 17.4 m²/g
Surface Weighted Mean D[3,2]: 0.344 um
Vol. Weighted Mean D[4,3]: 0.549 um

d(0.1): 0.188 um **d(0.5):** 0.372 um **d(0.9):** 1.132 um

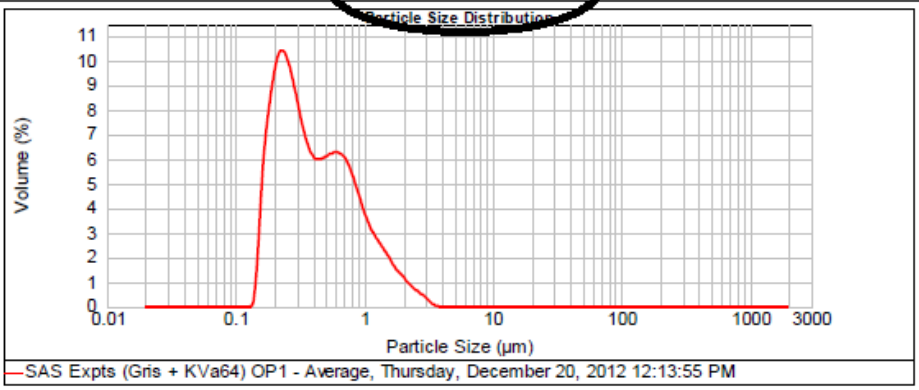

Size (µm)	Volume in %	Size (µm)	Volume in %	Size (µm)	Volume in %	Size (µm)	Volume in %	Size (µm)	Volume in %	Size (µm)	Volume in %
0.010	0.00	0.105	0.00	1.096	2.69	11.482	0.00	120.226	0.00	1258.925	0.00
0.011	0.00	0.120	0.00	1.259	2.26	13.183	0.00	138.038	0.00	1445.440	0.00
0.013	0.00	0.138	1.84	1.445	1.81	15.136	0.00	158.489	0.00	1659.587	0.00
0.015	0.00	0.158	6.20	1.660	1.36	17.378	0.00	181.970	0.00	1905.461	0.00
0.017	0.00	0.182	8.38	1.905	1.04	19.953	0.00	208.930	0.00	2187.762	0.00
0.020	0.00	0.209	9.42	2.188	0.73	22.909	0.00	239.883	0.00	2511.886	0.00
0.023	0.00	0.240	8.97	2.512	0.49	26.303	0.00	275.423	0.00	2884.032	0.00
0.026	0.00	0.275	7.74	2.884	0.27	30.200	0.00	316.228	0.00	3311.311	0.00
0.030	0.00	0.316	6.42	3.311	0.02	34.674	0.00	363.078	0.00	3801.894	0.00
0.035	0.00	0.363	5.60	3.802	0.00	39.811	0.00	416.869	0.00	4365.158	0.00
0.040	0.00	0.417	5.40	4.365	0.00	45.709	0.00	478.630	0.00	5011.872	0.00
0.046	0.00	0.479	5.55	5.012	0.00	52.481	0.00	549.541	0.00	5754.399	0.00
0.052	0.00	0.550	5.67	5.754	0.00	60.256	0.00	630.957	0.00	6606.934	0.00
0.060	0.00	0.631	5.57	6.607	0.00	69.183	0.00	724.436	0.00	7585.776	0.00
0.069	0.00	0.724	5.05	7.586	0.00	79.433	0.00	831.764	0.00	8709.636	0.00
0.079	0.00	0.832	4.20	8.710	0.00	91.201	0.00	954.993	0.00	10000.000	0.00
0.091	0.00	0.955	3.32	10.000	0.00	104.713	0.00	1096.478	0.00		
0.105	0.00	1.096		11.482	0.00	120.226	0.00	1258.925	0.00		

Operator notes: *Reproducibility study*

Malvern Instruments Ltd.
Malvern, UK
Mastersizer 2000 Ver. 5.22
Serial Number : 34264-82
File name: 20121220
Record Number: 14

Figure B.1: Particle size analysis report generated by Malvern instrument

Appendix C

Verification of miscibility of organic solvents in $scCO_2$

During the SAS process, when the organic solvent is added to the anti-solvent, the dissolution of massive amount of anti-solvent in the solvent causes enormous expansion of the liquid solvent. This phenomenon is called "volumetric expansion" which plays a vital role in the precipitation process. Volumetric expansion curves for acetone is available in the literature[38] at 33^0C. Researchers revealed that when CO_2 is added to a closed vessel containing acetone, the volume of acetone increases slowly with CO_2 mole fraction increasing from 0 to 0.8. However, acetone is expanded by 500 to 700% of its original volume, when the CO_2 mole fraction is > 0.85. DMSO also undergoes such large volumetric expansion in presence of CO_2, as reported by Kordiowski et al[39].

We wanted to observe and verify these phase behavioral changes when CO_2 is added to a closed vessel containing acetone or DMSO. These experiments were performed using RESS 50 apparatus as shown in Appendix A. We could observe through the view cell that both acetone and DMSO level levels would rise as more and more CO_2 was added to the vessel. The results are summarized in the Table C.1.

Table C.1. Miscibility and volume expansion of organic solvents with $scCO_2$

Contents of extraction vessel	Temperature (^{O}C)	Pressure (bar)	Observation (made through view cell)
25 ml Acetone + CO_2	30	50	Three phase system of acetone, liquid CO_2, and vapors of CO_2. Acetone level rises due to CO_2 being absorbed into it.
25 ml Acetone + CO_2	35	80	No phase boundary between acetone and $scCO_2$, indicating excellent miscibility.
25 ml Acetone + CO_2	100	300	No phase boundary between acetone and $scCO_2$, indicating excellent miscibility. Acetone level risen ~5-6 times.
25 ml DMSO + CO_2	30	50	Three phase system of DMSO, liquid CO_2, and vapors of CO_2. DMSO level rises due to CO_2 being absorbed into it.
25 ml DMSO + CO_2	35	75	No phase boundary between DMSO and $scCO_2$, indicating excellent miscibility.
25 ml DMSO + CO_2	100	300	No phase boundary between DMSO and $scCO_2$, indicating excellent miscibility. DMSO level risen ~5 times.

Appendix D

Verification of in-solubility of GF in acetone-CO_2 & DMSO-CO_2 system

At the beginning of the experiment, 100ml of acetone solution containing GF (25 mg/mL) was placed in the extraction vessel. Agitator was turned on to gently mix the acetone solution. When looked through the view cell, a clear acetone solution is seen, and agitator can be seen. After that, the CO_2 pump was turned on to fill the extraction vessel. Temperature was gradually raised from 35^0C to 60^0C, and pressure was gradually raised from 0 to 150 bar, and observations were made through the view cell. The solubility or insolubility of GF in CO_2 + acetone was judged by the visual appearance of cloudiness. We found that at 40^0C and 100 bar, the vessel was extremely cloudy, and agitator could not be seen, providing evidence that $scCO_2$ acts as an anti-solvent for GF. Experiments were then repeated by using DMSO as the organic solvent, at a GF concentration of 60 mg/ml. The results are summarized in the Table D.1. Even though these experiments were not quantitative in nature, they provided clear evidence that SAS technique can be applied for precipitation of GF from acetone or DMSO as the organic solvent.

Gioannis et al.,[40] conducted quantitative solubility determination of GF in presence of acetone. The solubility measurements for the GF–CO_2–acetone system were performed at 39^0C at 60 and 100 bar, and at 53^0C and 100 bar. They found that there was dramatic reduction in solubility of GF in acetone with increase in mole fraction of CO_2. At a CO_2 mole fraction of 0.9, pressure between 60 – 100 bar, and temperature between 39^0C to 53^0C, the solubility of GF in the binary system was approximately 0.0005 mol/mol .

Table D.1. Determination of solubility/insolubility of GF in acetone-scCO2, or DMSO-scCO2 system, by appearance of cloud point

Contents of extraction vessel	Temperature (^{O}C)	Pressure (bar)	Observation (made through view cell)
25 ml Acetone + GF (25 mg/mL)	35	1	Clear acetone solution.
25 ml Acetone + GF (25 mg/mL) + CO_2	35	80	Vessel cloudy, indicating drug is starting to precipitate out
25 ml Acetone + GF (25 mg/mL) + CO_2	40	100	Vessel extremely cloudy, indicating drug is almost insoluble at this condition. Agitator bar not visible due to extreme cloudiness.
25 ml Acetone + GF (25 mg/mL) + CO_2	60	150	Vessel extremely cloudy, indicating drug is almost insoluble at this condition. Agitator bar not visible due to extreme cloudiness.
25 ml DMSO + GF (60 mg/mL)	35	1	Clear DMSO solution.
25 ml DMSO + GF (60 mg/mL) + CO_2	35	75	Vessel very cloudy, indicating drug is starting to precipitate out
25 ml DMSO + GF (60 mg/mL) + CO_2	40	90	Vessel extremely cloudy, indicating drug is almost insoluble at this condition. Agitator bar not visible due to extreme cloudiness.
25 ml DMSO + GF (60 mg/mL) + CO_2	60	150	Vessel extremely cloudy, indicating drug is almost insoluble at this condition. Agitator bar not visible due to extreme cloudiness.

Appendix E

Physicochemical Characterization

E.1 Thermal Analysis and PXRD

Differential Scanning Calorimetry (DSC) profiles were obtained by using a DSCQ-2000 ® (TA Instruments, New Castle, Delaware) differential scanning calorimeter. Calibrations were performed prior to each day of analysis using pure samples of indium and zinc. The measurements were carried out in a hermetically sealed aluminum pans at a scanning rate of 10^0C per minute under nitrogen atmosphere using approximately 6 - 8 mg of sample. Melting point (T_m) values were determined by the Pyris software.

The crystalline properties of the samples obtained by SAS were determined by Powder X-Ray Diffraction (PXRD) using Bruker D8 Advance Powder X– Ray Diffractometer (Brukler Corporation, Madison, WI). Samples of interest were analyzed using a Cu (λ=1.54) K α radiation. The X-ray patterns were collected in the 2θ range of 1 to 40^0 by scan speed of 0.27^0/sec and step size of 0.0045°.

DSC curves of pure untreated GF, and an optimized SAS formulation (lot # OP1) are shown in Figure E.1. Pure GF gave a melting endotherm at around 219°C indicating that the drug is in crystalline form. As shown in Table E.1, melting of GF could be observed between 216°C to 219°C with all of the SAS formulations (N1 to N19, and OP1). Thermal analysis shows that processing and/or formulation variables did not affect the crystalline nature of drug.

Raw GF is crystalline in nature with well-defined peaks. PXRD of GF coprecipitates after SAS processing shows that the material morphology remained crystalline, independent of changes in processing and/or formulation variable. As shown in Figure E.2, the PXRD patterns of the optimized formulation produced from SAS were super imposable to the spectra of drug from the supplier. These findings were consistent with the results obtained by DSC.

In our study, there was multicomponent system comprising of drug, polymer and organic solvent. The presence of drug and polymer may have shifted the phase equilibrium and affected the solubility of acetone in scCO2, and hence the efficiency of SAS process to remove the solvent from the feed is reduced. This long duration likely allowed preferred packing of the molecules into its most stable form, the crystalline form.

Table E.1. Summary of thermal analysis and PXRD on SAS formulation of GF from DOE study

SAS Formulation Lot #	Melting Point from DSC (^{0}C)	Morphology from PXRD
Untreated as-is drug	218.28	Crystalline
N1	218.44	Crystalline
N2	219.02	Crystalline
N3	219.16	Crystalline
N4	217.31	Crystalline
N5	218.49	Crystalline
N6	218.44	Crystalline
N7	216.64	Crystalline
N8	218.42	Crystalline
N9	219.02	Crystalline
N10	219.16	Crystalline
N11	218.49	Crystalline
N12	217.31	Crystalline
N13	218.42	Crystalline
N14	219.02	Crystalline
N15	218.16	Crystalline
N16	217.95	Crystalline
N17	216.55	Crystalline
N18	216.90	Crystalline
N19	218.55	Crystalline
OP1	217.69	Crystalline

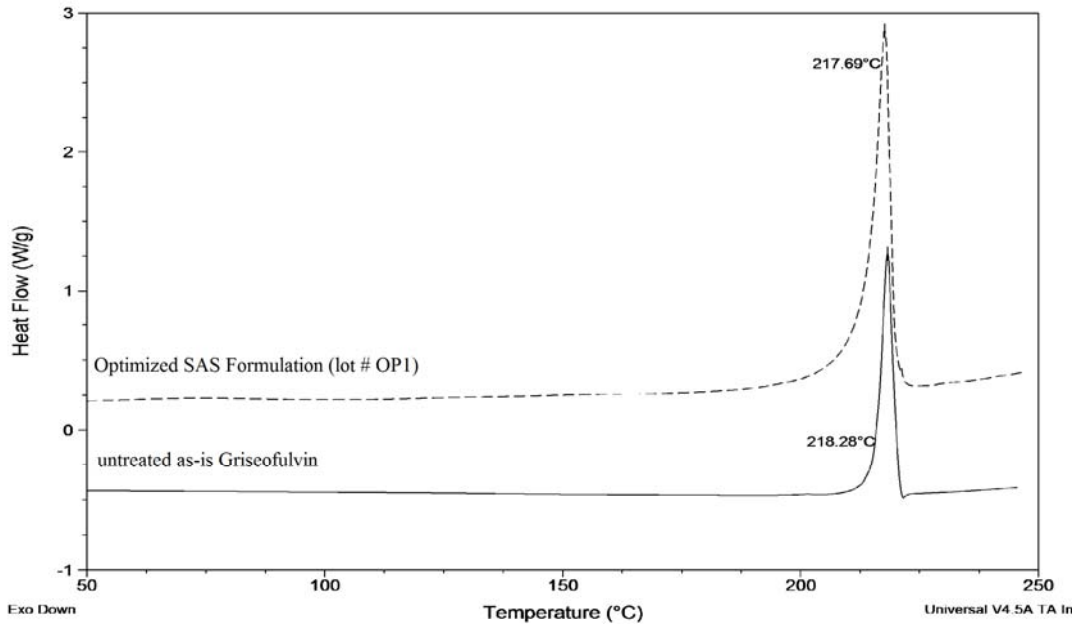

Figure E.1: DSC thermograms for optimized SAS formulation vs untreated as-is GF

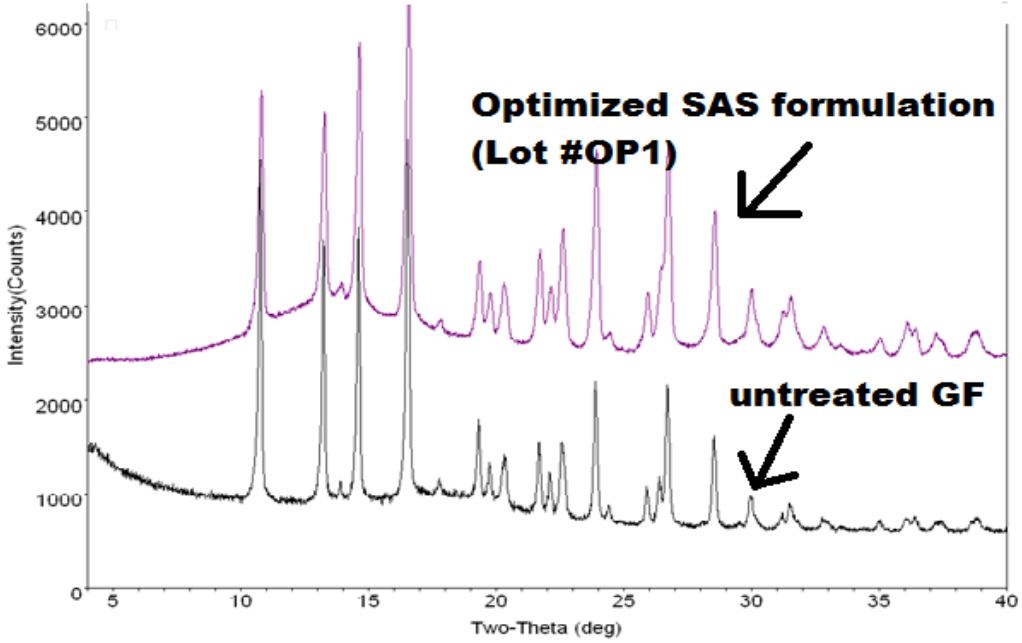

Figure E.2: PXRD spectra of optimized SAS formulation vs untreated as-is GF

E.2 Fourier Transform Infra-Red (FTIR)

FTIR spectra were collected on a Nicolet 6700 from Thermo scientific (Thermo Fisher Scientific Inc., Pittsburgh, PA) . Powders were measured directly using the smart orbit accessory. Spectra were collected from 400 – 4000 cm-1 using 64 scans at a resolution of 4 cm-1. Spectra were analyzed using the Omnic software (v.7.2).

FTIR spectrums were obtained for the untreated GF and an optimized SAS formulation (OP1), and are shown in Figure E.3 & E.4. The spectra of the GF in SAS formulation is similar to that of the untreated GF from supplier, with no shift of peaks due to SAS process. These results are in agreement with DSC and PXRD to show that there is no significant change in the physicochemical properties of GF. Also, there is no evidence of any interaction between drug and polymer.

a)

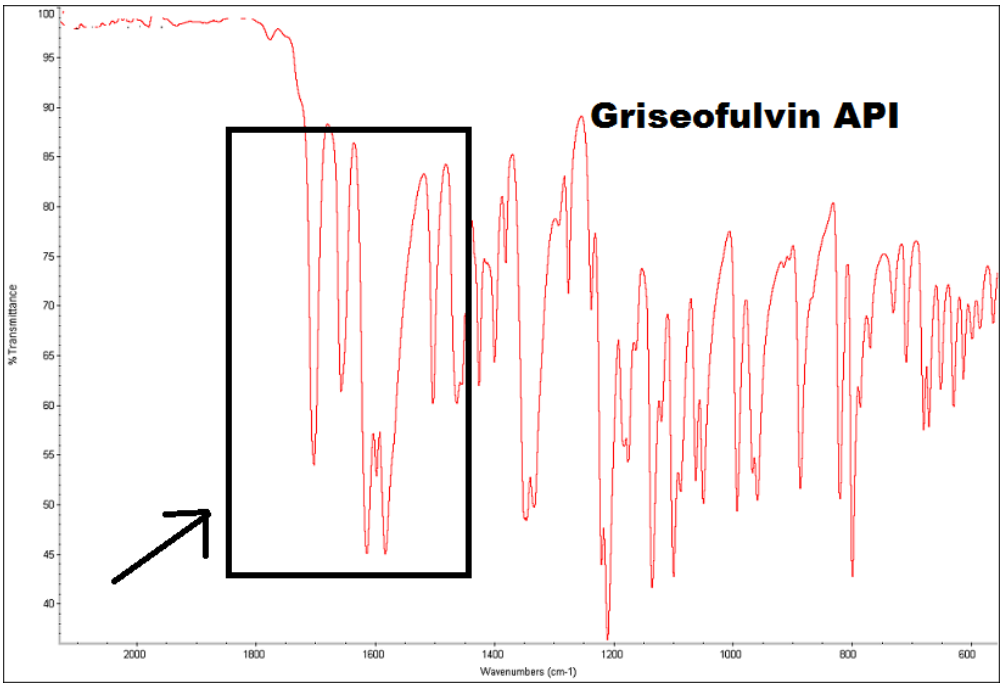

b)

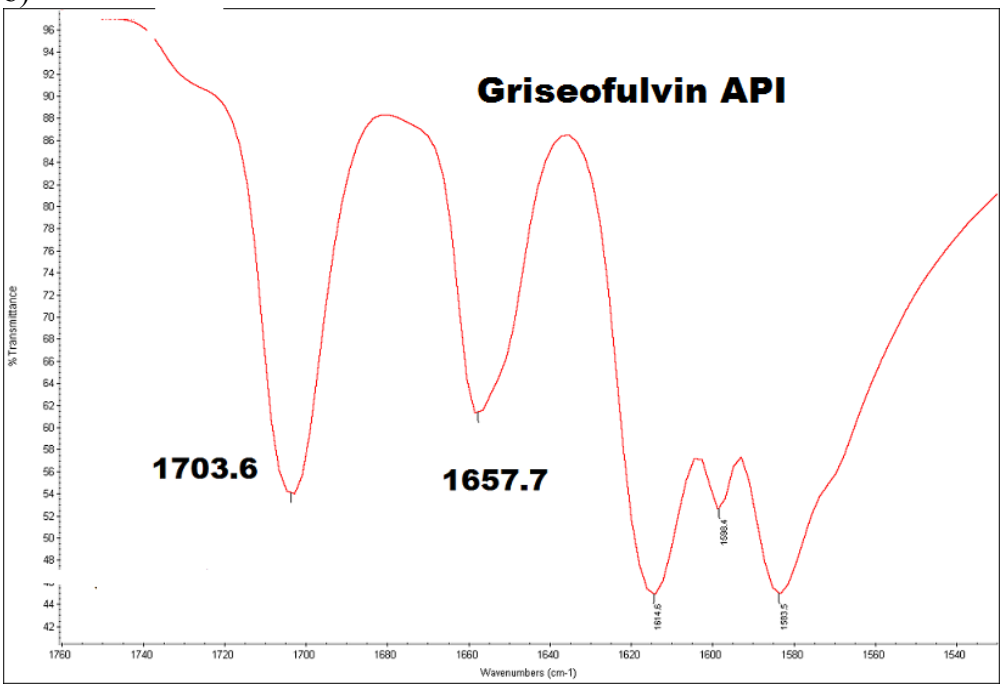

Figure E.3: FTIR Spectrum of griseofulvin API (un-processed) , showing entire spectrum (a), and the region of interest (b).

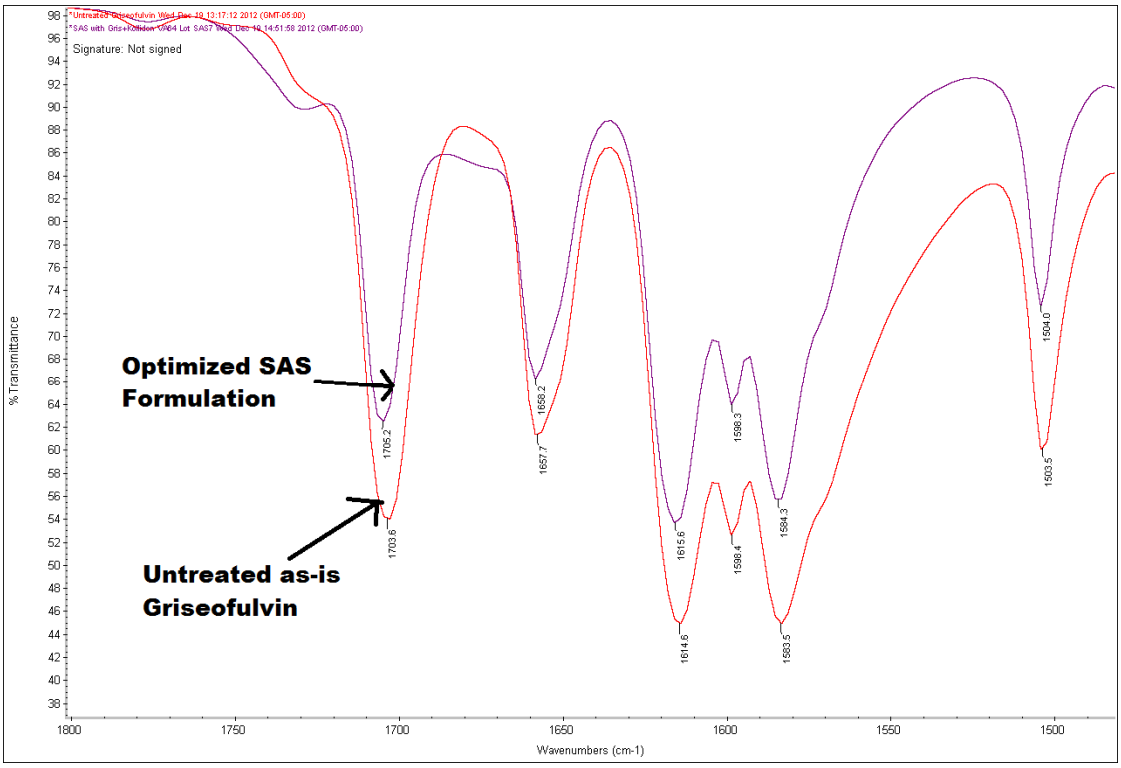

Figure E.4: FTIR spectra of optimized SAS formulation vs Griseofulvin API

E.3 Zeta Potential

The zeta potential value is an important particle characteristic as it can influence both particle stability as well as particle mucoadhesion. The electrostatic repulsion between particles with the same electric charge prevents the aggregation of the spheres[41]. Hence, more pronounced zeta potential values either positive or negative, can stabilize particle suspension. When SAS solid dispersion of drug and polymer is added to water, the polymer dissolves, leaving behind a suspension of drug particles. The zeta potential measurements were done to understand the characteristics of drug

suspension. A value lower than 30mV indicates that there is aren't enough charges on the particles to keep them in a stable, non-aggregated state. On the other hand, a large zeta potential value (>30mV) could support our argument that during particle size measurement we are measuring individual particles. The zeta potential values for our formulations (N1 to N19, and OP1) ranged from -31.1mV to -35.5mV, as shown in Table 6.

E.4 BET Surface area analysis

The specific surface area of samples was determined following the Brunauer–Emmett–Teller (BET) method of nitrogen adsorption/desorption at −196 °C with Tristar II® surface area and porosity measurement instrument manufactured by Micromeritics™ (Micromeritics Instrument, USA). BET surface area measurement was done only on the samples of optimized SAS formulation (lot # OP1).

BET surface area measurements were done for untreated GF from supplier and for optimized formulation of SAS coprecipitates (OP1). BET surface area value of 5.2457 m^2/g for SAS formulation was not significantly different from a value of 5.2095 m^2/g for untreated Griseofulvin. However, it should be noted that untreated GF is a micronized material. Secondly, SAS coprecipitates of drug and polymer together are not that much different in particle size compared to untreated GF. It is only in the *in-situ* conditions when the polymer is removed, the drug particle size is nano sized. Even though the BET surface area of SAS drug is similar to untreated drug from supplier, the SAS drug is expected to have better solubility and rate of dissolution.

E.5 Dissolution and intrinsic dissolution rate

Dissolution studies were performed by USP Dissolution Apparatus Type II , paddle method using Distek® dissolution apparatus (Distek, Inc., North Brunswick, NJ). The apparatus was equipped with UD-lite® fiber optic measurement capability. Solid Samples obtained with SAS processing were compressed into 100 mg tablets using a flat faced ¼" round tooling, under carver press. Each SAS formulation tablet contained equivalent of 7 mg of GF, the polymer Kollidon VA64 (1.75 mg) and the filler (Lactose). The physical mixture of GF (7 mg) and Kollidon VA64 (1.75 mg), were also compressed into 100 mg tablets using lactose as the filler. The dissolution analyses were performed in 500 ml of pH 6.8 phosphate buffers (0.05M), also called as simulated intestinal fluid (SIF), at 37^0C, 50 rpm stirring speed, and the drug dissolved was analyzed at UV wavelength of 295 nm.

Intrinsic dissolution rates (IDR) were determined by using Distek stationary disk (Distek Inc., USA) system. Approximately 200 mg of SAS processed sample were compressed with the aid of a benchtop Carver press (Carver, Inc., Wabash, IN, USA) at 4000 psi with a dwell time of 10 s to form a compact pellet of 0.5 cm^2 exposed surface area. Assemblies, each composed of the pellet, die, gasket, and a polypropylene plastic cap, were immersed with the pellet side up, into the bottom of flat-bottom dissolution vessels containing 500 mL of SIF at 37°C. The USP Apparatus II paddle was positioned 1 inch above the assembly and rotated at 50 rpm.

The dissolution profiles of tablets containing SAS formulation are compared in Figure E.5 to that of physical mixture of GF and Kollidon VA64 in the same ratio as in SAS

formulation. After 100 minutes, the amount dissolved from SAS formulation (80%) was more than 8 fold better compared to only 10% dissolved for micronized drug from supplier. The increased dissolution of the SAS drug is due to the decrease in particle size. According to Noyes Whitney equation[42], particle size reduction leads to increase in surface area and that leads to improvement in the rate of dissolution. In addition, we carried out an intrinsic dissolution study. As shown in Figure E.6, intrinsic dissolution rate (IDR) of a SAS formulation (0.0065 $\mu g/cm^2/min$) was 58% better than that of micronized GF (0.0038 $\mu g/cm^2/min$) in physical mixture.

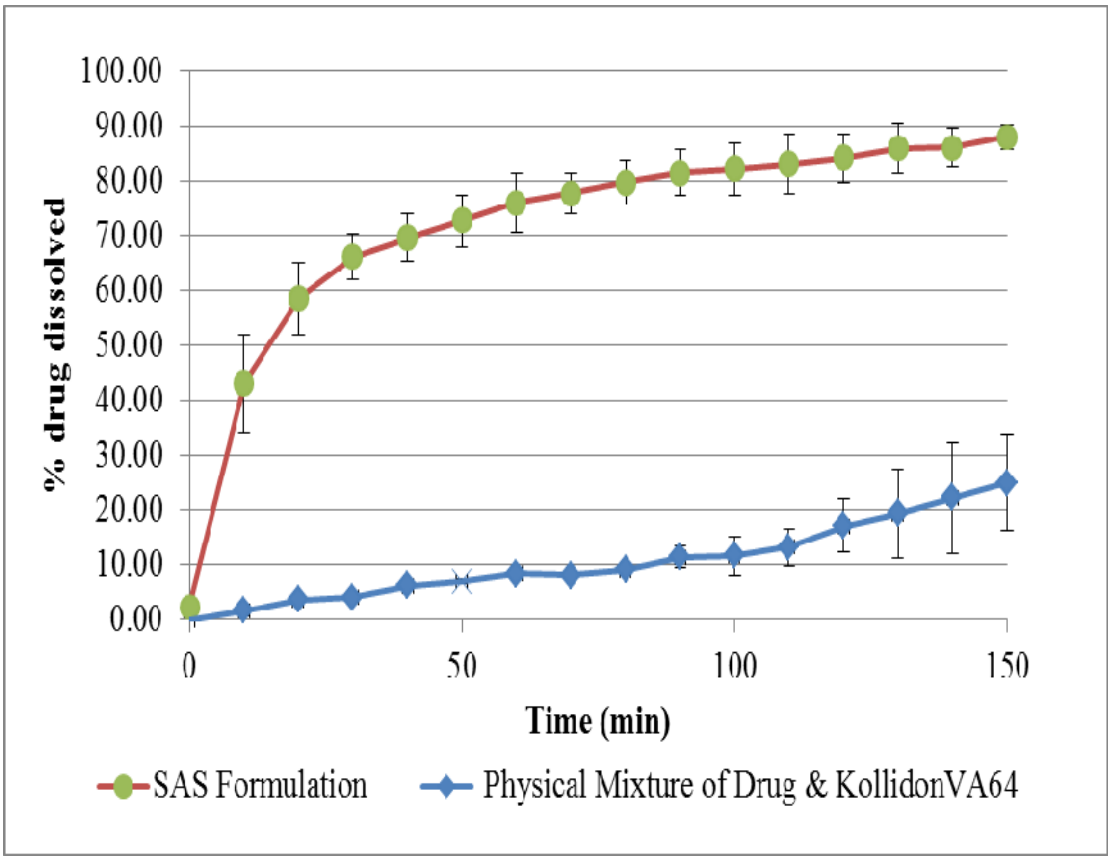

Figure E.5: Comparative dissolution of optimized SAS formulation vs physical mixture of as-is drug with Kollidon VA64.

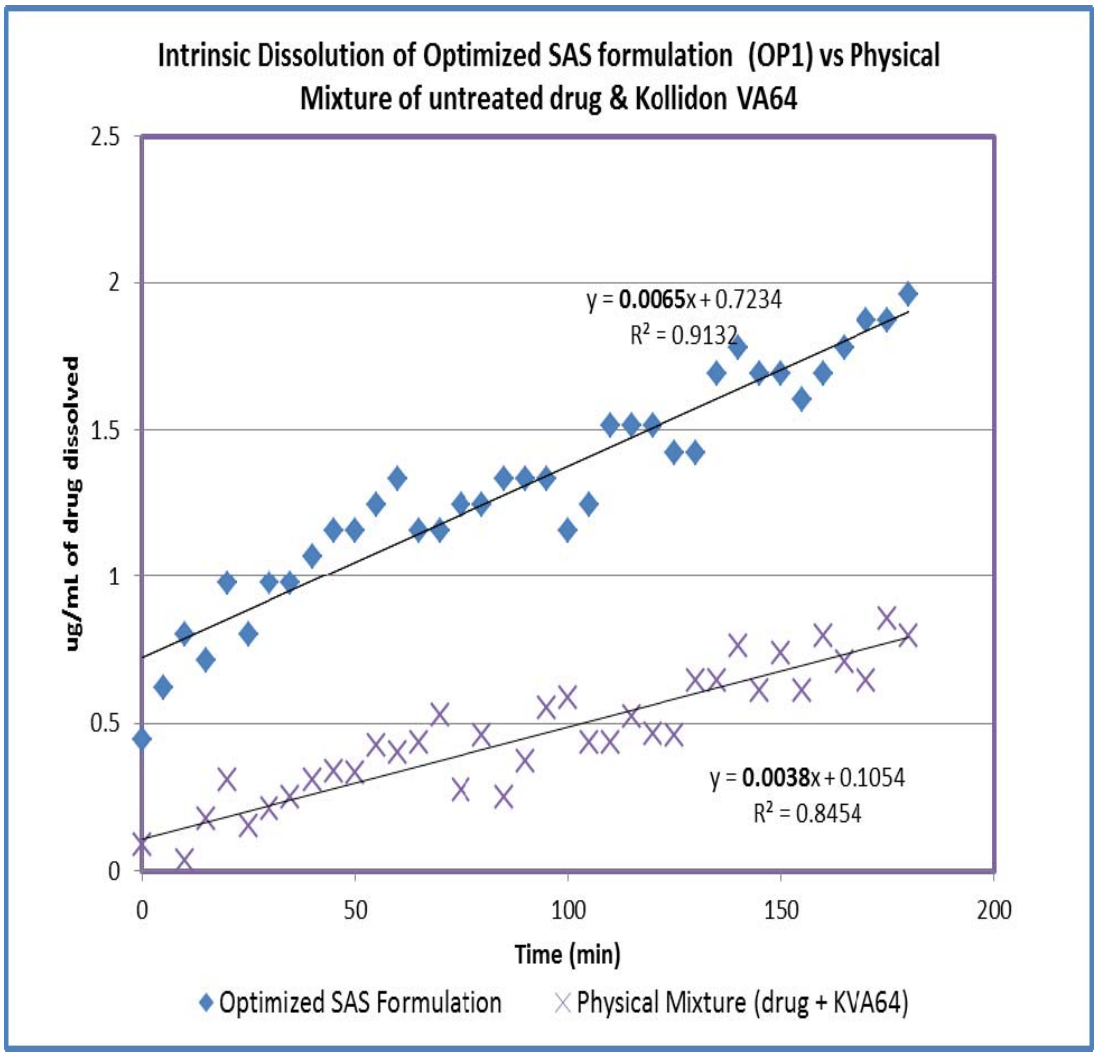

Figure. E.6: Intrinsic dissolution of optimized SAS formulation vs physical mixture of as-is drug with Kollidon VA64.